الجمهورية الجزائرية الديمقراطية الشعبية

République Algérienne Démocratique et Populaire

وزارة التعليم العالي والبحث العلمي

Ministère de l'Enseignement Supérieur et de la Recherche Scientifique

جـــامعة محمـــد خيضر-بسكرة
كليـــــة العلـــــوم والتكنولوجيا
قســـم الهندسة المدنيـــة والري
المرجع: .....

Université Mohamed Khider – Biskra
Faculté des sciences et technologies
Département : Génie civil et hydraulique
Réf: .....

Thèse présentée en vue de l'obtention du diplôme de

Doctorat

Spécialité : Génie civil, Option : Géomécanique et structures en interaction

Investigation expérimentale du comportement mécanique et hydraulique d'un sol pulvérulent traité à la chaux et/ou au ciment.

Présenté par:

BELMANA ADEL

Soutenue publiquement le 23/06/2025

Devant le jury composé de :

Mr. Benmeddour Djamel	**Professeur**	**Président**	**Université de Biskra**
Mr. Mellas Mekki	**Professeur**	**Encadrant**	**Université de Biskra**
Mr. Cavaleiro Victor	**Professeur**	**Co-encadrant**	**Université de Beira Interior**
Mr. Mabrouki Abdelhak	**Professeur**	**Examinateur**	**Université de Biskra**
Mr. Demagh Rafik	**Professeur**	**Examinateur**	**Université de Batna 2**
Mr. Mansouri Mouloud	**Professeur**	**Examinateur**	**Université de Sétif 1**

الجمهورية الجزائرية الديمقراطية الشعبية

Democratic and Popular Republic of Algeria

وزارة التعليم العالي والبحث العلمي

Ministry of Higher Education and Scientific Research

Mohamed Khider University – Biskra
Faculty of Science and Technology
Department: Civil Engineering & Hydraulics
Ref: .....

جـــامعة محمـــد خيضر-بسكرة
كليـــــة العلـــــوم والتكنولوجيا
قســـم الهندسة المدنيـــة والري
المرجع: .....

Thesis presented for the award of the Diploma of

Doctorate

Specialty: Civil Engineering, Option: Geomechanics and interacting structures

Experimental investigation of the mechanical and hydraulic behavior of a pulverulent soil treated with lime and/or cement.

Presented by:

ADEL BELMANA

Publicly defended on 06/23/2025

In front of the jury composed of:

Mr. Djamel Benmeddour	**Professor**	**Chairman**	**University of Biskra**
Mr. Mekki Mellas	**Professor**	**Supervisor**	**University of Biskra**
Mr. Victor Cavaleiro	**Professor**	**Co-supervisor**	**University of Beira Inertior**
Mr. Abdelhak Mabrouki	**Professor**	**Examiner**	**University of Biskra**
Mr. Rafik Demagh	**Professor**	**Examiner**	**University of Batna 2**
Mr. Mouloud Mansouri	**Professor**	**Examiner**	**University of Setif 1**

To my family and friends

Acknowledgments

I would like to express my gratitude to Professor Mellas Mekki, my thesis director, and Professor Victor Cavaleiro, my co-director, for their invaluable guidance and oversight of this work, as well as for imparting their expertise.

I extend my gratitude to the panel members who consented to evaluate this work in its unconventional format: Mr. Abdelhak Mabrouki, Mr. Rafik Demagh, Mr. Mouloud Mansouri and especially the chairman Mr. Djamel Benmeddour as well as the reporters Mr. Mekki Mellas and Mr. Victor Cavaleiro.

I wish to extend my heartfelt gratitude to Dr. Luis Pais, Dr. Isabel Falorca, Dr. Gabriel Marchi, and Pr. Abílio Manuel of the GeoBioTec laboratory for their indispensable support in laboratory testing, their attentive listening, and their application of technical expertise and experience to improve my work.

I pay my sincere thanks to the entire team and administration of Laboratoire des Travaux Publics de l'Est (LTP) for their substantial assistance in the development of the devices, as well as for their patience and recommendations. Likewise, I am pleased to have frequently engaged in discussions on technical matters with Mr. Rabeh Hachimi.

My thanks also go to Pr. Castro Gomes, Mr.Addalhakim Benhamouda, Mr.Naim Sedira, and Mr.Imed Beghoura, from whom I frequently sought assistance in conducting the MIP and TGA tests.

I wish to express my gratitude to the administrative managers: Professor Antonio Albuquerque, Ms. Maria José, Ms. Sandra Miguel, Mr. Hugo Pinto, Ms. Monica Gabriel, and Ms. Maria Abalada.

I am pleased to have collaborated with Mr. Leonado Marchiori, Mr. André Studart, Ms. Vanessa Alvané, and Ms. Victoria Morais. Having had the opportunity to cooperate, their friendship remains a great pleasure for me.

I would like to express my heartfelt gratitude to those individuals who, directly or indirectly, have contributed to the preparation and execution of this thesis by their presence, expertise, and feedback. The acknowledgements encompass numerous elements not articulated in the manuscript, although they significantly develop the whole work. I hope I have not forgotten anyone, whether professionally or personally.

Résumé

Les ouvrages hydrauliques utilisés pour l'irrigation, la production d'électricité et la navigation sont sujets à la détérioration due à l'exposition à l'eau et à l'érosion, ce qui altère les propriétés mécaniques et hydrauliques des sols au fil du temps. De nombreux sols extraits sont impropres à une application directe en raison du risque d'érosion, ce qui nécessite l'utilisation de sols de substitution provenant de régions éloignées. Cela entraîne des dépassements de délais et des coûts d'exécution accrus, entraînant des déchets et des frais de transport et de stockage supplémentaires. Cela nuit également au développement durable en augmentant l'impact environnemental.

L'objectif principal de cette thèse est d'examiner les améliorations apportées à l'application de traitements à la chaux ou au ciment pour stabiliser un sol granulaire à teneur spécifique en argile jugé inadapté à l'érosion. Pour atteindre cet objectif, plusieurs obstacles doivent être surmontés : le premier problème concerne le manque de données expérimentales concernant l'érosion dans ce type de sol spécifique. Aucune recherche n'a été menée sur des sols présentant un large spectre granulométrique, allant de quelques microns à plusieurs millimètres. Le second problème est lié à la méconnaissance de l'efficacité des traitements à la chaux ou au ciment sur les sols à faible teneur en argile. La levée de ces différents obstacles nécessite la mise en œuvre d'une approche multicritère pour comprendre et estimer les améliorations apportées par un traitement à la chaux ou au ciment sur ce type de sol. Dans un premier temps, la sensibilité du sol est évaluée par les essais HET et Crumb. Un traitement à la chaux ou au ciment a été appliqué au sol, avec différents pourcentages et durées de cure, et des essais d'érosion ont été réalisés afin d'évaluer l'efficacité du traitement, le dosage optimal et le temps de cure. Parallèlement, une étude du comportement mécanique a été réalisée par des essais triaxial pour évaluer la résistance au cisaillement et la cohésion du sol traité. Cette étude a été complétée par des essais déterminant l'évolution de la minéralogie du sol tout au long du traitement, ainsi que sa porosité, notamment par rayons X, MEB, ATG et porosimétrie au mercure MIP.

Mots-clés : sol grossier, érosion interne, érosion de conduit, traitement à la chaux, traitement au ciment, Crumb test, essai triaxial.

الملخص

إن الهياكل الهيدروليكية المستخدمة في الري وتوليد الكهرباء والملاحة معرضة للتدهور نتيجة لتعرضها للمياه والتآكل، مما يؤدي إلى تغييرات في الخصائص الميكانيكية والهيدروليكية للتربة بمرور الوقت. كما أن العديد من أنواع التربة المستخرجة غير مناسبة للتطبيق المباشر بسبب خطر التآكل، مما يستلزم استخدام تربة بديلة من مناطق نائية. ويؤدي هذا إلى تجاوز المواعيد النهائية وزيادة تكاليف التنفيذ، مما يؤدي إلى الهدر ونفقات النقل والتخزين الإضافية. كما يؤثر هذا سلبًا على التنمية المستدامة من خلال زيادة التأثير البيئي.

الهدف الأساسي من هذه الأطروحة هو دراسة التحسينات في تطبيق معالجة الجير أو الأسمنت لتثبيت التربة الحبيبية ذات محتوى الطين المحدود الذي يعتبر غير مناسب ضد التآكل. ولتحقيق هذا الهدف، يجب التغلب على بعض العقبات: تتعلق المشكلة الأولية بنقص البيانات التجريبية المتعلقة بالتآكل في هذا النوع المحدد من التربة. لم يتم إجراء أي بحث على التربة التي تظهر طيفًا واسعًا من حجم الحبيبات، يتراوح من بضعة ميكرونات إلى عدة ملليمترات. أما السبب الثاني فيتعلق بعدم كفاية فهم فعالية معالجة الجير أو الأسمنت على التربة ذات المحتوى المنخفض من الطين.

إن إزالة هذه الحواجز المختلفة تتطلب تنفيذ نهج متعدد المعايير لفهم وتقدير التحسينات التي يجلبها معالجة الجير أو الأسمنت على هذا النوع من التربة. في البداية، يتم تقييم حساسية التربة من خلال اختبارات HET و Crumb .تم تطبيق معالجة باستخدام الجير أو الأسمنت على التربة التي تم تحليلها، باستخدام نسب مختلفة وفترات معالجة، يتم خلالها إجراء اختبارات التآكل لتقييم فعالية المعالجة والجرعة المثلى ووقت المعالجة. وبالتوازي، يتم إجراء دراسة على السلوك الميكانيكي باستخدام اختبارات ثلاثية المحاور لتقييم قوة القص وتماسك التربة المعالجة. تم استكمال هذا التحقيق باختبارات تحدد تطور معادن التربة طوال المعالجة، بالإضافة إلى مساميتها، بما في ذلك تحليلات الأشعة السينية والمجهر الإلكتروني الماسح وتحليل الوزن الجزيئي ومسامية الزئبق.

الكلمات المفتاحية: التربة الخشنة، التآكل الداخلي، الأنابيب، المعالجة بالجير، المعالجة بالإسمنت، اختبار التفتت، اختبار ثلاثي المحاور.

Abstract

Hydraulic structures utilized for irrigation, electricity generation, and navigation are susceptible to deterioration from water exposure and erosion, resulting in alterations to the soil's mechanical and hydraulic properties over time. Numerous extracted soils are unsuitable for direct application due to the risk of erosion, necessitating the utilization of substituted soils from remote areas. This results in deadline overruns and increased execution costs, leading to waste and additional transportation and storage expenses. This also adversely affects sustainable development by increasing environmental impact.

The primary aim of the thesis is to examine the enhancements in the application of lime or cement treatment to stabilize a granular soil with a specific clay content deemed unsuitable against erosion. To attain this goal, certain some obstacles must be overcome: The initial issue pertains to the deficiency of experimental data regarding erosion in this specific soil type. No research has been performed on soil exhibiting a broad grain size spectrum, ranging from a few microns to several millimetres. The second is related to the insufficient understanding of the efficacy of lime or cement treatment on soil with a low clay content.

The removal of these various barriers requires the implementation of a multi-criteria approach to understand and estimate the improvements brought by lime or cement treatment on this type of soil. Initially, the soil's sensitivity is evaluated by the HET and Crumb tests. A treatment using lime or cement was applied to the analyzed soil, utilizing various percentages and curing durations, during which erosion tests are performed to assess the treatment's efficacy, optimal dosage and curing time. In parallel, a study on the mechanical behavior was performed utilizing triaxial tests to assess the shear strength and cohesiveness of the treated soil. This investigation was supplemented by tests determining the evolution of soil mineralogy throughout treatment, as well as its porosity, including X-Ray, SEM, TGA, and mercury porosimetry analyses.

Keywords: coarse soil, internal erosion, piping, lime treatment, cement treatment, crumb test, triaxial test.

Summary

List of figures

Introduction

Chapter I

Chapter II

Chapter III

Chapter IV

ANNEXE

LIST OF TABLES

Chapter I

Chapter II

Chapter III

Introduction

The purpose of this work is to develop our understanding of erosion and dispersion phenomena, particularly in hydraulic structures made of earth or transportation infrastructure embankments. The rupture of dikes or dams represents some of the most catastrophic environmental disasters, causing irreversible ecological, social, and economic repercussions.

There are numerous reports detailing dam failures that have caused significant problems worldwide. For instance, the Marib Dam in Yemen experienced a breach in 575, an earthen dam near Grenoble, France, suffered a failure in 1219, and as evidenced by incidents in Aude in 1999 or 2005, in Gard in 2002, or during the passage of storm Xynthia in 2010 in Vendée (Haghighi 2012); in Italy, dam failures occurred in 1923, 1935, and 1985, resulting in the loss of many lives in the regions of Gleno, Molare, and Stava, respectively (Luino et al. 2014). In Algeria, the 'Fergoug' dam claimed the lives of approximately 200 people in 1881 in the Mascara region (Gaagai et al. 2020).

Problematic

The main function of earthworks such as dikes and dams is water retention. At a broader scale, these structures consist of porous media in permanent or temporary contact with moving water on the surface and within the pores. By nature, they are linear structures, meaning that a failure in any section, also known as rupture, results in the total loss of their function (Figure.1). This rupture can be caused either mechanically along a slip surface or by hydromechanical forces gradually displacing soil particles. These phenomena can manifest on the surface of the structure, known as external erosion, or within the soil mass, termed internal erosion. External erosion is typically triggered by overflow beneath the crest of the structure, potentially leading to the formation of a breach, mainly during extreme floods where the water level exceeds the design capacity of the structure. Internal erosion, on the other hand, is caused by flow within the earthwork, displacing soil particles until a preferential pathway forms, where flow velocity gradually increases until partial or total rupture occurs. This process can accelerate during exceptional events. However, its initiation is difficult to detect as it is invisible from the outside and does not result in significant leakage or settlement. When either of these phenomena is observed, the consequences can be dramatic, as it is often too late to intervene and maintain the functionality of the structure.

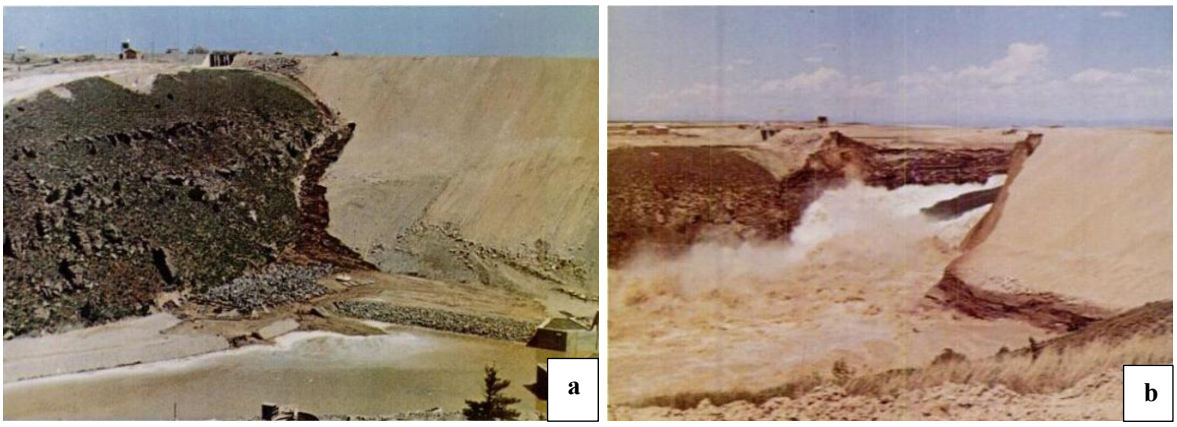

Figure. 1: Failure of Teton Dam (Idaho, États-Unis, 1976) ;(a) before failure; (b) After failure. (Teton Dam Failure Review Group (US). (1977)). Teton Dam Failure Review Group (US). (1977)

Hydraulic earthworks are constructed using sandy and clayey materials, and their primary function is to ensure both mechanical strength and waterproofing throughout their lifespan. What sets them apart is their ability to combine the behaviors of porous media both frictional and cohesive with the physicochemical interactions between water and clay. These behaviors and interactions can be influenced by the manner in which materials are placed and by the impact of mechanical and hydraulic stresses.

The decree of February 27, 2012, from the High Commissioner of the Republic, mandates owners, operators, or concessionaires of high-risk dams to carry out a hazard study by a competent organization. This study must outline the levels of risk considered, the measures capable of reducing them, and the residual risks. The implementation of the decree requires the project engineer to identify various rupture mechanisms, leading them to explore and develop tools and methods to characterize and quantify the erodibility of materials (DIMENC 2014).

Additionally, transport infrastructure embankments can also be subjected to hydraulic loads (Bertaina 2009). Road routes occasionally traverse valleys, with the longitudinal profile adjusted to suit car speeds, so many of these valleys are crossed by low-height road embankments (from a few tens of centimetres to a few meters). When even a modest watercourse delineates hydraulic pathways at the bottom of these valleys, hydraulic discharge structures are planned. However, when the valley is dry, poorly defined, or when discharge structures have been undersized, it can happen, during exceptional weather events, that these road embankments become an obstacle to water flow, leading to water accumulation against the "upstream" slope of the infrastructure.

The road embankments were not designed to withstand such hydraulic loading against their slopes. As water levels rise upstream, internal flows find pathways through the embankment, facilitated by potential vulnerabilities at the interfaces between the road embankment, the subgrade layer, and the overall pavement structure. If the resulting degradation does not directly lead to the collapse of the infrastructure, water levels may continue to rise until reaching the top of the embankment, overflowing onto the roadway and reaching the downstream embankment. Regressive erosion of the embankment then undermines the infrastructure, reducing its overall stability under water pressure and elongating the hydraulic path, which slows internal flows. If these phenomena persist long enough, they pose a threat to the road embankment, potentially leading to the rapid formation of a breach that damages the infrastructure irreversibly.

Furthermore, the structure of a road embankment is exposed to degradation mechanisms under lateral hydraulic loading, with a vulnerability of a distinct nature compared to that of a dam: the layers of homogeneous permeability feature horizontal interfaces conducive to the development of internal flows, while the road surface covers the crest of the slope, retaining almost all of the hydraulic energy that transforms into torrential velocity on the downstream slope, potentially hastening degradation through significant slippage due to its own weight. The distribution of stresses between internal erosion and surface erosion, as well as their respective predominance, differ significantly from those observed for a dam.

Another significant concern regarding erosion problems is the scouring of foundations of structures such as bridges or offshore wind turbines. The materials found in riverbeds primarily consist of sediments subjected to continuous and variable hydrodynamic forces over the lifespan of the structure. These forces are intensified at the site of shallow or deep foundations due to the discontinuity created by the structure. Erosion resulting from these intensified forces can degrade the bearing capacity of the foundation, or even wash away the entire supporting soil, ultimately leading to the failure of the crossing structure.

Indeed, most hydraulic structures are made up of ancient embankments, some dating back to the Middle Ages. These embankments were constructed gradually, with varying levels of maintenance, and generally, their structure is not well understood. Furthermore, newer structures often do not consider their susceptibility to erosion during the design phase. Hence, it is crucial to develop, apply, and validate dedicated testing methods to evaluate their sensitivity to erosion.

The primary goal of this document is to develop testing methods necessary for characterizing the different aspects of erosive processes, particularly within hydraulic earthworks.

Scientific approach

In our quest to deepen our understanding of erosion phenomena, beyond their practical application, we have explored existing experimental methods. Our goal was twofold: to improve and develop testing devices and to conduct studies using these testing methods and equipment. This was done to better understand how various parameters influence soil sensitivity to erosion.

The primary aims of this study were to refine devices, protocols, and experimental techniques for enhanced characterization of structures within practical engineering, and to gain a deeper insight into the various phenomena within a broader scientific framework. Consequently, this research was bifurcated into two segments: the first entailed refining and suggesting new testing methodologies, whereas the second involved the application of these developed testing methods in two distinct studies. The resulting conclusions will furnish a synthesis of these studies and the potential perspectives they open up.

Thesis plan

This document is composed of four chapters:

The first chapter offers fundamental insights into soil erosion and dispersion, delving into various measurement methodologies. It underscores the challenges associated with quantifying erosion phenomena.

The second chapter provides an in-depth description of the experimental devices used in this thesis, introduces the soil subject, and explains the experimental technique used for the research.

The third chapter explores a parametric study on the influence of certain parameters on the initiation and development of soil erosion, using tests with the Hole Erosion Test (HET) apparatus to characterize internal soil erosion through a simplified approach. The test involves tracking the temporal enlargement of a flow channel within a soil sample. A new version of the apparatus, equipped with improved instruments and interpretation methods, is proposed to estimate the erosion rate based on the mass of eroded particles and independently of hydraulic loading. Furthermore, an enhanced crumb test (ECT) designed to study soil sensitivity to dispersion is introduced, which refers to the soil's tendency to break apart in water without any

external mechanical movement or effort. Specifically, a new quantitative temporal tracking method for the geometry of unsaturated soil specimens is introduced.

The fourth chapter focuses on the research and studies conducted using these two experimental devices (HET, ECT) to characterize the behaviour of soil treated with quicklime or cement in relation to erosive processes. Hydraulic characteristics such as permeability and mechanical as well as physicochemical evolution are examined. The test results are compared for all studied configurations between treated and untreated soil.

The fourth chapter deals with the characterization of the behaviour of lime and cement-treated soil in relation to erosive processes, using the same procedures as those in Chapter Three.

The final section provides a summary of the key findings from this study, along with recommendations for future research endeavours.

I CHAPTER 1. SOIL EROSION AND DISPERSION: STATE OF THE ART

I.1 Introduction

The main objective of this chapter is to provide a state-of-the-art review of the research conducted to better understand the phenomenon of internal erosion in hydraulic structures.
Initially, we will briefly recall the various types of earthworks, and the materials used, while synthesizing the various observed modes of failure. Then, the second part will delve deeper into the study of internal erosion processes, focusing specifically on piping erosion and dispersion phenomena, primarily based on previous studies conducted using experimental techniques.
The third part of this chapter will focus on the lime and cement treatment technique previously employed in the context of stabilizing fine soils to address soil erosion.

I.2 Earthworks structures

Among the hydraulic structures affected by internal erosion, we can distinguish:

- Flood protection levees, which are not under load under normal conditions, are designed to protect downstream areas from flooding.
- Canal embankments for navigation,
- Hydroelectric canals for conveying water to dams.
- Earthen dams and earth water retention structures often have shorter lengths than the other three types of dams. However, in some large earthen dams, the hydraulic load can be considerably higher.

I.2.1 Types of hydraulic earthworks and their constitution

River management, navigation, irrigation, energy generation, and flood protection are just a few of the uses for which hydraulic structures are made. It is imperative to comprehend the composition, arrangement, and compaction of the components (fine and coarse soils) utilized in these constructions to guarantee efficient examination and upkeep.

I.2.1.1 Dikes

There are two distinct kinds of dikes:

- Mixed dikes: they are composed of a core of clayey materials covered with filtering layers of sandy-gravelly materials upstream and draining downstream.

- Gravel dikes: they are made of sandy and gravelly alluvium from the site, with increasing permeability towards the downstream.

I.2.1.2 Earth dams

Four types of dams are distinguished based on available materials and their implementation:

- Homogeneous dams: primarily constructed with fine soils, they are typically built when these materials are readily available and in sufficient quantity near the construction site, making the project economically feasible. In cases where materials are arranged based on their particle size and moisture content without the use of a separation filter, they are referred to as pseudo-zoned dams. For example, a dam may be constructed with the finest particles upstream and the coarsest downstream, or with the wettest materials in the center.
- Zoned earth dams: a more expensive option, considered when the available quantity of fine materials is insufficient. These dams include a core or upstream mass providing waterproofing.
- Dams with sealing: used when fine materials are not available for construction, these dams are made waterproof by geomembranes, molded walls, and sheet pile curtains.

In Algeria, the construction of dams began in the 19th century. At the end of the colonial period, the country had only 15 dams across its entire territory (Table 1). Today, after considerable investments in the hydraulic sector, 79 dams are in operation, distributed across the various regions of the country.

- • 14 in the Western region.
- 17 in the Chélif region.
- 18 in the Central region.
- 30 in the Eastern region.

Tableau I-1: Algerian dams before 1962 (Bouzid 2010)

Name	Oued	Construction year	Initial volume (hm^3)
Meurad	Djabroun	1852-59	0.8
Tlelat	Tlelat	1869-70	0,7
Fergoug	Habra	1865-71 puis 1882	30
Cheurfas	Sig	1880-82	3
Cheurfas	Sig	1886-92	18
Djidiouia	Djidiouia	1857-77	0,7
Hamiz	Hamiz	1869-94	14
O.Fodda	Fodda	1932	228
Boughzoul	Chelif	1934	55
Bakhadda	Mina	1936	56
Ghrib	Chelif	1939	280
Foum El Gueiss	Gueiss	1939	3,4
K'sob	K'sob	1940	12,4
Zardezas	Saf-Saf	1946	14,9
Beni Bahbel	Tafna	1946	63
Bouhanifia	Hammam	1948	73

Projections for 2030 estimate that the number of dams will rise to 139, with a total storage capacity of 12 billion cubic meters nationwide.

I.3 Hydraulic structure failure

The primary function of a hydraulic structure is to retain water, and the loss of this capability can result in significant material and human damage. The failure of such a structure can arise from various causes, which can be broadly classified into mechanical and hydrodynamic origins.

Mechanical failure typically involves the structural integrity of the soil, such as a failure along a slip surface. This type of failure occurs when the forces within the soil exceed its strength, causing it to slide and lose its ability to support the structure. This can happen due to changes in load, water saturation, or seismic activity.

Hydrodynamic failure, on the other hand, involves the gradual movement of soil particles that make up the structure. This displacement is driven by the forces exerted by water flow within and around the structure. There are two primary types of erosion associated with hydrodynamic failure: external erosion and internal erosion (Figure. I.1).

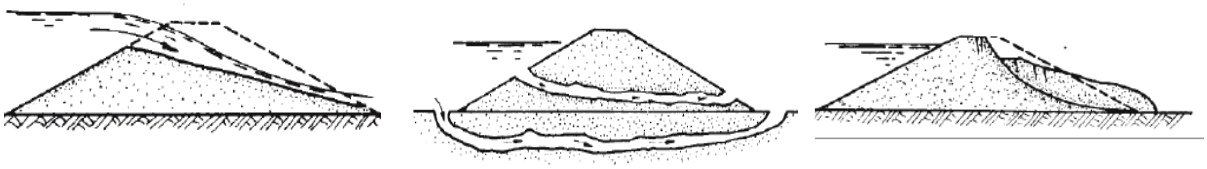

Figure I-1: Phenomena of rupture of hydraulic structures: External erosion (a); Internal erosion (b), External instability (c) (Elandaloussi R. (2015))

External erosion is caused by water flow over the surface of the structure. This can occur when water levels rise and flow over the top of the dam or embankment, carrying away soil particles in a process known as overtopping. This can gradually weaken the structure, leading to its eventual failure.

Internal erosion, also known as piping, occurs within the body of the structure. It is characterized by the movement of soil particles caused by subsurface hydraulic flow. This type of erosion starts at a microscopic level, with water seeping through the soil and gradually displacing particles. Over time, this can create voids and channels within the structure, which can grow and eventually lead to a catastrophic collapse. This process is particularly insidious because it is initially invisible at the surface, often going undetected for years. However, during events such as heavy rainfall or flooding, the process can accelerate rapidly, causing the structure to fail in a very short period (Figure. I.2).

Figure I-2: An example of piping failure at Upper clear Boggy in the USA (Lim 2006)

Erosion is the primary cause of soil degradation (Souidi 2011), particularly in Mediterranean regions. These areas are fragile and have historically been the most affected by erosion (Kheir 2002).

Researches (Demmak 1982; Meddi 1992; Morsli et al. 2015; Laouina et al. 2000) has demonstrated that erosion is very active in the Maghreb countries. The extent of soil erosion in this region requires greater attention, as it causes significant damage (Roose et al. 1998).

I.3.1 Hydraulic structure failure in Algeria

Embankment dams are structures made of loose materials, ranging from fine clay to very coarse elements like rock fill. They are categorized based on the method used to ensure impermeability. This very old type of dam is the most commonly used, representing nearly 70% of dams worldwide. In Algeria, many dams are constructed with loose materials, such as the Hammam Boughrara, Sidi Abdelli, Cheffia, Guenitra, Beni Zid, Mexa, Zit El Emba, Fontaine des Gazelles, Deurdeur, Oued Cherf, Foum El Gueiss, Ghrib, Bakhadda, Beni Amrane, El Agrem dams, and many others.

Algeria ranks among the most affected countries by erosion worldwide (Touaibia 2010). The factors that contribute to this phenomenon include the climate and torrential water flows, weak geological formations, low density of vegetation cover, overexploitation of land and overgrazing, inappropriate land use practices, and the type of agricultural mechanization.

I.3.1.1 Fergoug Dam Breach

The first time was on November 25, 1927, as the water level continued to rise, the 32-meter-high Oued-Fergoug dam began to vibrate. Suddenly, the dam bowed in its middle, opened up, and a huge torrent of water gushed out at the point of rupture (Figure I-3).

Forty-five minutes after the announcement of the dam breach, the tumultuous waters rushed into the streets of Perrégaux, with an impressive and unsettling noise. The powerful wave swept away the railway's metal bridge and the state railway depot, carrying locomotives and wagons that were overturned and transported to the city streets. Roads were cut off, orchards uprooted, and crops destroyed. Water flooded and damaged the road connecting Perrégaux to Oran. In the city, about fifty houses couldn't withstand the pressure of this natural force that had been attempted to be controlled. In the streets, the height of the muddy waters reached two meters.

Fortunately, thanks to the telephone call from the dam engineer and the fact that the event occurred during daylight, no casualties were reported in Perrégaux. However, a few individuals were found drowned in the plain (Comité technique permanent des barrages 1998).

The second time was on March 10, 1872, an exceptional flood estimated at 700 m^3/s caused the spillway to break, creating a breach. On December 15, 1881, a flood of 850 m^3/s swept away 125 meters of the dam on the right bank. This tragic event resulted in the drowning of 250 people and the destruction of bridges and houses by the raging waters. The dam reconstruction, carried out between 1883 and 1885, included a profile modification and cost 1,300,000 francs (Comité technique permanent des barrages 1998).

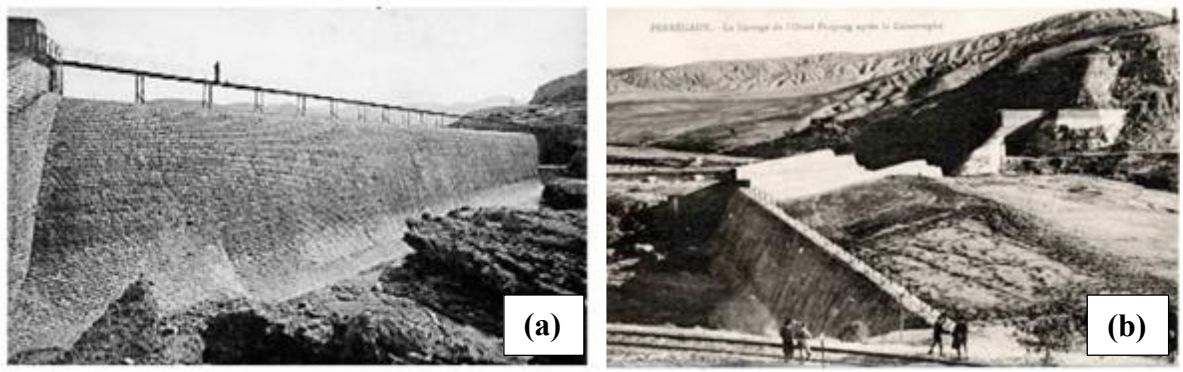

Figure I-3: Breach of the Fergoug Dam; (a) Before the breach 1907, (b) after the disaster 1928. (Comité technique permanent des barrages, 1998)

I.4 Erosion typology

Internal erosion is shown to be the most common cause of recent earth structure collapses in France and around the world, according to databases created for the national ERINOH project (Internal Erosion of Hydraulic Structures) by Fry et al. (2012). A total of 46 failures were reported over the 26-month monitoring period that began in 2010. Of those failures, 43 (or more than 97%) were attributed to erosion. Twenty of these forty-three erosion-induced failures resulted from overtopping, and the other 22 were due to internal erosion.

Figure I-4: Rupture of the Bom Conselho dam (Brazil) in June 2010 by overflow (Fry et al. 2012)

Prior research evaluating dam collapse risk indicated that the risk of breaching and the failure process can be anticipated based on historical dam failure incidents (Luino et al.2014; Gaagai et al. 2020).

I.4.1 External erosion

It refers to the degradation of a soil or rock's surface due to the separation and movement of particles brought on by external natural agents such water, air, heat, humidity, freezing, or drying. Rain erosion, river erosion, and coastal erosion are the three primary forms of water-induced external erosion that can be distinguished (Pham 2008).

Water circulation over the crests of structures, no matter how small, can lead to external erosion. During floods or periods of excessive rainfall, for example, this happens when drainage systems are unable to cope with the excess water during floods or intense rainfall, resulting in the water overflowing, where it becomes torrential and extremely erosive. Erosion commences from the slope's downstream edge and advances until a breach appears when flow velocities surpass the particle detachment threshold. Continuity, cohesiveness, crest coating, and water depth above the structure all affect how long this phenomenon lasts, ranging from minutes to hours. A breach can be created by partial or total embankment collapse brought on by damage to the slope's base or steepening of the downstream slope.

I.4.2 Internal erosion

According to Blai (2004), "internal erosion" often refers to the phenomenon of particle separation and transport caused by water flow within a structure. The definition provided by the ICOLD (1990) is "the movement of soil particles inside an embankment dam or its

foundation due to seepage in the direction of the flow." This phenomenon is divided into various categories. Four primary mechanisms are identified by Fry et al. (2012) as the causes of internal erosion: (1) suffusion; (2) backward erosion; (3) contact erosion; and (4) conduit erosion, also known as focused leak erosion.

I.4.2.1 pipe erosion

Notably, differential settlements, rat burrows, conduits within the dike bodies, tree roots, and more are among the causes of erosion identified in the publications published by the French Committee on Large Dams (CFGB) (Blai 2005). Apart from the fact that the flow is under pressure and the erosion happens at the interface of a conduit within the soil mass, this phenomenon is remarkably similar to external erosion, which happens at the interface between a typically turbulent flow and the soil surface. As a result, in comparison to the structure's surface, the soil's condition and the typically turbulent flow conditions differ. In general, there is tension in the soil (Reddi and Bonala 1997; Indraratna et al. 2009). The ERINOH database indicates that this process is the most frequent reason for internal erosion failures.

I.4.2.2 Contact erosion

Contact erosion is the process in which particles detach from the interface between two porous media that have significantly differing grain sizes (Béguin 2012). When a layer of gravel comes into touch with a layer of fine sand, the sand grains at the boundary may get detached and move through the small pores in the gravel layer. This occurrence is alternatively referred to as interface erosion or contact suffusion. The relationship between the two layers is strongly influenced by the difference in grain size and permeability. This discontinuity fulfils two essential prerequisites for erosion. The coarse material demonstrates a high level of permeability, resulting in flow velocities that are capable of dislodging and carrying particles. This phenomenon is known as the hydraulic condition. Furthermore, the dimensions of the pores and constrictions in this material are far greater than the size of the smaller dirt particles, enabling them to pass through without becoming trapped. This situation is known as the geometric condition.

I.4.2.3 Regressive erosion

Erosion that begins downstream and moves upstream is referred to as regressive erosion. This happens when the pressure of fluid seeping through the structure dislodges soil particles. The components that make up the soil's framework become unstable at the base of the slope due to

drag forces from the flow. The flow gradually carries these elements away, which destabilizes the upstream materials, which are subsequently displaced as hydraulic gradients increase, the process continues, and the hydraulic path becomes shorter.

I.4.2.4 Suffusion

Suffusion is a phenomenon that causes the movement of small particles within the soil, as explained by Bendahmane et al (2005). While the general distribution of particle sizes in the soil remains constant, its permeability diminishes. The rearrangement of particles in a flow creates a concentrated increase in pressure downstream, which has the potential to trigger landslides. Typically, suffusion progresses at a modest pace, which enables its diagnosis and suitable intervention. Various criteria have been suggested in the literature to assess the commencement and progression of internal erosion. These procedures primarily rely on the analysis of the particle size distribution of materials, or the assessment of the minimum hydraulic gradient required for erosion.

I.5 Characterization of erosion

I.5.1 Internal erosion and laboratory tests

According to the literature, the erodibility of a soil is defined as the correlation between the erosion rate (e), which represents the amount of soil eroded per unit of time and area, and the flow velocity (v) at the water surface (Heize 1975). This definition is limited since the flow velocity varies in both intensity and direction throughout the flow field, and it is specifically zero at the interface between the fluid and solid. It would be pertinent to examine the correlation between the erosion rate and the shear stress (τ) at the water-soil interface in order to establish a more rigorous definition of erosion.

$$\dot{\varepsilon} = f(\tau) \qquad [I.1]$$

The definition based on shear stress is an improvement over the one based on velocity. However, it remains incomplete because shear stress, according to the mechanism described earlier, is not the only force involved in erosion. Briaud (2008) proposed a more comprehensive description:

The definition relying on shear stress is a better alternative to the one relying on velocity. Nevertheless, the erosion process described earlier is not solely dependent on shear stress, as outlined in the previous explanation. Briaud (2008) brought up a more thorough explanation:

$$\frac{\dot{\varepsilon}}{u} = \alpha \left(\frac{(\tau-\tau_C)}{\rho_w u^2}\right)^m + \beta \left(\frac{(\Delta\tau)}{\rho_w u^2}\right)^n + \delta \left(\frac{(\Delta\sigma)}{\rho_w u^2}\right)^p \qquad \text{[I.2]}$$

Where:

$\dot{\varepsilon}$ the erosion rate, u the longitudinal flow velocity, τ the hydraulic shear stress, τ_c the critical erosion stress below which erosion does not occur, ρ_w the density of water, Δ_τ the fluctuations in hydraulic shear stress, and $\Delta\sigma$ the fluctuations in hydraulic normal stress. The other variables are parameters that characterize the soil.

Identifying the six parameters (*α, β, δ, m, n, p*) involved in the model [I.2] is not feasible, and it is still empirical.

A curve for granular and fine soils had been created by Hjulström (1935). Nevertheless, Briaud (2008) found that his suggestions for fine soils were overly simplified. Shields (1936) introduced a formula, to determine the smallest particle size required to prevent erosion and the shear stress generated by particle motion.

An "Ex situ Scour Test Device" (ESTD) was used in an attempt to assess overall shear and normal stresses by Shan (2010), as reported by Haghighi (2012). Still, there isn't a workable way to measure local stresses and variations in the model [1.3]. The Shields (1936) model, commonly referred to as the "erosion law," is still used and can be stated as follows:

$$\dot{\varepsilon} = k_{er}(\tau - \tau_C) \qquad \text{[I.3]}$$

I.5.2 Typology and mechanisms of dispersion

Soil dispersion is the suspension of individual clay particles in stagnant water (Ingles 1968; Sherard 1976; ASTM D4647; ASTM D4221 2011), influenced by the nature of the clays and their reactivity in water which is often interpreted as a sensitivity to erosion. The susceptibility to dispersion is determined by the amount of sodium (Na+) in the clay, which acts as a compensating cation for the negative charge carried by the clay layers. Other factors influencing this phenomenon include the presence of sodium, calcium, or magnesium ions, the stacking

mode of the clay layers, salt concentration in the erosion fluid, the pH of the erosion fluid, and the structure of the clay mineral (Holmgren and Flanagan 1977; Raudkivi and Tan 1984).

The decrease in the size of clay particle agglomerates can facilitate their mobility or block a preferential exit route. There is no direct correlation between dispersiveness and erodibility, but dispersion is often recognized as a cause of particle pulling in internal erosion. Soil dispersiveness is closely related to the nature of the clay and its reactivity to water (Blai 2004).

The susceptibility to dispersion is determined by the amount of sodium (Na+) in the clay, which acts as a compensating cation for the negative charge carried by the clay layers. Other factors influencing this phenomenon include the presence of sodium, calcium, or magnesium ions, the stacking mode of the clay layers, salt concentration in the erosion fluid, the pH of the erosion fluid, and the structure of the clay mineral (Holmgren and Flanagan 1977; Raudkivi and Tan 1984).

Hydration refers to the process of exposing unsaturated soil to water, resulting in the breakdown of the particles that make up the soil. The disintegration occurs due to the quick breakup of the particle assemblies when molecular water reaches its equilibrium position on the particle surfaces, based on energy considerations. Deaeration is the process of removing air from the soil, which happens when water infiltrates the soil. The compressible air subsequently creates pressure, causing a significant change in the original composition of the soil, resulting in total saturation. The previously mentioned processes are typically characterized by their rapidity and typically endure for only a little duration, typically a few minutes, in the area where the soil directly interacts with water (Tarog 2000, Pham 2008, and Haghighi 2012).

Swelling arises when the concentration of ions within the soil matrix exceeds that of the liquid causing erosion. The disparity in concentration prompts water to permeate the soil pores, augmenting osmotic pressure and resulting in the enlargement of the soil mass. The ionic concentration in the soil's interstitial solution is determined by two factors: the amount of unbound salts in the water between soil particles, and the presence of ions that are balanced by electrical charges within the particles. The swelling induced by soluble salts eventually diminishes as the salts are dissolved by water. Conversely, ions that are bound cannot be released through diffusion. As a result, soil particles hold water and salts, leading to the absorption of water and swelling of the soil. As the particles gradually disperse and the

attraction forces weaken, this process leads to the fragmentation of the solid mass (Pham 2008; Haghighi 2012).

I.6 Experimental tests and devices

Many studies with less complex apparatus have been conducted to evaluate different aspects of erosive processes. These devices allow for the measurement of fluid-induced stresses and geometric changes, under certain interpretation assumptions. There are several significant differences between these testing equipment. As an illustration, some use a vertical water current (JET), while others provide a horizontal tension directly to the soil contact (HET). Measurements might be taken are taken either continuously or at specific time intervals during tests that are carried out in the field or in a lab as defined (Jerez Loaiza 2011). It is possible to make measurements both directly and indirectly.

I.6.1 Tests at the structure scale

In this test, extensive measurements such as temperature, displacement, flow rate, and failure time are taken while simulating large-scale events within a controlled experimental structure. The hydraulic load is applied by the upstream water level, and the phenomenon's kinetics are assessed over time. Unlike natural failures where data is scarce and measurements are made both before and after the incident, this approach offers databases for numerical modelling of structures.

Sensors for dike breach warning systems are developed at the IJkdijk experimental site in Booneschans, Netherlands. The findings demonstrate that early failure stages can be efficiently identified by measuring the temperature and pore pressure in layers that are susceptible to internal erosion (De Vries et al. 2010).

To determine the critical flow velocity for contact erosion and investigate the scale effect, Béguin (2012) carried out tests at the Hydraulic Laboratory of the "Compagnie Nationale du Rhône" in Lyon (Figure I-5). He perceived how failure progressed from the upstream onset of instability to the downstream advancement. Temperature and resistivity measurements provided less insight about the beginning and development of the erosion conduit than did fiber optic deformation data. There was no discernible scale effect, and the critical velocities achieved were comparable to those observed in the lab.

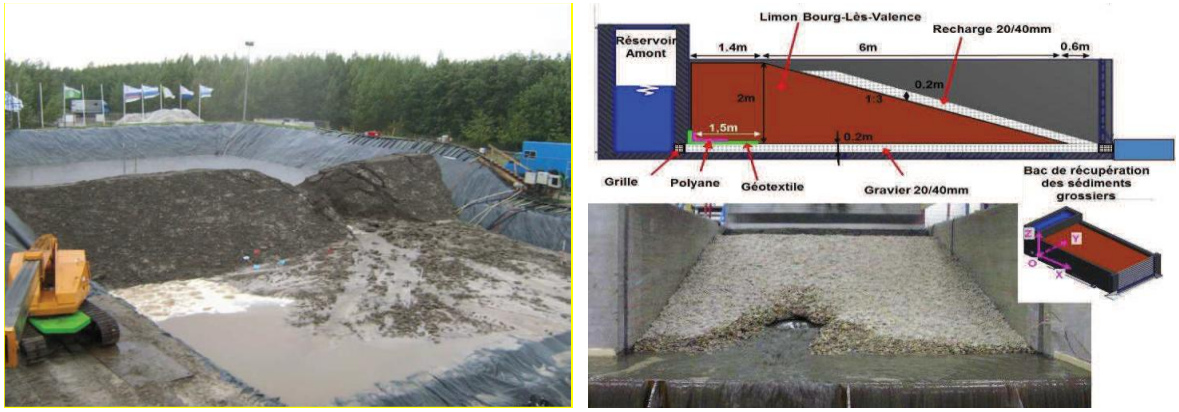

Figure I-5: large-scale internal erosion tests; a) IJkdijk test just after rupture (Vries et al. 2010); b) diagram of experimental structure and example of rupture at the hydraulics laboratory of the Compagnie Nationale du Rhône in Lyon (Béguin 2012)

The test has several significant limitations, including elevated implementation costs, insufficient direct parameter characterisation, difficulties in environmental control, and adherence to safety regulations. Consequently, few experiments have been conducted so far. In addition, the absence of equipment within the mass has hindered several test campaigns.

I.6.2 Internal erosion tests

The internal erosion test devices are designed to simplify the simulation of real conditions. They make it possible to track and measure the processes that lead to particle detachment and movement in soils. These tools are essential for comprehending the dynamics of erosion and creating precise models. The tests range in size, complexity, and experimental circumstances to suit the objectives of each study, but they all strive to collect accurate and comprehensive data on internal erosion events**.**

I.6.2.1 Hole Erosion Test (HET)

This test entails forcing a flow through an already-existing hole in the material, similar to the "pinhole test", but it is fully instrumented. A determination of the shear stress and an evaluation of the erosion rate can be made by monitoring factors such as flow rate, hydraulic gradient, and the evolution of the hole's diameter. The equipment for the Hole Erosion Test (HET), created by Wan and Fell (2002), is shown in Figure I-6. This test aids in accurate measurement and tracking of geometric changes.

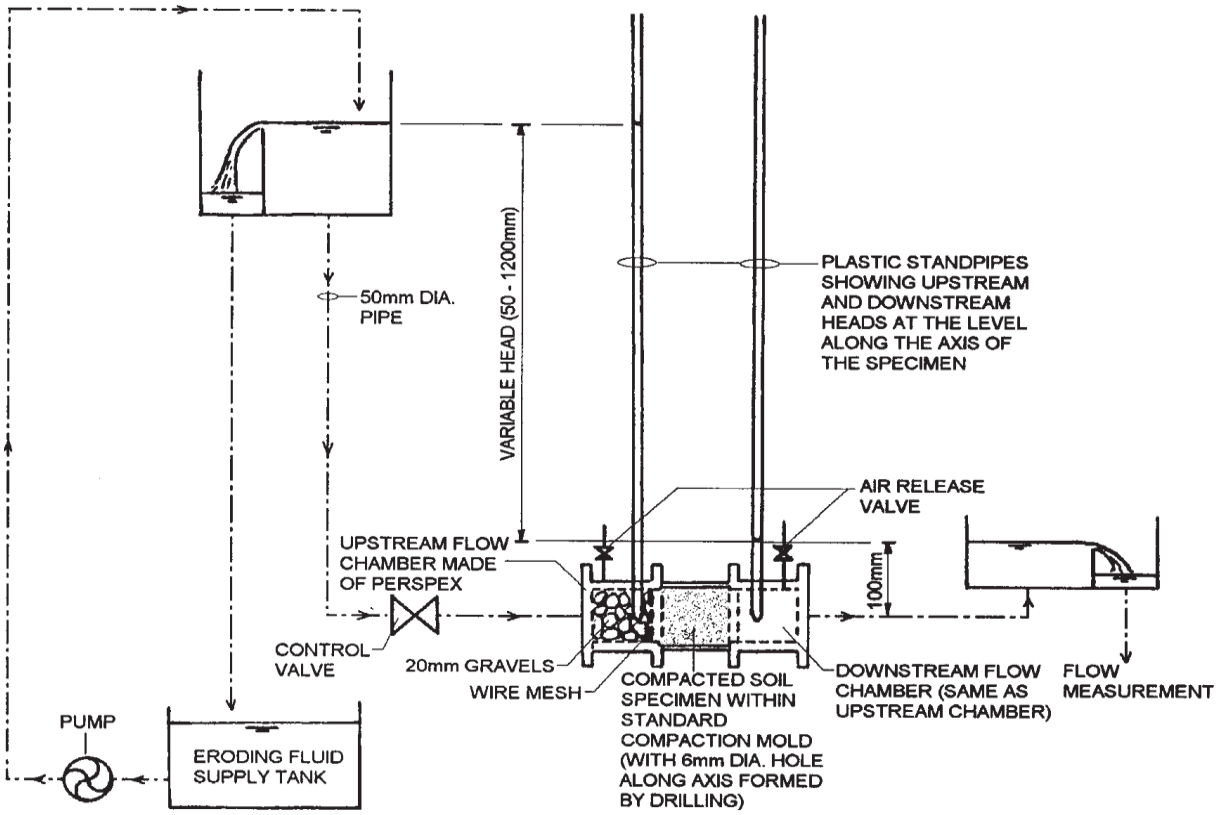

Figure I-6: Diagram of the Hole Erosion Test experimental device (source Wan and Fell, 2002)

The evaluation of the erosion resistance of 14 different types of core materials used in dams was the main goal of Wan and Fell (2004) study. To categorize this resistance, they developed a "erosion rate index". The objective was to create a straightforward approach to estimate the risk of internal erosion and earth dam piping. However, the method chosen by the researchers to estimate the critical shear stress has been criticized for its disputable nature.

I.6.2.2 Flow Pump Test

Testing that compares internal and surface erosion is referred to by this term (Reddi et al. 2000). Similar to the hole erosion test, the procedure involves pumping water through the pore network of a sample that is placed in a laboratory permeameter or through a hole that is drilled in the center of a soil sample. The test's name comes from the pump that creates the hydraulic gradient in this experiment. The pump is set up to increase the flow rate over a 15-minute period, gradually, from 0 to 200 ml/min (Figure I-7).

Experiments on a reconstructed soil texture consisting of 70% Ottawa sand and 30% kaolinite showed that the soil's internal and external critical shear stresses differed by almost 1000 times. An analogous variation was noted in the erosion coefficients. The probable blockage and

redeposition of eroded soil particles within the pore network is the reason given by the authors for this discrepancy.

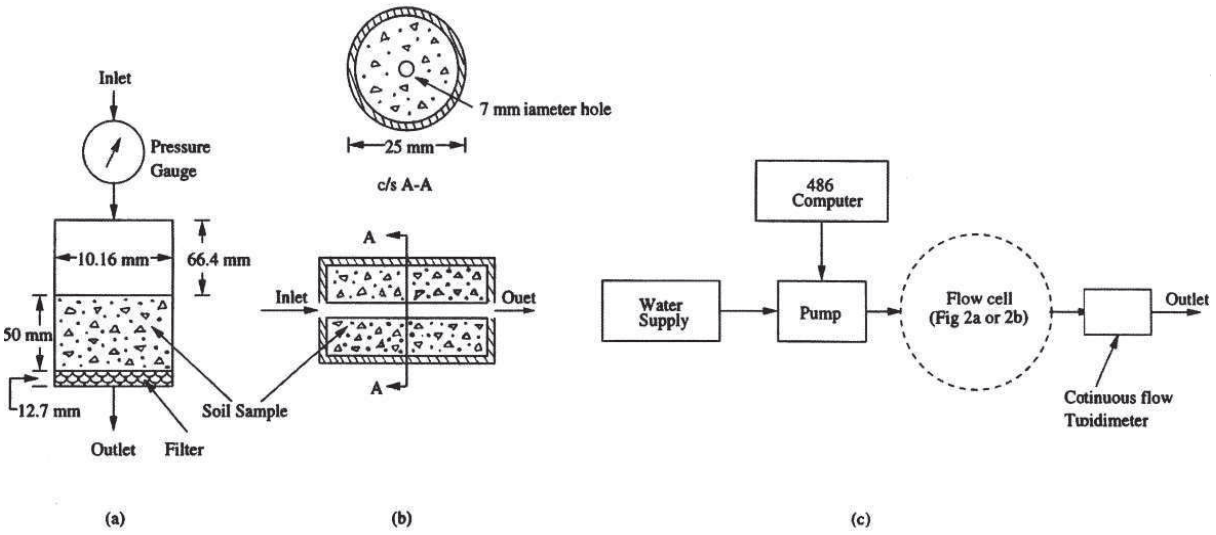

Figure I-7: Diagram of the "Flow Pump Test" experimental device a) internal erosion test cell b) test cell for surface erosion (pipe) c) diagram of the experimental setup (source Reddi and al. 2000)

I.6.2.3 Triaxial Erosion Test

In order to study suffusion in a uniform volume, this modified version of the conventional triaxial apparatus can be used to apply mechanical and hydraulic strains to soil samples. It effectively prevents the occurrence of parasitic flows surrounding the samples and allows for precise control over confinement during tests. Sanchez et al. (1983) utilized this instrument to examine materials from five distinct earth dams and measure shear stress and erosion rate. Researchers found that silt soil erosion is more influenced by increased water content compared to clay soil erosion. Bendahmane et al. (2008) improved the process by effectively injecting interstitial fluid and collecting the resulting effluent. They proposed doing testing, consolidation, and saturation in the same cell under strict control of humidity and temperature. The device allows for the application of both static and dynamic hydraulic stresses, and it also enables automatic monitoring (Figure I-8).

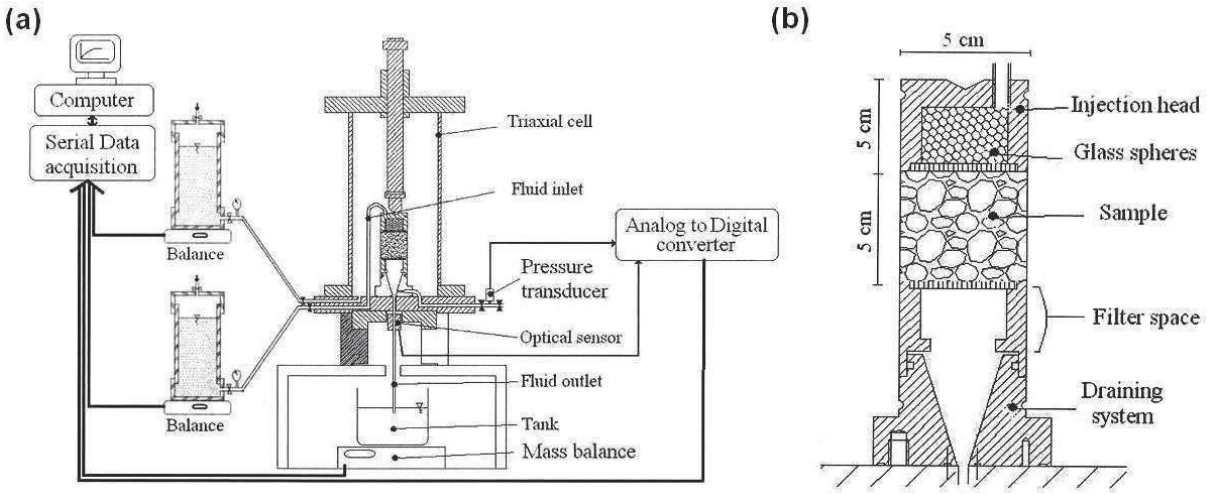

Figure I-8: Diagram of the experimental device of Triaxial Erosion Test; (a) assembly of the device; (b) test cell (source Bendahmane et al. 2008)

I.6.2.4 Suffusion column test

The research conducted by (Elandaloussi et al. 2019) focuses on the creation of a suffusion column equipped with an automated hydraulic loading device, a data acquisition system, an effluent collection system, and a measurement system to monitor the changes in pore pressure, effluent turbidity, flow rate, and fragment mass. Calculating the total mass of eroded particles requires collecting the effluent (Figure I-9).

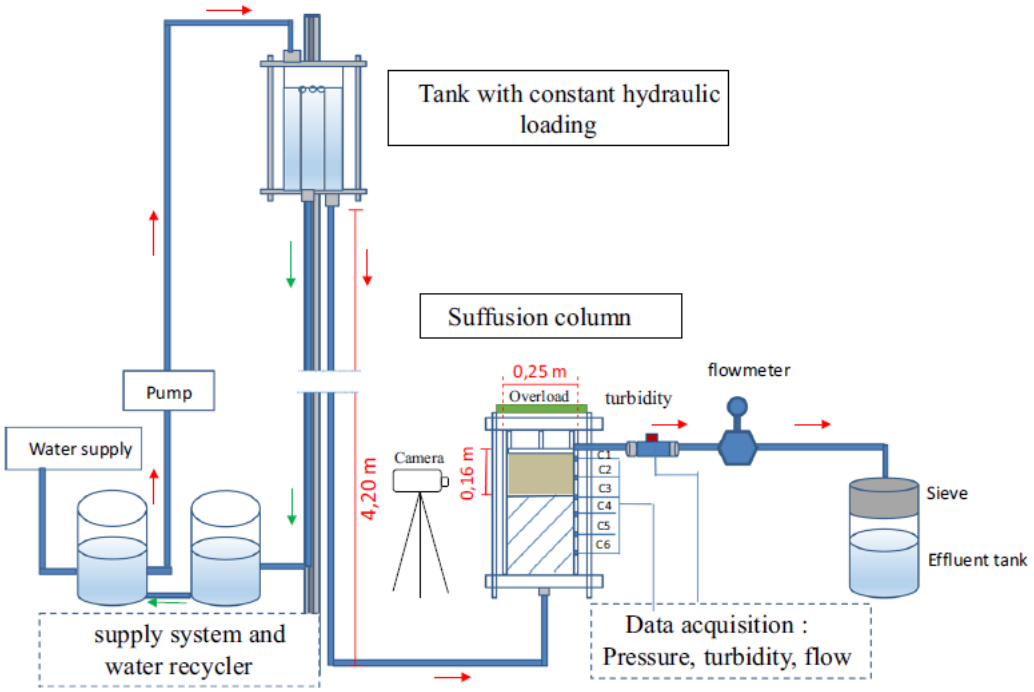

Figure I-9: General diagram of the test device (Elandaloussi et al. 2019)

I.6.2.5 Experimental device for contact erosion

Through tangential flow, this apparatus investigates erosion at the interface between two materials (Béguin 2012). It uses a steel cell containing fine and coarse soil layers and was first created to investigate geotextile devices (Ho 2007). The boundaries of the cell align with the upper surface of the fine soil layer. Through a glass pane, interface phenomena are seen. The upper surface of the sample is surcharged, and water can pass through the layer of coarse dirt thanks to a hydraulic system.

Using geometrically open filters, the apparatus evaluates particle detachment and transport conditions in coarse soil. The nominal flow velocity is estimated, and the flow is primarily localized. A turbidimeter is used to measure solid discharge, and tangential flow is produced by pressure differential. The sample is placed within a latex bladder, and the turbidity and outflow are gauged (Figure I-10).

The study used 30-minute increments of increased flow velocity to examine different types of soil. The coarseness of the soil particle size increased the threshold velocity as diameters increased, indicating a crucial velocity for erosion initiation. Similar effects were seen by fine soil particle size, which in clay and sand domains had a minimum and an enhanced critical velocity. The erosion process showed signs of instability at the interface and a consistent rise in erosion rate with increasing velocity.

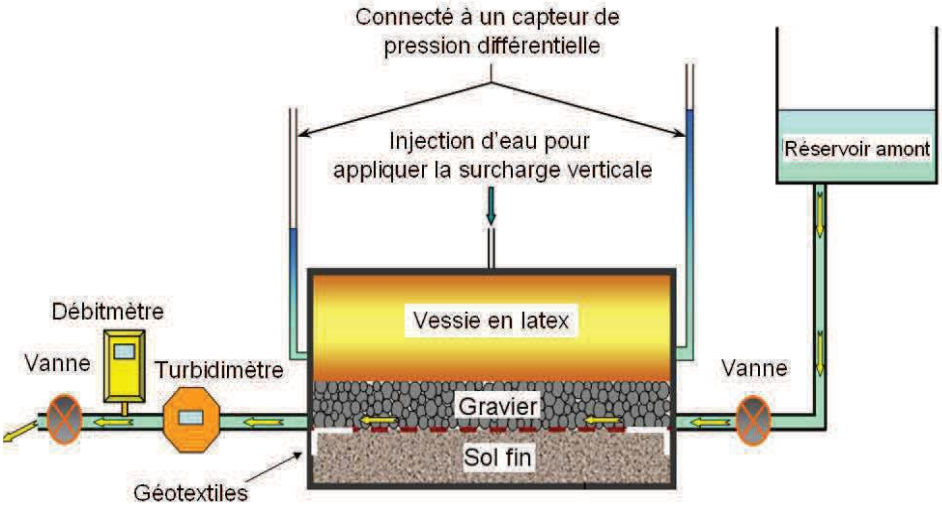

Figure I-10: Schematic of the contact erosion experimental device (source Béguin 2012)

I.6.3 Dispersion characterization tests

There is no need for mechanical stress in the basic experiments used to determine soil dispersion, and the results are qualitative. In the literature, several tests are mentioned to assess soil dispersibility, including:

I.6.3.1 The Double Hydrometer Test

Tarog (2000) states that the testing approach was initially introduced by Sherard et al. (1972), whereas the concept for the method was proposed by Volk (1937). The primary goal of this method is to compare the particle size distribution of a clay using two distinct approaches.

First method: Perform a sedimentation-based study to determine the distribution of particle sizes, following the guidelines outlined in the NF P 94-057 standard. This process entails the utilization of a dispersion agent, specifically sodium hexametaphosphate, along with a mechanical agitator that operates at a speed of 1000 revolutions per minute.

Second method: Conduct the particle size distribution analysis without the use of a dispersion agent or an agitator.

The natural dispersibility tendency of the tested soil can be found by comparing the curves produced by these two approaches (Figure I-11).

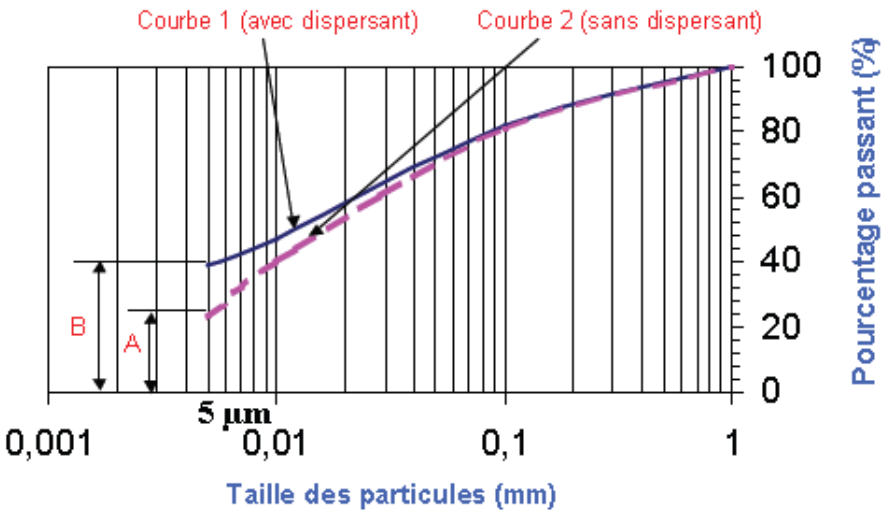

Figure I-11: Typical Double Hydrometer Test results (Haghighi 2012)

The test involves evaluating the dispersion rate (D), defined as the ratio between the percentage of fine particles smaller than 5 microns without dispersant and the percentage of fine particles smaller than 5 microns with dispersant, according to the following formula:

The dispersion rate (D), which is determined by dividing the percentage of fine particles less than 5 microns with dispersant by the percentage of fine particles less than 5 microns without dispersant, is what is measured during the test using the following formula:

$$D = \frac{A}{B} = \frac{\%<5\mu m\ without\ dispersant}{\%<5\mu m\ with\ dispersant} \times 100 \qquad [I.4]$$

If (D) approaches 100%, i.e., (A = B), the soil is totally dispersive; in other words, the clay naturally deflocculates in water. On the other hand, if (D) is nearly zero, the material is completely non-dispersive.

Three categories for soil classification were suggested by Sharad et al. (1976) based on (D):

- (D < 30\%): non-dispersive

- (30\% < D < 60%): probably dispersive

- (D > 60%): dispersive

Only 85% of the time can dispersive soils with (D > 30\%) be identified using the double hydrometer test, according to Decker and Dunnigan (1977).

I.6.3.2 Crumb test and modified Crumb test experimental protocol

As per ASTM D 6572-00, the "Crumb Test" is a standardized examination. This is a straightforward test, which is simple to execute and does not necessitate a substantial amount of resources. This test can be conducted either in the laboratory or right at the site of interest. Nevertheless, it depends entirely on the visual observations given by the operator, resulting in totally qualitative results (Figure I-12).

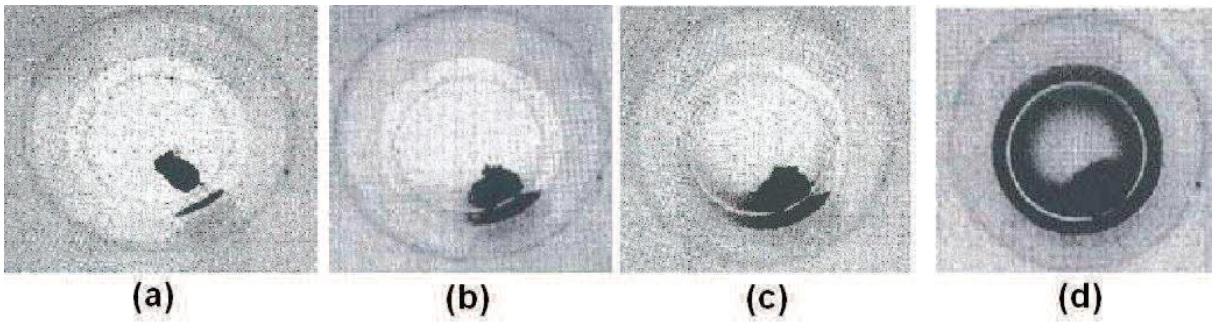

Figure I-12: Typical "Crumb test" tests, a) level 1: non-dispersive, b) level 2: intermediate, c) level 3: dispersive, d) level 4: highly dispersive (source ASTM D6572-00)

The "Crumb Test" involves preparing a small 15mm cubic sample in 250ml of distilled water, which is then placed in a container and classified into one of four dispersion levels based on the turbidity of the colloidal suspension as it is shown in Figure I-13.

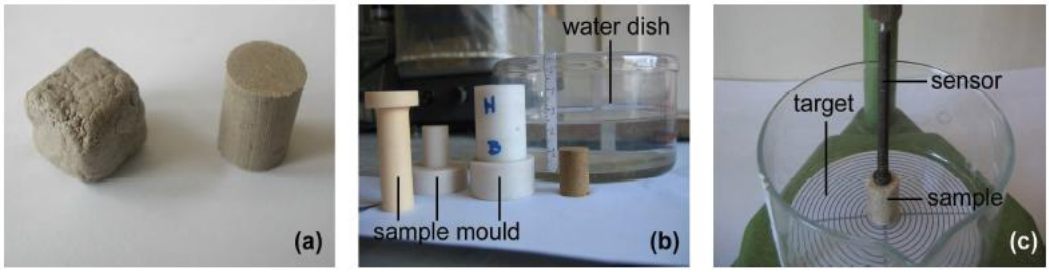

Figure I.13: New Crumb test (a) classic and new samples (b) compaction mold and water container (c) mechanical probe and graduated bottom (Pham et al. 2008)

Pham et al. (2008) faced difficulties related to the cubic form of the samples throughout his experimental study (Figure I-13(a)). In order to overcome this challenge, they proceeded with the test using cylindrical samples with same volume (measuring 20 mm in height and 15 mm in diameter), as depicted in Figure I-13(b).

Pham et al. (2008) developed a device to measure the swelling and flattening of a soil sample over time, equipped with a palpator and target. The palpator measures soil swelling, while the target assesses the sample's diameter at its base (Figure I-13)).

Haghighi (2012) and Elandaloussi (2019) employed two cameras on a more advanced apparatus (Figure I.14) to measure the degradations that were observed. The first camera is positioned above the sample to measure changes in diameter, and the second camera is positioned horizontally to monitor differences in the specimen's geometry.

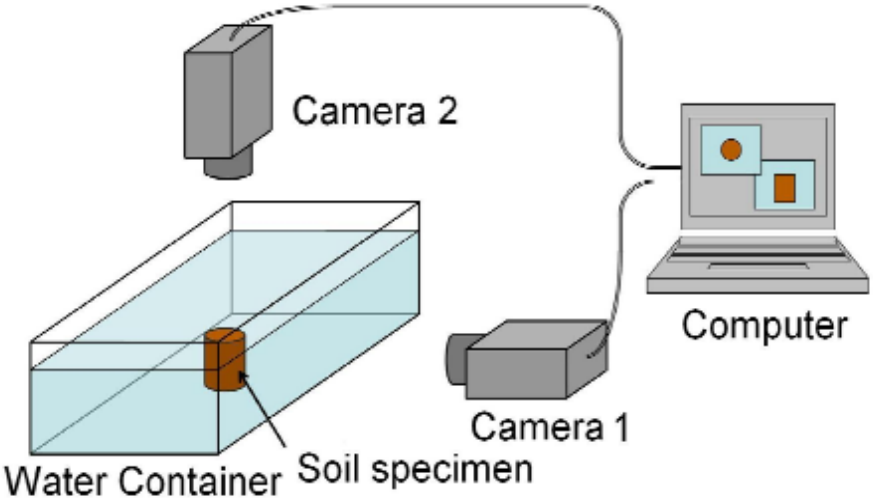

Figure I-14: General diagram of the improved Crumb test device by Haghighi (2012)

I.6.3.3 Sand Castle Test

The test aims to assess the collapse and filling capacity of filtering materials by submerging a soil sample in distilled water, and classifying it based on its collapse time.

Figure I-15: Experimental setup and procedure of the "Sand Castle Test" (Park 2003)

Using the following procedure, Park (2003) used this method to define various soil textures: Using a metal bar, the soil is compacted in a 261 ml plastic mold. The sample is then unmolded onto a grid and carefully submerged using two hooks in a container holding 3.75 Liters (1 gallon) of distilled water. The sample is captured on camera at intervals of 0.1, 2.4, 8.16, and 32.64 minutes to track the development of its collapse (Figure I-15).

For our study, we will focus only on some of these tests, specifically the Double Hydrometer Test, the Crumb Test, and the Sand Castle Test. These tests inspired the development of our own dispersion testing device.

I.7 Mineralogy and soil chemistry

Soils consist of particles of different sizes, with varying shapes, size distributions, and arrangements that vary between different soil types. Sand and gravel, which are the largest grains, are often made up of silica crystals that have three-dimensional structures with identical dimensions. On the other hand, tiny particles, which are commonly found in clayey soils, have a flat, two-dimensional shape, with a thickness that is far smaller than their other dimensions.

The disparity in composition leads to discernible variations in the behavior of fine soils and granular soils. Gravity has a minimal effect on the arrangement of particles in clayey soils, as the primary forces at play are electrical attraction and repulsion, which determine the volume occupied by a specific quantity of clay particles. This phenomenon can be attributed to the tendency of clay sheets to aggregate and form either flakes or agglomerates. The configurations of these change depending on the moisture content of the soil. (Haghighi 2012).

Clays are formed through the decomposition of siliceous rocks via physical and mechanical disintegration, followed by chemical alterations. All hydrated silicates belonging to the phyllosilicate group are considered part of the family of clay minerals. Clay minerals possess an ionic structure that results in strong bonds with polar water molecules. These minerals are enveloped by a layer of strongly bound water, which significantly impacts the overall behavior of the material. A clay particle is composed of a series of primary sheets that are made up of two fundamental structural units: the silica tetrahedron and the alumina octahedron (Craig 2004). The silica tetrahedron is composed of a silicon atom at its center, with four oxygen atoms evenly spaced around it. The tetrahedra form a hexagonal planar structure, with the oxygen atoms lying in the same plane and each oxygen atom being shared by two tetrahedra (Figure I-16a). One of the oxygen atoms possesses a free valence and can form a covalent bond with another sheet. The alumina (or magnesium) octahedron is composed of six hydroxyls (OH-) that surround one aluminum (or magnesium) atom, with each hydroxyl equidistant from the central atom. The octahedra combine with one another to create a flattened layer (Figure I-16b)

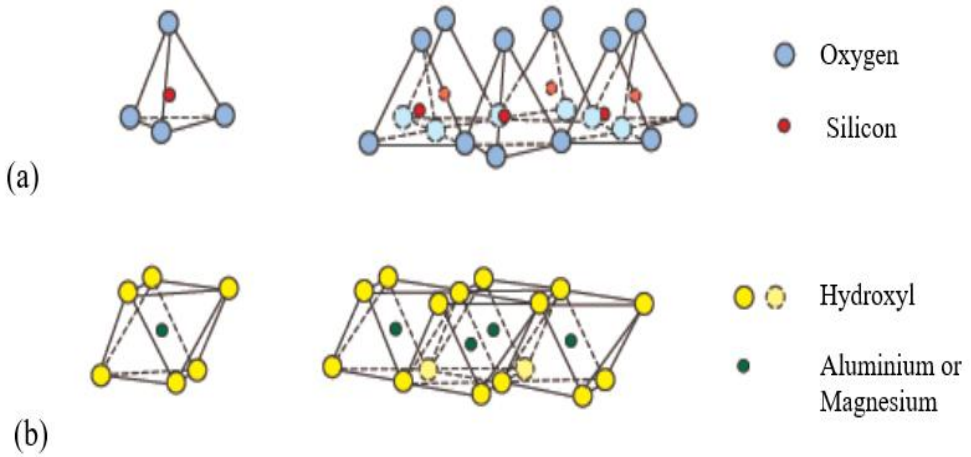

Figure I-16: Crystalline layers of clay (a) octahedral layer of silica (b) octahedral layer (Cuisinier 2002)

Clay sheets are then a combination of these basic units, with the ideal elementary sheet consisting of 2 or 3 units. Covalent and ionic bonds ensure rigidity, while less strong bonds form clay particles with varying numbers depending on the type of clay. These bonds are essential for the assembly of elementary sheets.

The forces that bind these layers together are mainly of three types:

- **Van der Waals forces**: Refer to weak molecular attraction forces but present between the layers.
- **Hydrogen bonds:** They are formed with strongly electronegative atoms, such as oxygen, and play a crucial role in the cohesion of the layers.
- **Isomorphic substitutions:** They consist of the substitution of certain cations of the crystal lattice by other cations of lower valence, creating a charge deficit. For example, a silicon ion (Si_4^+) can be replaced by an aluminum ion (Al_3^+) in the tetrahedral layer, or an aluminum ion (Al_3^+) by a magnesium ion (Mg_2^+) in the octahedral layer of alumina. This gives clay particles a negative charge, allowing them to adsorb cations and water molecules to reach electroneutrality.

The cation exchange capacity (CEC) is a crucial metric for understanding clays' ion exchange behavior, which is influenced by water content and isomorphic substitutions. The deposition environment, particularly the medium's salinity, significantly impacts the behavior of clay particles.

Figure I-17 shows the most common types of clays are:

- **Kaolinite:** It is comprised of elementary particles that consist of a layer of silica and a coating of alumina. Hydrogen bonds are responsible for holding the layers together. A single kaolinite particle typically consists of 100 to 150 layers, with each layer measuring approximately 0.1 μm in thickness and 1 μm in width.
- **Illite:** It possesses a structure characterized by the presence of an alumina layer sandwiched between two layers of silica. Potassium ions are used to balance the charge deficit in this structure, resulting in the formation of robust bonds between the layers. An average illite particle consists of around 10 layers, each measuring 10 nm in thickness and 0.3 μm in width.
- **Smectite (or montmorillonite):** This clay also consists of an alumina layer sandwiched between two layers of silica. However, what sets smectite apart is that the spaces between these layers contain water and cations, such as sodium (Na^+) or calcium ($Ca2^+$). The bonds between the layers are weak, which makes this clay highly sensitive to changes in water content. As a result, it has a high potential for swelling and shrinkage. The particles of montmorillonite can be extremely fine, sometimes consisting of a single elementary layer that is approximately 1 nm thick and 0.1 μm wide.

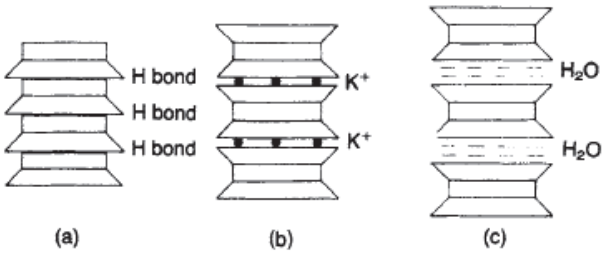

Figure I-17: Structures of clay sheets (a) kaolinite (b) illite (c) Montmorillonite (Craig 2004)

I.8 Soil treatment

Soil treatment with hydraulic binders is an effective and sustainable solution to combat soil erosion. By improving soil mechanical properties and increasing soil resistance to erosion, this technology protects infrastructure and the environment while optimizing construction costs. To maximize benefits, it is essential to understand soil characteristics and to adapt the selection and dosage of binders to the specific needs of the project.

Since treatment products are of a diverse nature, they can have different effects on the same material. We distinguish between traditional methods such as lime and cement treatments, these materials are derived from non-renewable raw materials, but they have been the subject of

significant developments, particularly in the field of earthworks. Less traditional methods use materials that are derived from the transformation of renewable raw materials, such as lignosulfonate.

I.8.1 Soil lime treatment

Since the middle of the last century, soil stabilization with lime has been a classic technique in earthworks. In the review of literature, Soil lime treatment is a widely recognized method for improving and stabilizing soil, especially in earthworks. It is particularly effective for enhancing the workability of silty and clayey materials, resulting in improved mechanical qualities when compacted (Herrier et al., 2012).

This treatment process is associated to soft soils, such as clayey soils (Al-Mukhtar et al. 2010; Lemaire et al. 2013; Tran et al 2014; Khemissa and Mahamedi 2014), silty soils (Cuisinier et al. 2011; Makki et al. 2015; Le Runigo et al. 2011), sandy soil (Consoli et al 2014).
In the last twenty years, lime treatment methods have made substantial progress as a result of economic and ecological considerations. Lime treatment has been employed for decades in the United States and Australia to enhance the quality of dikes, levees, and earthen dams (Howard et al. 1976; Perry 1977; ANCOLD 1978), so guaranteeing no borrowing or waste (Herrier et al. 2012).While the implementation this technique in hydraulic structures in France has been recently applied, with recent works by Haghighi(2012), Chevalier et al. (2015), Bennabi (2016), and Elandaloussi et al 2019 serving as examples. However, the use of lime-treated soils in hydraulic applications is poorer known and less documented in Algeria, no study has been carried out to understand the mechanisms of piping erosion in both cases untreated and treated soil.

Lime is generally a powdery, white material obtained by calcining limestone, industrially in a lime kiln. It has been used since antiquity, particularly in construction. Chemically, it is calcium oxide (CaO) containing varying amounts of magnesium oxide, but the term "lime" can refer to different chemical states of this product: quicklime, hydrated lime, and hydraulic lime. For this project, quicklime is used for soil treatment.

I.8.1.1 Interactions between lime and soil clay particles

I.8.1.1.1 Cationic exchange

An exothermic hydration reaction forms calcium hydroxide (Ca(OH)2) and releases thermal energy when lime (CaO) is added to a soil-water environment. As a result of this reaction, the interstitial water in the soil becomes rich in calcium ions (Ca2+) and hydroxide (OH^-) (Figure I-18).

$$CaO + H2O \rightarrow Ca(OH)2 + 15.5\ kJ/mol \qquad [I.5]$$

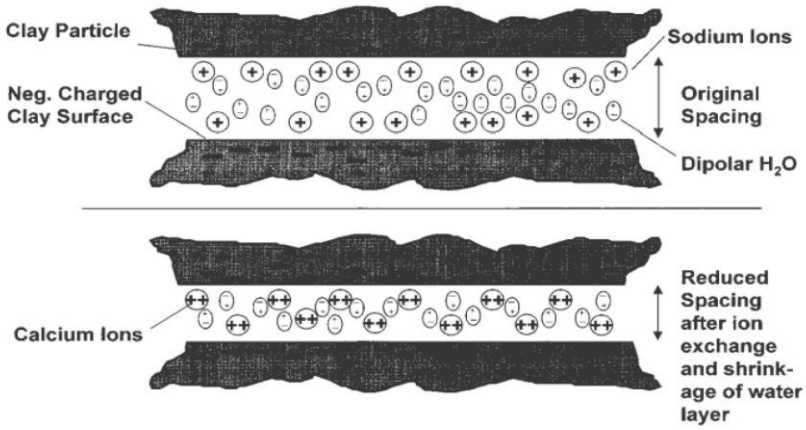

Figure I-18: Schematic of cation exchange in clay, (Prusinski and Bhattacharja 1999) cited by (Tran, V. D. 2013)

The primary interactions that take place are as follows:

1. *Hydration and Ionic Dissociation*: The hydration reaction produces high concentrations of Ca2+ and OH− ions in the interstitial water, initiating a series of chemical reactions depending on the soil composition, its mineralogy and the chemistry of the interstitial water.
2. *Cationic exchange*: Immediately after mixing, the dissolved calcium cations are absorbed and intercalated in the inter-folia space of the clay (TOT structure), replacing the existing cations. Divalent calcium cations replace monovalent cations and high concentration ions replace low concentration cations (Eades and Grim 1960; Choquette et al. 1987).
3. *Lyotrope Series*: Calcium replaces most of the cations available in the system by following the lyotrope series, which stipulates that cations of higher valence replace

those of lower valence, and that large cations replace smaller ones of the same valence (Little 1995).

I.8.1.1.2 Flocculation and agglomeration

Clay particle flocculation and agglomeration are direct consequences of the cationic exchange initiated by the addition of lime. This process changes the texture of the clay, transforming it from a fine-grain plastic material into a granular soil (Figure I-19). Here are the main steps and effects:

1. *Texture Modification:* Cationic exchange causes clay particles to flocculate and aggregate, changing their texture from plastic and fine to granular.
2. *Structure Change:* Flocculation alters the structure of clay particles, making them move from a horizontal and parallel orientation to a more random and edge-to-face orientation.

Flocculation is attributed to several factors:

- *High Electrolyte Content*: The presence of a large amount of ions in the solution promotes flocculation.
- *High pH:* The increase in pH, caused by the addition of lime, plays a crucial role in this process.
- *Double Layer Thickness Reduction*: Cation exchange reduces the thickness of the double electrochemical layer surrounding clay particles, facilitating their closeness and agglomeration.

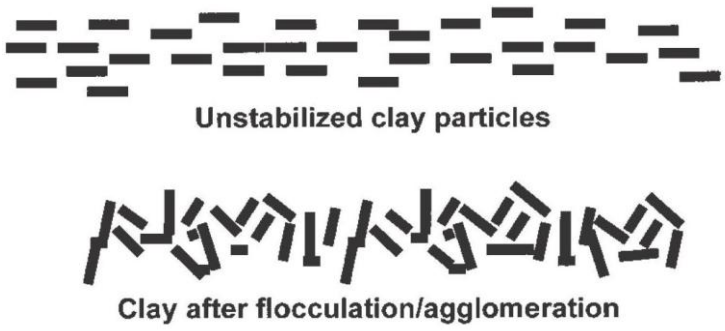

Figure I-19: Flocculation and agglomeration of lime-treated soil, (Prusinski and Bhattacharja 1999) cited by (Tran, V. D. 2013)

Agglomeration occurs when flocked clay particles begin to form weak bonds at the particle edge-surface interfaces. This is due to the deposition of cement-based materials on these interfaces. Here are the main steps and effects of this process:

When weak connections are formed between flocking clay particles at the particle edge-surface contacts, agglomeration takes place. The reason for this is because materials based on cement have been deposited on these surfaces. The primary actions and outcomes of this process are as follows:

1. *Formation of Weak Bonds:* The flocculated clay particles begin to bond weakly to each other due to cement deposits at their interfaces.
2. *Aggregate Formation:* Agglomeration leads to the formation of larger aggregates from the finely divided clay particles, which further improves the texture of the clay soil.
3. *Reduction of the Diffuse Double Layer:* Cation exchange reduces the thickness of the electrochemical double layer surrounding the clay particles, facilitating their convergence and agglomeration.
4. *Increased Internal Friction:* Flocculation and agglomeration increase internal friction between clay particles, which has several beneficial effects:

    - Reduced Plasticity: The soil becomes less plastic and an improved workability.
    - Increased Shear Strength: The soil gains strength, which is crucial for construction applications.
    - Improved texture: The soil becomes more granular and less sticky, making it easier to use.

Studies by Diamond et al. (1963); Hilt and Davidson (1960); and Boardman et al. (2001) confirm that these combined factors lead to effective flocculation and agglomeration, thus significantly altering the structure and texture of clay soil treated with limestone.

I.8.1.1.3 Pozzolanic reaction

The lime initiates complex reactions in the clay soil, including the pozzolanic reactions, which improve the texture and mechanical properties of the soil by forming cement-binding compounds. These processes, depending on time and pH conditions, gradually transform the soil structure (Figure I-20).

The tetrahedral and octahedral layers of clay leaves, particularly those at their edges, are subjected to a pozzolanic reaction with limestone once the calcium cations ((Ca^{2+}) have saturated the available sites in the soil. The interfolia-attached calcium cations are not a part of this process.

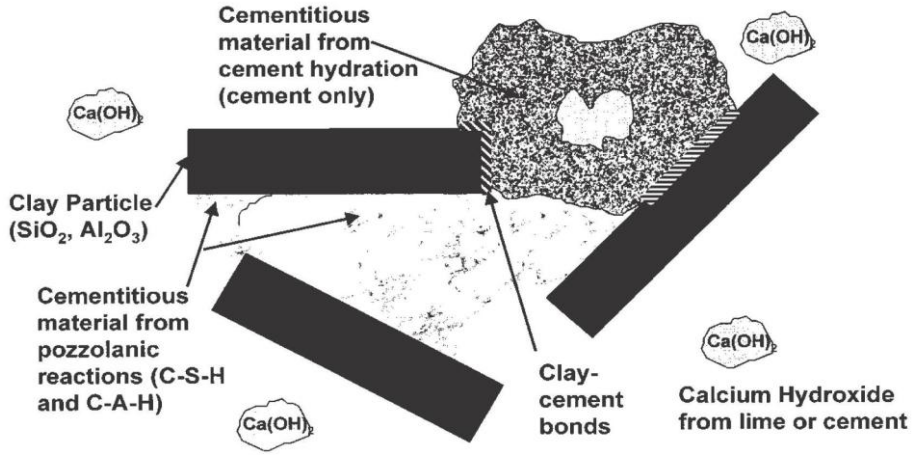

Figure I-20: Pozzolanic reaction (Prusinski and Bhattacharja 1999)

- Basic Environment and Reactivity

The basal medium with a high pH increases the solubility and reactivity of silica and alumina present in clay particles. Calcium ions are combined with dissolved silica and alumina to form additional cement compounds, such as calcium silicates hydrated (CSH) and calcium aluminates (CAH) (Rao and Rajasekaran 1996; Kavak and Akyarl 2007; Al-Mukhtar et al. 2010a)

$$SiO2 + (Al2O3, SiO2) + Ca(OH)2 + H2O \rightarrow CSH, CAH, CASH \qquad [I.6]$$

- Precipitation Mode: The high pH ined by the calcium hydroxide dissolves the edges of the silica particles. The reaction products then precipitate and form bonds between the particles of the soil (Diamond et al. 1963).
- Direct Reaction: Calcium hydroxide reacts directly with adjacent clay surfaces, forming pozzolanic products like precipitation.

Through consuming of the clay and the production of new minerals with binding properties, the reactions contribute to flocculation by binding the adjacent soil particles.

The pozzolanic reaction develops slowly over a period of months or years. A pH of 12.4 must be maintained for an extended amount of time to enhance reactivity since silicon and aluminum ions are highly soluble at this Ph.

I.8.1.1.4 Lime Carbonation and its Effects on Soil Stabilization

Although carbonation may provide slight initial soil reinforcement, it is not suitable for long term stabilization. The reaction between lime and air CO_2 forms calcite crystals that disrupt soil stabilization processes by inhibiting the essential pozzolanic reactions (Cabane 2004).
The carbonation of lime is the result of a reaction between lime (CaO) and carbon dioxide (CO2) in the air. This reaction can occur during the maturation of lime-treated soils,
according to the following chemical equation:

$$CO2+CaO \rightarrow CaCO3 \qquad [I.7]$$

Carbonation is more pronounced at high percentages of lime, as a greater amount of free lime is available for this reaction.

Adverse Effects include:
-Poor Binding Property: formed calcite crystals (CaCO3) have very weak binding properties, which disrupt soil stabilization.
- Inhibition of the Pozzolanic Reaction: The formation of calcite consumes part of the available lime, thereby reducing the amount of lime needed for the Pozzolanic reactions. This leads to a decrease in the final resistance of the soil.
- Short-term effect: Although calcite may initially strengthen the soil slightly, its effect is not sustainable in the long term.

I.8.2 Erosion tests on lime-treated soils

I.8.2.1 Lime treatment at the Kern Canal in the USA

The Kern Canal in California, built in the 1940s, is 240 km long and made of plastic clay soils (Ip>40). It has been subjected to frequent damage, requiring repairs and prevention measures, particularly in the 1970s. A 3.2 km long section was repaired by widening the trapezoidal section and coating it with a layer of lime-treated soil (Howard and Bara 1976). After 40 years, the lime-treated sections were significantly less affected compared to sections coated with concrete or rockfill. The project manager found that installation and maintenance costs for the section reinforced with lime-treated soil were significantly lower, making the lime treatment technique more economical and effective than other techniques (Haghighi 2012) cited by (Elandaloussi 2015).

I.8.2.2 Laboratory Testing Campaign by Haghighi (2012)

(Haghighi 2012) conducted a laboratory testing campaign utilizing three test methods: HET (Hole Erosion Test), Mojet, and ECT (Enhanced Crumb Test). Two soil types, silt and clay, were utilized for testing purposes. The soils were evaluated in their original, untreated state as well as after being treated with 2% and 5% lime, respectively. The testing conditions were carefully established and controlled. Comparisons were made after curing periods of 7 and 90 days post lime treatment.

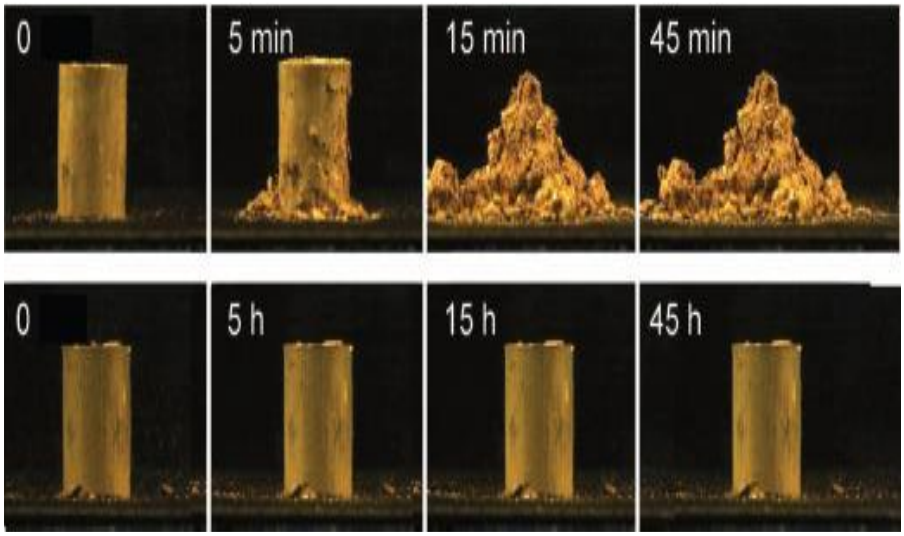

Figure I-21: ECT on Hericourt silt after 7 days of maturation; untreated (top), treated (bottom) according to Haghighi (2012)

According to Haghighi (2012), lime-treated soils were found to be significantly more resistant than untreated soils. In the HET test, erosion was likely to be initiated at a critical shear stress at least four times higher than that of the untreated state. In the Mojet test, the eroded mass at the surface was at least 300 times higher for untreated soils compared to treated soils. Finally, in the ECT test (Figure I-21), treated soils were found to be insensitive to erosion. This indicates a considerable increase in the hydraulic resistance of the treated materials.

Haghighi (2012) lime-treated soils were found to be significantly more resistant than untreated soils. During the HET test, erosion was likely to be initiated when the critical shear stress reached a level that was at least four times higher than the untreated state. The Mojet test revealed that the eroded mass at the surface was at least 300 times greater for untreated soils compared to treated soils. Ultimately, the ECT test revealed that the treated soils exhibited no

sign of sensitivity to erosion. This signifies a substantial augmentation in the hydraulic resistance of the processed substances.

I.8.2.3 Laboratory Testing Campaign by Elandaloussi (2015)

The study aimed to verify the relevance of using lime treatment on coarse soil for hydraulic structures, improving its resistance to internal erosion by suffusion. The soil had a wide granulometric range and a certain percentage of fines. A test device was developed and implemented to study the behavior of lime-treated soils and understand the mechanisms involved (Figure I-22). Tests were conducted on reconstituted soil from reference soils like Hostun sands and kaolinite.

Figure I-22: Preliminary column configuration for downflow and Suffusion column (Elandaloussi 2015)

A parametric study was conducted to understand the influence of different parameters such as lime dosage, curing time, height of the specimen, weight of the surcharge, and direction of flow. Results showed two distinct hydraulic behaviors: internal erosion in untreated soil with suffusion in the upward direction and hydraulic fracturing in treated soil, conditioned by lime dosage and curing time.

To interpret the results, a parallel study was conducted to evaluate the soil's mechanical behavior by evaluating its resistance to simple compression. Samples were immersed in an aquarium, simulating a dispersion test (Crumb test) before undergoing simple compression tests. The main results showed that lime treatment stabilizes the dispersion. However, the mechanical resistance measured after immersion is lower compared to the resistance before immersion, despite the trend of evolution according to the curing time remains maintained.

The synthesis of experimental results showed that while lime treatment stabilizes the soil with respect to suffusion, the mechanisms involved in improving mechanical properties do not entirely intervene in its stabilization with respect to internal erosion by suffusion. The development of cementitious products in the long term does not seem to contribute to the properties making the soil stable with respect to internal erosion by suffusion (Elandaloussi 2015).

I.8.3 Soil cement treatment

Cement treatment is more conventional one, widely used in earthworks stabilization several decades ago, it can be opted to improve the engineering properties of this particular soil vis-a-vis piping, to increase the strength, consequently reducing the environmental impact, the project's cost and delivery time furthermore ensuring a long service period.

In the review of literature, this treatment process is associated to soft soils, such as clayey soils (Ghadakpour et al. 2020; Croft 1967; Millogo and Morel 2012; Osula 1996; Khemissa and Mahamedi 2014; Bhattacharja and Bhatty 2003 (clay and sandy clay soil)), clayey silt soil (Jafer et al. 2015), silty soils (Al-Rawas et al. 2005; Eid et al. 2015; Jauberthie et al. 2010; Saussaye et al. 2012; Lemaire et al. 2013; Eskisar 2015), sandy soil (Consoli et al. 2007, 2010), sandy to clayey soils (Bellezza and Fratalocchi 2006), and other nature of materials like: marl (Melbouci 2017), sediment (Rekik et al. 2009), Sabkha soil (Al-Amoudi 2002), silty sand and clay as fine soils and gravelous sand and alterite as granular soil (Ranaivomanana and Razakamanantsoa 2018).

The application of soil-cement treatment in hydraulic earthworks is poorer known and less documented in literature, the only published work was by Nussbaum and Colley (1971). Especially works about internal erosion, Mehenni et al. (2016) carried out a research on silty soil.

Cement stabilization is quick, does not require mellowing time, and provides a non-leaching platform. It can be used for a large range of soils (Melbouci, 2017; Sariosseiri and Muhunthan, 2009). The best results of cement have been observed on silt as well as coarse grained materials Currin et al. (1976).

Portland cement is a finely ground material resulting from the inter-grinding of clinker and gypsum. The clinker, a hydraulic product, consists of four main oxide phases:

1. Tricalcium Silicate (C_3S)
2. Dicalcium Silicate (C_2S)
3. Tricalcium Aluminate (C_3A)
4. Tetracalcium Aluminoferrite (C_4AF)

A sequence of complex physico-chemical phenomena with extremely variable kinetics are induced by the interaction of a binder (lime or cement) with the fine particles of the soil. This results in an improved workability in the short-term, and an enhanced mechanical property of the soil in the long term such as compressive strength and bearing capacity. ((e.g., Al-Amoudi 2002; Sariosseiri and Muhunthan 2009; Eid et al. 2015). Moreover, (Catton 1940; Wooltorton, 1955 and Handy 1953) demonstrated that the formation of cementitious links between soil particles and hydration products resulted in a higher strength. Likewise, the effect of soil composition is also evident in the varying recorded strengths for stabilizing similar graded soils with equal proportion of cement. Pakbaz and Alipour (2012) reported that the soil showed a substantial increase in strength, even for very low cement content, and that the rigidity of the soil samples was dependent on the curing time and water content of the soil.

The stabilization process involves hydration reactions where C_3S and C_2S, play crucial roles and react with water to form calcium silicate hydrate (CSH) and calcium hydroxide ($Ca(OH)_2$):

1. Hydration of Tricalcium Silicate (C_3S):

$$2C3S + 6H \rightarrow CSH + 3Ca(OH)2 \qquad [I.8]$$

This reaction is vital for early strength development.

2. Hydration of Dicalcium Silicate (C_2S):

$$2C2S+4H \rightarrow CSH + Ca(OH)2 \qquad [I.9]$$

This reaction contributes to strength over a longer period.

These compounds significantly enhance the soil's mechanical properties, making cement treatment a widely used method in geotechnical engineering for improving the stability and strength of clayey soils.

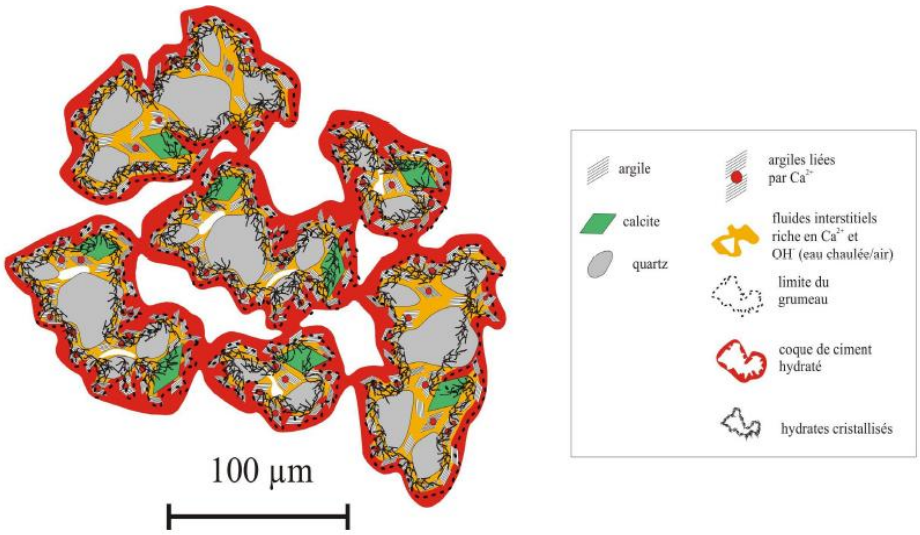

Figure I-23: Schematic representation of silt treated after 90 days of curing, (Cabane, 2004) cited by (Tran, V. D 2013)

Therefore, primary and secondary cementitious materials are produced in the soil-cement matrix when cement is mixed into moist clay soil (Chew et al. 2004). The primary cementitious materials are formed by the hydration reaction, and consist of hydrated calcium silicates (C_2SH_x, $C_3S_2H_x$), calcium aluminates (C_3AH_x, C_4AH_x) which provide strength and structure to the soil matrix, and hydrated lime $Ca(OH)_2$,which provides available calcium for cation exchange resulting in flocculation and agglomeration. This is therefore the particular difference in terms of mechanism compared to lime treatment of soils. A secondary pozzolanic reaction between hydrated lime and silica and alumina contained in clay minerals leads to the formation of other hydrated calcium silicates and hydrated calcium aluminates as in the case of lime (Tran, V. D. 2013).

Like lime, cement, after mixing with soil, reduces swelling/shrinkage which causes reduction in plasticity of the swelling soil, improves workability, increases strength.

I.8.3.1 Erosion tests on cement-treated soils

I.8.3.1.1 Indraratna et al (2008)

The study was conducted by Indraratna et al (2008). To assess the effectiveness of cement and ammonium lignosulfonate in stabilizing erodible silty sand from Wombeyan Caves, NSW, Australia. Four dosages of cement (0.5%, 1%, 1.5% and were tested. Samples were compacted to 90% and 95% of their maximum dry density to study the effect of compaction on erodibility. Internal Erosion Apparatus (IEA) designed to simulate internal crack erosion (Figure I-24). Samples were prepared, cured for seven days, saturated, and subjected to erosion tests.

Continuous monitoring of erosion rate was achieved using an inline process turbidity meter and a data acquisition system.

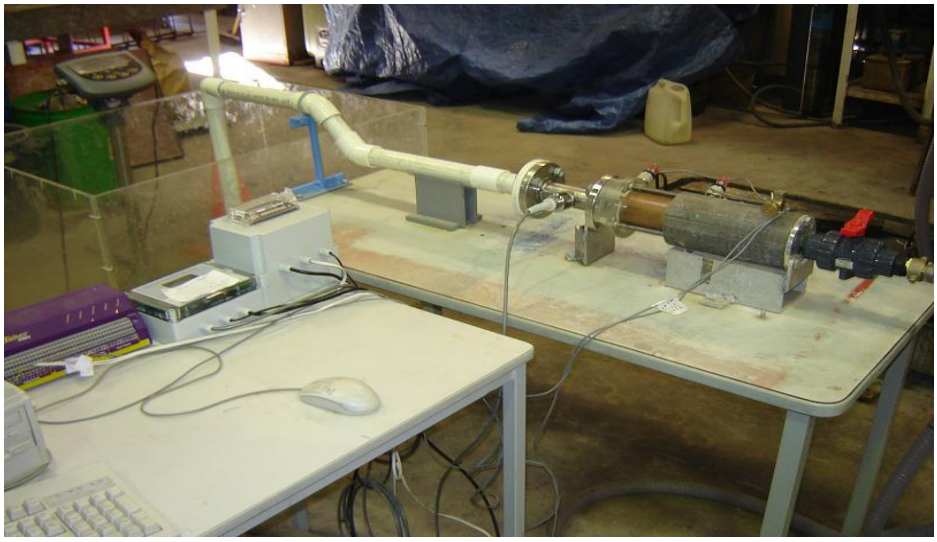

Figure I-24: Photograph of the Internal Erosion Apparatus (IEA)

Cement increased resistance to erosion. Critical shear stress increased linearly with the amount of stabilizer. Coefficient of soil erosion decreased as a power function of critical shear stress. A key observation was that Higher levels of chemical additives resulted in better performance in terms of reducing erosion rate and increasing critical shear stress. The study found that chemical additives helped in binding soil particles more effectively, which increased soil cohesion and erosion resistance. Compaction level and chemical dosage had significant effects on erosion resistance.

I.8.3.1.2 Mehenni et al (2016)

Conducted by Mehenni et al (2016) and focuses on the effects of different soil treatments on the internal erosion resistance of compacted silt.

The primary aim is to investigate how treatments with clay, cement, and lime affect the internal erosion characteristics of compacted silt. Internal erosion was measured using the hole erosion test (HET). A new enhanced HET device was developed, capable of applying high inlet pressure (up to 650 kPa) and generating hydraulic shear stress (up to 10,000 Pa) (Figure I-25).

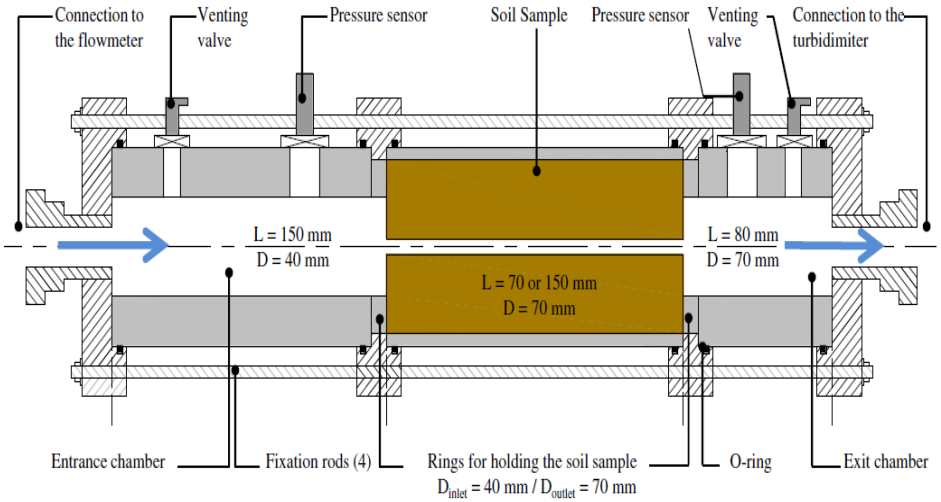

Figure I-25: Schematic of the enhanced HET testing cell (Mehenni et al 2016)

The study quantified the internal erosion resistance using the coefficient of soil erosion and critical shear stress. The findings showed that cement treatment is effective in improving the internal erosion resistance of compacted silt, with cement showing a stronger impact in comparison with other lime and clay. With an increased the critical shear stress, with the effect being proportional to the amount of cement added. Curing time had a notable impact on the erosion characteristics of cement-treated soil, enhancing the resistance over time.

I.8.4 Cement and lime treatment's impact on the permeability of soil

It is crucial to assess the effects of lime or cement treatment on the soil's hydraulic conductivity in addition to the mechanical enhancement for earthen structures that are in regular contact with water, such as dikes, canals, reservoir bottoms, and river levees.

There is limited qualitative and quantitative evidence available about the impact of lime treatment on hydraulic conductivity. The prevailing notion is that soil treatment improves the hydraulic conductivity of lime-treated soil as compared to untreated soil. Some scientists discovered these results when researching a variety of soil types, ranging from very expansive clays to low plasticity silts (e.g., Ranganatham, 1961; Brandl, 1981; Nalbantoglu and Tuncer 2001).

Lime treatment creates a new small pore class and alters the overall pore size distribution, resulting in a more complex structure with varying impacts on hydraulic conductivity depending on compaction conditions. El-Rawi and Awad (1981) found that if the water content is below or equal to the optimum water content, the hydraulic conductivity of lime-treated silt

is almost one order of magnitude higher than untreated soil. However, on the wet side of the optimum, the hydraulic conductivity of lime-treated soil is of the same order of magnitude as untreated soil. McCallister (1990) also found that even if lime treatment is associated with a decrease of the optimum dry density under a given compaction energy, the hydraulic conductivity of a soil would not be systematically increased by the lime treatment. James (1976) demonstrated that variations of several orders of magnitude in hydraulic conductivity between samples compacted at the same dry density but with different initial water contents and compaction energy are related to the soil's microstructure, i.e., its pore size distribution (e.g. Garcia-Bengochea et al., 1979; Delage et al.,1996).

Cement deep soil mixing is widely employed in construction and has markedly reduced soil permeability. Mousavi and Wong (2016) demonstrated that the permeability of cement-stabilized clay decreases when the cement content rises from 8% to 18%.

The influence of cement on hydraulic conductivity has been analyzed in relation to variables such as cement content, curing duration, and curing conditions (e.g., Brandl, 1992; Bellezza, 1996; Bellezza and Pasqualini, 1997), but the impact of soil properties is still insufficiently clarified. The addition of cement to sandy soils often reduces their hydraulic conductivity; nevertheless, the precise soil parameters affecting the hydraulic characteristics of sandy soil-cement mixtures are still insufficiently defined. In contrast, conflicting results have arisen concerning fine-grained soil-cement mixtures, suggesting that soil permeability may either increase or decrease (Adaska, 1985; Pasqualini et al., 2002). This conduct necessitates particular focus when hydraulic performance is a primary design objective. The addition of cement is expected to increase the short-term permeability of clays by modifying the surface chemistry of clay particles via cation exchange and subsequent flocculation (Mitchell, 1992; Chew et al., 2004).

I.9 Conclusion

Erosion is the primary cause of collapse in earth structures, including dikes, dams, and foundations. This phenomenon, affected by numerous causes, compromises the stability and durability of our infrastructures. Nevertheless, the physical and mechanical properties conventionally employed to define soils do not allow the prediction of their susceptibility to erosion. Consequently, it is imperative to establish testing methodologies to evaluate their

resistance to this process, so facilitating the construction of more resilient buildings and mitigating the risks linked to breakdowns.

Following a comprehensive evaluation of erosion assessment methodologies, we opted for HET and dispersion experiments to define soil deemed inappropriate for dike structure. A specialized experimental apparatus was developed to assess the erosion sensitivity of this soil, both in its natural condition and following the application of a treatment intended to enhance its characteristics.

II CHAPTER 2. EXPERIMENTAL PROTOCOLS

II.1 Introduction

This chapter provides a comprehensive description of the experimental devices that were created and utilized throughout this thesis. The soil that will be the focus of the investigation is next introduced, and lastly, we will provide a detailed explanation of the experimental technique established for this research.

II.2 Experimental device for Hole Erosion Test (HET)

The Hole Erosion Test (HET) is an experimental procedure used to evaluate the erodibility of soils, particularly cohesive soils like clay. The test involves creating a small, pre-formed hole or tunnel through a soil specimen and then allowing water to flow through it under controlled hydraulic conditions. As the water flows, it exerts shear stress on the soil, leading to erosion of the soil along the hole (Chevalier et al 2010). By measuring the rate of erosion and the corresponding hydraulic conditions, researchers can determine critical parameters such as the critical shear stress for erosion and the soil's erosion rate. This test is commonly used in geotechnical engineering to assess the vulnerability of soils to internal erosion, which is a significant concern for the stability of earth structures like dams and levees.

II.2.1 Apparatus and test principle

A hole Erosion apparatus inspired from the one developed by Wan et Fell (2002, 2004) was developed to carry out laboratory tests, and can be considered an efficient tool to assess piping erosion initiation and to characterize the internal erosion of soils (Herrier and Bonelli 2014).

The test device is schematically shown in Figure II-1. The whole system consists of the following elements:

- The erosion cell containing the soil sample
- The eroded particle collection tank
- A tank with constant hydraulic head, with overflow recovery
- A water supply tank
- A hydraulic pump and a suppressor

The different elements of device are connected using sections set of tubes fitted with quick couplings and valves.

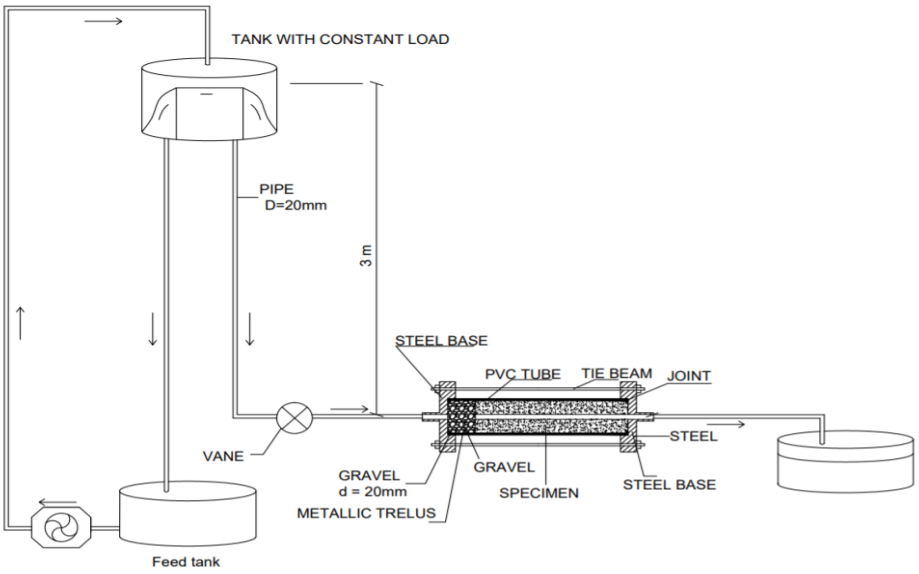

Figure II-1: General schema of the developed HET device

II.2.1.1 The erosion cell

Figure 2: The erosion cell

As it is illustrated in Figure II-2 and Figure II-3. The erosion cell consists of three parts, the first one is an upstream base with an inlet diameter of 30 mm, which ensure a constant inflow for each hydraulic load. The central (second) part is a PVC cylinder of 100 mm in diameter and 250 mm in length, 50 mm of it is reserved to receive gravels which the role is to make the

inflow homogeneous, and 200 mm for the specimen with a preformed hole; Separated by means of a metal grid of 1 mm from the gravels. Downstream there is another base, and it has an outlet with a 30 mm diameter.

Figure II-3: The erosion cell parts

II.2.1.2 Eroded particle collection system

After being relocated to the outlet and dropped into a tank the eroded particles are recovered by decantation (Figure II-4) and dried in an oven and finally weighed.

Figure II-4: Eroded particle collection

II.2.1.3 Hydraulic loading system

Water circulation in the test equipment is based on the employment of a supply tank, a pump, a constant water level tank and a ruler

II.2.1.3.1 Constant load feed tank

The constant level tank is suspended on a sliding vertical system and has a ruler installed so that the position may be determined instantly.

The feed tank, which has a capacity of 500 liters, is gets its supply from two sources: the drinking water network and the overflow from the constant water level tank.

Figure II-5 depicts a comprehensive schematic of the hydraulic loading mechanism, emphasizing the interconnections among its many components. Figure II-6 shows an overall view of the loading apparatus.

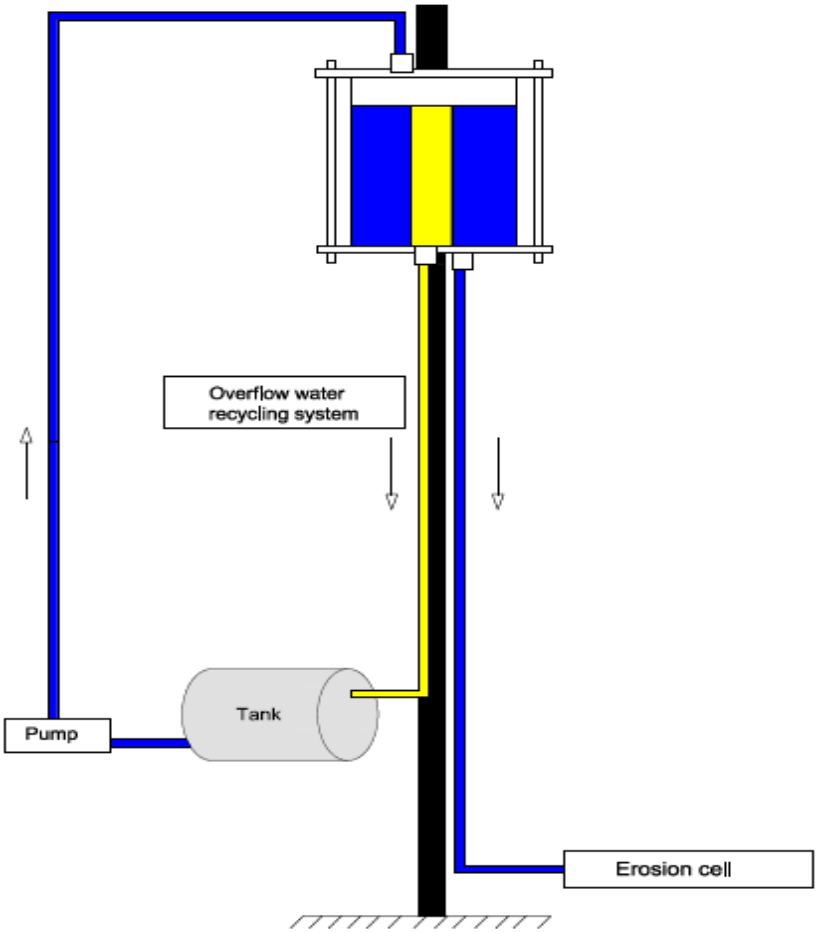

Figure II-5: a comprehensive schematic of the hydraulic loading mechanism

Figure II-6: An overall view of the loading apparatus

II.2.1.3.2 Pump

The pump is an essential part of the device since it is responsible for generating and sustaining a continuous flow of water. The pump in question is a Pentax PM/BR pump. It is utilized to provide a consistent load to the tank.

II.2.2 Flow rate measurement

The measurement of the flow rate is as follows: The graduated container is positioned beneath the outlet. Initiate the timer once the flow commences. When the predetermined amount has passed, stop the timer (Figure II-7). Repeat the same procedure for the second and the third trial under the same conditions. calculate the flow rate for each trial using the formula and the average is taken:

$$Q = \frac{V}{t} \qquad \text{(II.1)}$$

Where:

- V = Volume of liquid collected (liters)
- t = Time taken (s)

Figure II-7: Flow rate measurement

II.2.3 Inflow Calibration Procedure

The calibration of water flow at the entrance of the erosion cell is demonstrated in Figure II-8, following the previously described technique.

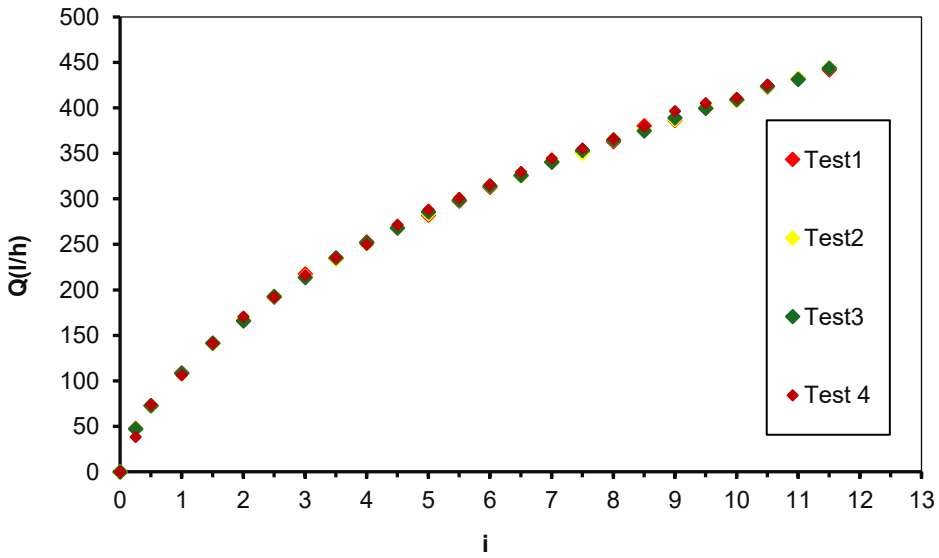

Figure II-8: Inflow curve

The four tests demonstrate a similar trend of increasing flow rate with the hydraulic gradient "i".

All four tests demonstrate a clear linear or slightly curved increase in flow rate as the value of the hydraulic gradient "i" increases.

II.3 Dispersion test (modified Crumb test)

The principle of this test is based on that called Crumb Test described in standard (ASTM D 6572-13). However, it is adjusted to fit the specimen dimension. The specimens reserved for this test were prepared with the same method as that of the erosion (HET) test. The specimens were deposited on a metal support allowing the contact of water below the specimen and then emerged in a glass tank. The test consists of immersing a specimen of known density and dimensions in a tank of water and following its morphological evolution over time and assessing its dispersion in water as it is illustrated in Figure II.9. (Belmana et al 2024).

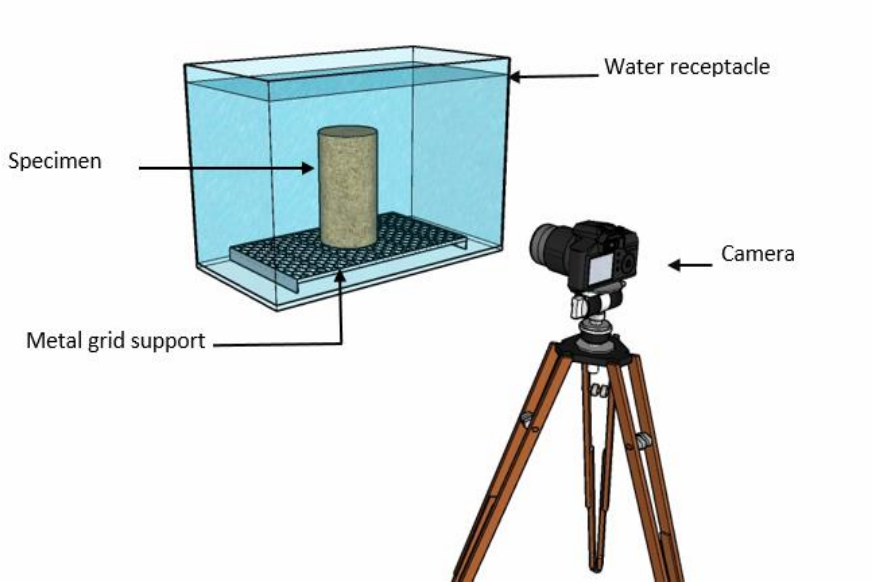

Figure II-9: Sketch of crumb test device (Belmana et al 2024)

The whole device comprises:

- A PVC mold measuring 100*200 mm, which is used for producing the compaction.
- A glass tank with dimensions of 500×500×500 mm.
- A metallic grid.
- A camera used for capturing and recording visual images.

The tank utilized is a 500*500*500 mm glass tank with a practical capacity of 125L. The glass has a thickness of 0.5 mm (Figure II-10).

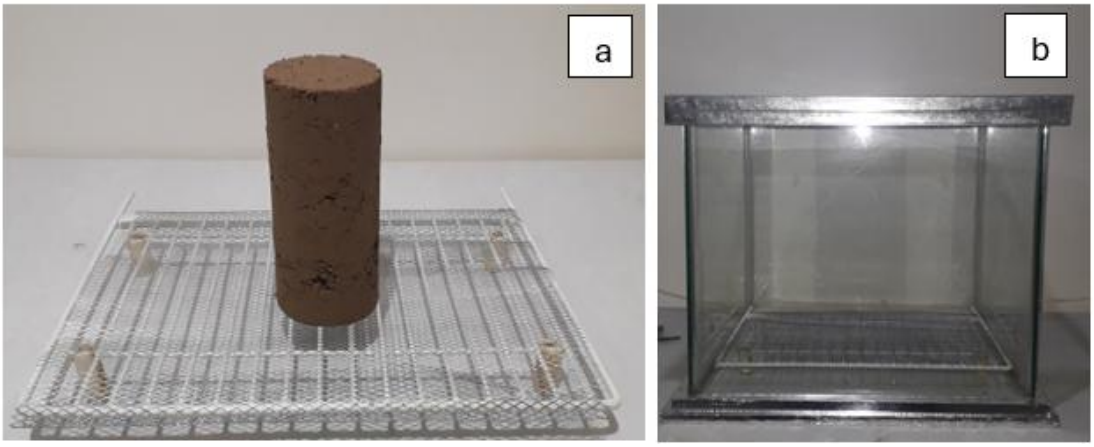

Figure II-10: Crumb test device;(a) metallic grid with specimen; (b) glass tank.

II.4 Triaxial tests

Triaxial tests are a fundamental type of soil mechanics test used to assess the mechanical properties of soils under various loading conditions. These tests are crucial in geotechnical engineering for evaluating the strength, stiffness, and stability of soils, particularly in the design and analysis of foundations, embankments, and earth-retaining structures.

Triaxial tests were performed according to AFNOR (1994) NF 94-074 on specimens of 70 mm in diameter and 140 mm in and compacted to same dry density as specimens prepared for HET tests. To study the influence of lime / cement treatment on the mechanical behavior of the soil after compaction, Consolidated Undrained (CU) tests were carried out on untreated and treated specimens in order to evaluate the shear strength evolution of the soil before and after treatment as well as after curing time of 1,7,28 and 90 days.

The used device is a GDS Triaxial Automated System (GDSTAS), it is a load frame-based triaxial testing system. The system is configured by choosing from a range of load frames, triaxial cells, pressure controllers and software (Figure II-11).

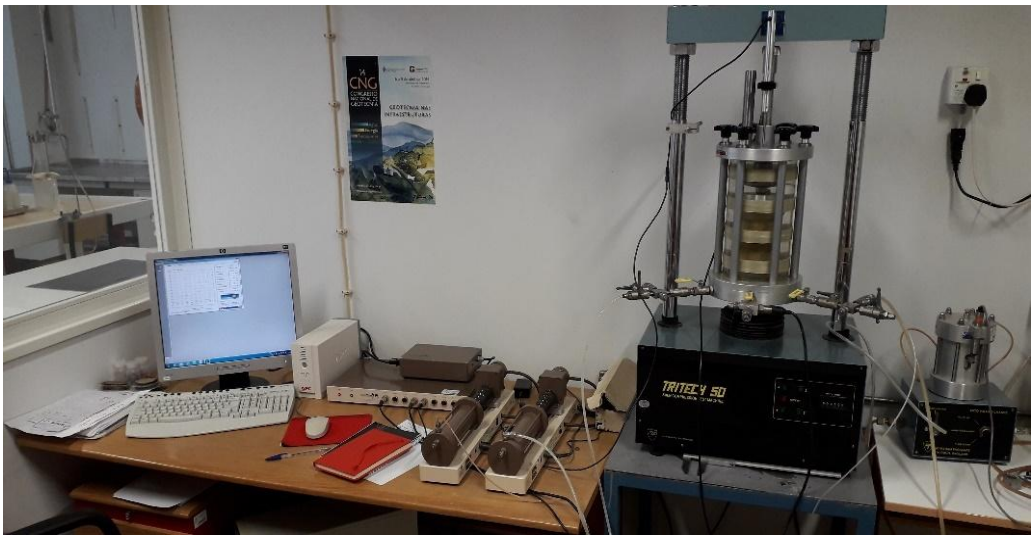

Figure II-11: The GDS Triaxial Automated System (GDS TAS)

II.4.1 Components of a Triaxial Test

To perform a triaxial test the system must contain a number of components to enable the desired specimen stress state to be reached and shear the specimen whilst recording the soil response. Table 1 lists each primary component of a GDS triaxial system, along with its main function. A complete system diagram is presented in Figure II-12

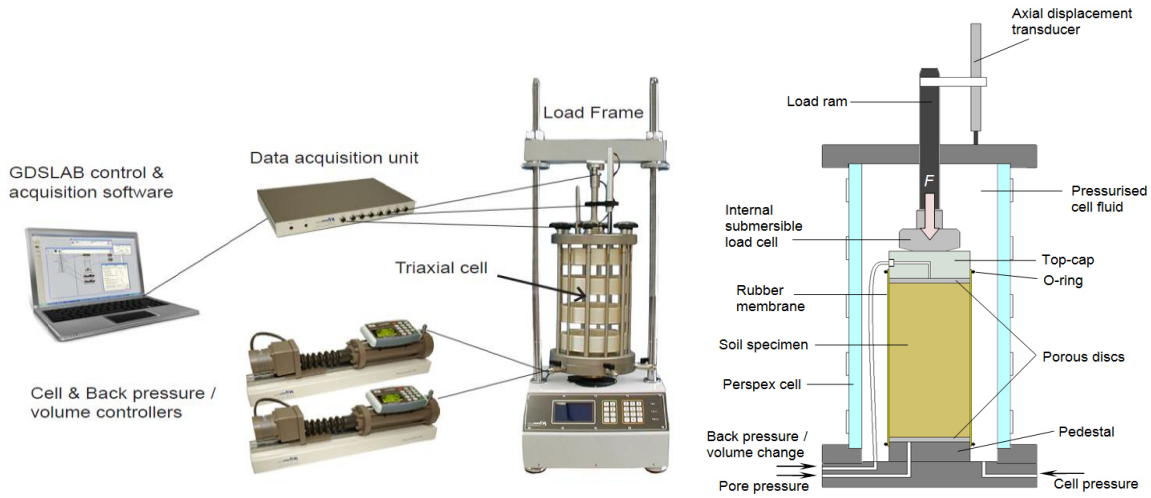

Figure II-12: Components of a GDS triaxial automated system

Table II-1: Primary components of a GDS triaxial automated system

Component	**Main function**
Triaxial cell	House the specimen and cell fluid
Pedestal & top-cap	Provide specimen seating and drainage ports
Rubber membrane, O-rings & porous discs	Seal the specimen from the cell fluid, allowing control over the effective stress and drainage
Cell pressure / volume controller	Apply confining stress to the specimen ($\sigma c = \sigma 3$) by pressurising the cell fluid
Back pressure / volume controller	Apply back / pore pressure u to the specimen and measure volume change ΔV
Velocity–controlled load frame	Shear the specimen through axial movement of a loading platen at a constant rate
Internal submersible load cell	Measure the change in axial load F applied to the specimen during shear
Pore water pressure (PWP) transducer	Measure the change in pore water pressure u within the specimen
Axial displacement transducer	Measure the change in height (and hence axial strain εa) of the specimen
Data acquisition unit	Convert analogue readings from the load cell, PWP and axial displacement transducers to digital data
GDSLab control & acquisition software	Control test hardware and record digital readings taken from the data acquisition unit

II.4.2 Type of Triaxial Test

In this study as it is mentioned previously a Consolidated-Undrained (CU) Test is performed; The soil is allowed to consolidate under the confining pressure before loading, but no drainage is allowed during the shearing phase. This test provides valuable information on pore pressure development.

The consolidated undrained (CU) test is the most common triaxial procedure, as it allows strength parameters to be determined based on the effective stresses (i.e. ϕ' and c') whilst

permitting a faster rate of shearing compared with the CD test. This is achieved by recording the excess pore pressure change within the specimen as shearing takes place.

II.4.3 Key Parameters Measured

The key parameters measured are the following:

- **Shear Strength:** The maximum stress the soil can withstand before failure.
- **Deformation Characteristics:** How the soil deforms under loading, which is essential for understanding settlement behavior.
- **Stress-Strain Relationship:** The relationship between the applied stress and the resulting strain, which helps in assessing the soil's stiffness.

II.5 Microstructure characterizations and analyses

Several techniques were used to analyze the microstructure of the soil before and after treatment in order to give an explanation for the improvements in geotechnical qualities that result from lime/cement interactions.

II.5.1 SEM

Scanning electron microscope (SEM) observations at the micro level are performed on both untreated and treated samples after 28 days of curing time, using HITACHI S-3400N (Figure II-13).

Figure II-13: Scanning electron microscope device

II.5.2 TGA

Thermo-Gravimetric Analysis (TGA) is a technique that involves measuring changes in weight as temperature increases. The fine soil elements were characterized using the (*TA Instruments Q50, nitrogen*), to assess changes in physico-chemical properties at high temperatures as a function of increasing temperature, both before and after treatment (Coats 1963). Thermogravimetric analysis (TGA) was conducted on samples weighing 8±0.5mg. The samples were heated at a rate of 20 °C/min, starting from the ambient temperature and reaching a maximum temperature of 1000 °C (Figure II-14).

Figure II-14: Thermogravimetric analysis (TGA) device

II.5.3 MIP

The Mercury Intrusion Porosimetry (MIP) technique was adopted to analyze the fabric and porosity of the soil samples using the *Micromeritics AutoPore IV 9500 apparatus* (Figure II-15). This technique enables the determination of a wide range of pore sizes, ranging from a few nanometers to several tens of micrometers, and allows for the identification of different types of soil pores. The principle behind this technique is the intrusion of mercury into a porous structure under carefully controlled pressures, following the capillary law that governs the penetration of liquid into small pores. In the case of a non-wetting liquid like mercury, this law is expressed by the Washburn equation (Eq. 1).

$$P = \frac{-4\gamma cos\,\theta}{D} \qquad \text{(II.2)}$$

Where P is the applied pressure, D is the apparent pore diameter, γ is the surface tension of the mercury, and θ is the contact angle between the mercury and the sample.

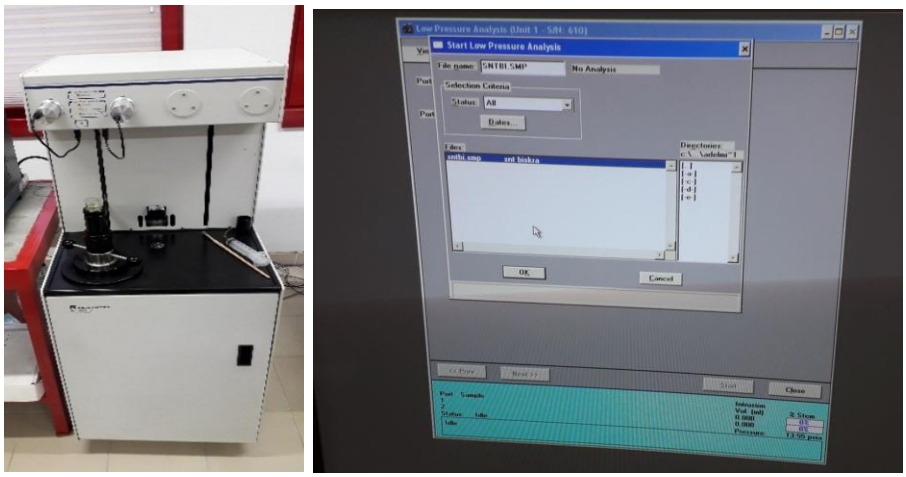

Figure II-15: Mercury Intrusion Porosimetry (MIP) device

II.5.4 Hydraulic conductivity (Permeability)

Hydraulic conductivity is measured for all three soil types: untreated, cement-stabilized, and lime-stabilized. The test process employed was the falling-head method as outlined by Bowles (1973) and the ASTM D2434 standard.

The equipment required for this type of test is illustrated in Figure II-16:

- Permeability apparatus
- Timer
- Thermometer
- Burette
- Ring stand with burette clamp for establishing a differential head throughout the soil sample

Figure II-16: Hydraulic conductivity testing device

The permeability coefficient will be determined from the linear segment of the curve using equation (II.3):

$$k_T = \frac{a \times l}{A \times t} \times ln \frac{h1}{h2} \qquad \text{(II.3)}$$

Where:

a is the cross-sectional area of the piezometric tube (m^2)

l is the specimen height during the test (m)

A is the cross-sectional area of the specimen (m^2)

t is the interval between measurements (s)

h_1 is piezometric head at the start of the selected interval (m) (see note)

h_2 is the piezometric head at the end of the selected interval (m) (see note)

Note that h_1 and h_2 are measured with reference to the outlet head.

$$k_{20} = k_T\left(\eta_T / \eta_{20}\right) \qquad \text{(II.4)}$$

Where (η_T/ η_{20}) is the viscosity correction.

II.6 Materials and methods

II.6.1 The soil

The soil was obtained from the vicinity of the 'Fontaines des Gazelles' dam in the Biskra region (Figure II-17).

Figure II-17: Origin of the studied soil

The granulometric analyses reveal that the grain size distribution curve is primarily composed of 10% clay, 23.09% silt, 56.91% sand, and 10% gravel (Figure II-18). The uniformity factor is 187, and the curvature factor is 6.9. According to the French standard AFNOR NF P1992, 11-300, it is classed as B5, which means it is a is very silty medium gravel.

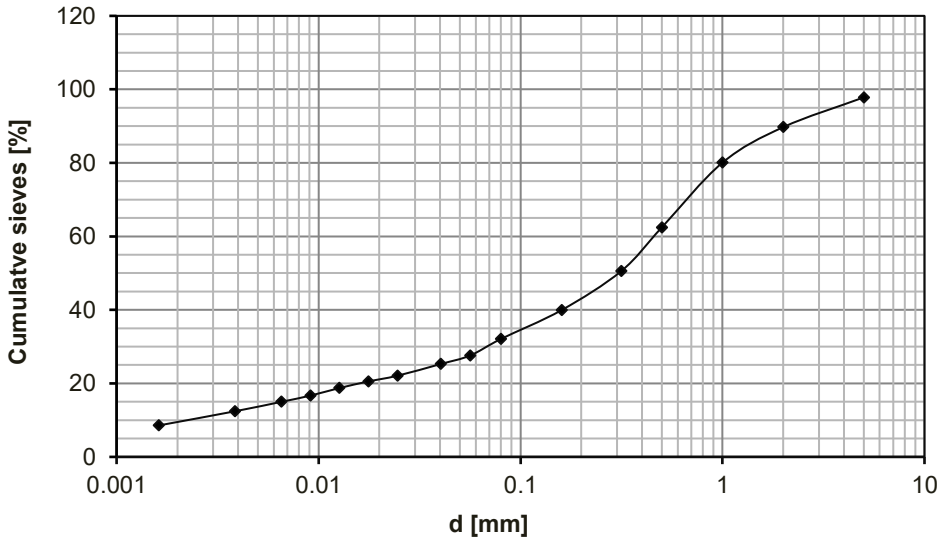

Figure II-18: Particle size distribution of the soil

Atterberg limits of the soil are found to be as follows: liquidity limit W_L = 31 (Figure-19), plasticity limit W_P = 15 and a plasticity index (I_P = 16).

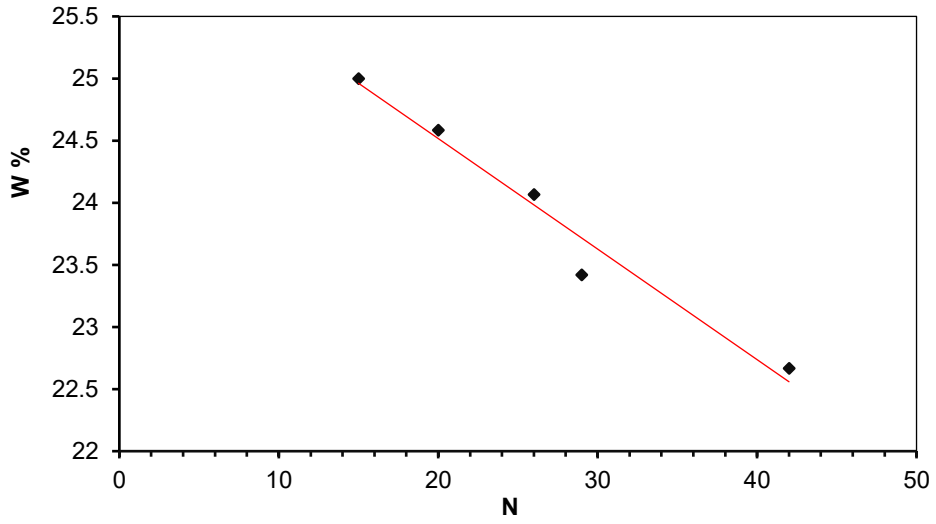

Figure 19: Liquid limit curve

According to French classification AFNOR XP P 94-011 is classed as as having low plasticity and being consistent (I_c =0,69). The clayey fraction of the soil is characterized by its significant activity (A_{CB} N 1.25; presence of calcic montmorillonite) (Figure II-20).

Figure II-20: The studied soil

Furthermore, mineralogical investigations are conducted using X-ray diffraction (DRX) and Energy-dispersive X-ray spectroscopy (EDX) in addition to the granulometric analyses. The DRX analyses permitted the identification of the essential crystalline phases contained in the materials, it indicates that the primary crystalline minerals present are quartz (Q) and calcite (Cl) (Figure II-20). The results showed that the predominant elements present are silica (SiO_2), calcium oxide (CaO) and alumina (Al_2O_3). On top of that SEM observations are presented in figure -22.

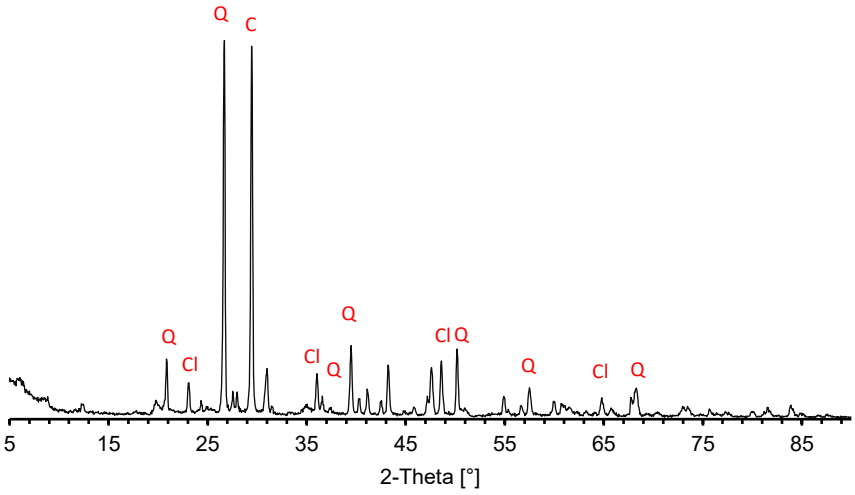

Figure II-21: Soil's X-ray diffraction analysis

While the utilization of EDX analyses allowed the quantification of the various oxidized chemical components present in the soil (Table II-2), which lists the geotechnical characteristics of the soil as well.

Table II-2: Geotechnical and chemical properties of the soil

Physical properties		**Physical properties**	
%80 µm	33.09	Na_2O	0.77
%<4 µm	12.5	MgO	3.38
% <2 µm	10	Al_2O_3	12.43
D_{10} [µm]	2	SiO_2	36.15
D_{30} [µm]	70	K2O	2.05
D_{60} [mm]	0.45	CaO	37.06
C_u	187	TiO_2	0.73
C_c	6.9	$Fe2O_3$	6.54
M_{BV}	0.5	SO_3	0.60
I_P	16	/	
A_{CB}	1.6	/	
ρ [t/m3]	2.66	/	

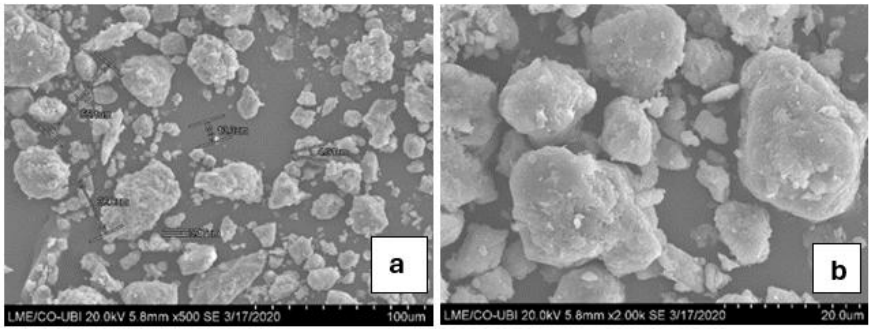

Figure II-22: SEM Aspects of the fine fraction of soil: (a) magnification x500. (b) magnification x2000

II.6.2 Lime

The lime utilized for the treatment was a quicklime supplied by BMSD Company in the wilaya of Saïda. Its characteristics are given in Table II-3.

Table II-3: Chemical composition of lime used by Energy-dispersive X-ray spectroscopy (EDX).

Table II-3: Physical and chemical analyses of lime

Lime			
Physical properties		***Chemical composition***	
Specific gravity	3,24	Na_2O	0.36
		MgO	-
Maximum dry density (t/ m^3)	--	Al_2O_3	0.29
		SiO_2	0.54
Bulk density (t/ m^3)	0,7–1,2	K_2O	-
		CaO	98.81
(%) < 80 µm	86	TiO_2	-
		Fe_2O_3	-
pH	12,4	SO_3	-

Furthermore, we conducted a mineralogical examination using X-ray diffraction. The results indicate that this quicklime contains 98.81% calcium oxide (Figure. II-23).

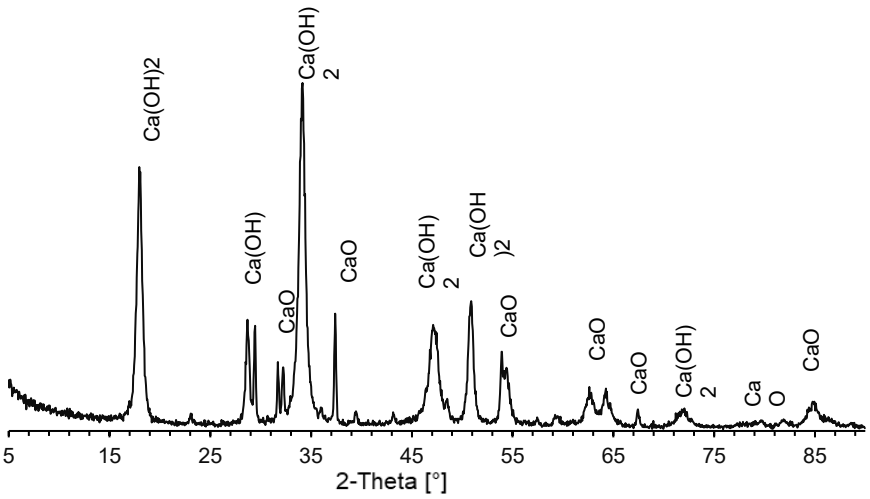

Figure II-23 : Lime X-ray diffraction analysis

II.6.3 Cement

The cement utilized for the treatment is a Portland cement referred to as CEMII/B-L42,5N, supplied by LAFARGE Company. It is approved and meets the standards of both Algerian (NA442 –2013) and European (EN197-1) standards. The clinker consists of 63% C_3S and 8.5% C_3A. The chemical compositions and properties of soil and cement are detailed in Table II-4.

Table II-4: Chemical composition of used cement by Energy-dispersive X-ray spectroscopy (EDX)

Oxide analysis	Cement
Na_2O	—
MgO	1.37
Al_2O_3	3.16
SiO_2	10.75
K_2O	1.10
CaO	77.93
TiO_2	—
Fe_2O_3	2.84
SO_3	2.85

The X-ray diffraction investigation (Figure II-24) revealed that the primary constituents of the soil were Calcite ($CaCO_3$) and Quartz (SiO_2). Calcite ($CaCO_3$) and calcium silicate (Ca_3SiO_5) are used in the production of cement.

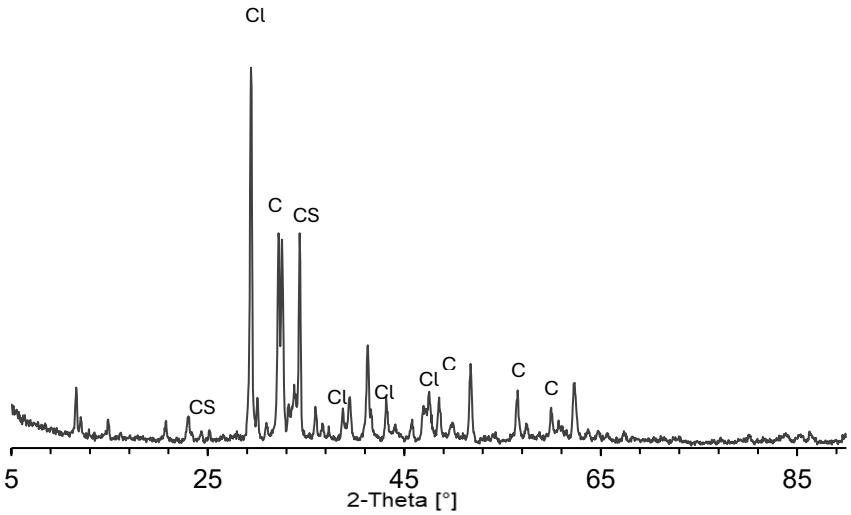

Figure II-24: Cement X-ray diffraction analysis

II.7 Experimental protocol

II.7.1 Specimen preparation

To prepare the test specimens, the soil is dried in an oven and then mixed using a MATEST 30 litres mixer with a power of 1.1Kw (Figure II-25). Subsequently, it is also employed for blending the soil with lime or cement.

Figure II-25: MATEST mixer

The soil was prepared in advance by mixing to a given water content, then sealed in a bag for 24 hours for maturation (Figure. II-26).

Figure II-26: Storage of soil samples

For HET tests, a cylindrical PVC mold measuring 100 mm in diameter and 200 mm in length was used to prepare the soil specimen (Figure II-27).

Figure II-27: Compaction mold

For Triaxial tests, a cylindrical copper mold measuring 70 mm in diameter and 140 mm in length was used to prepare the specimen (Figure II-28).

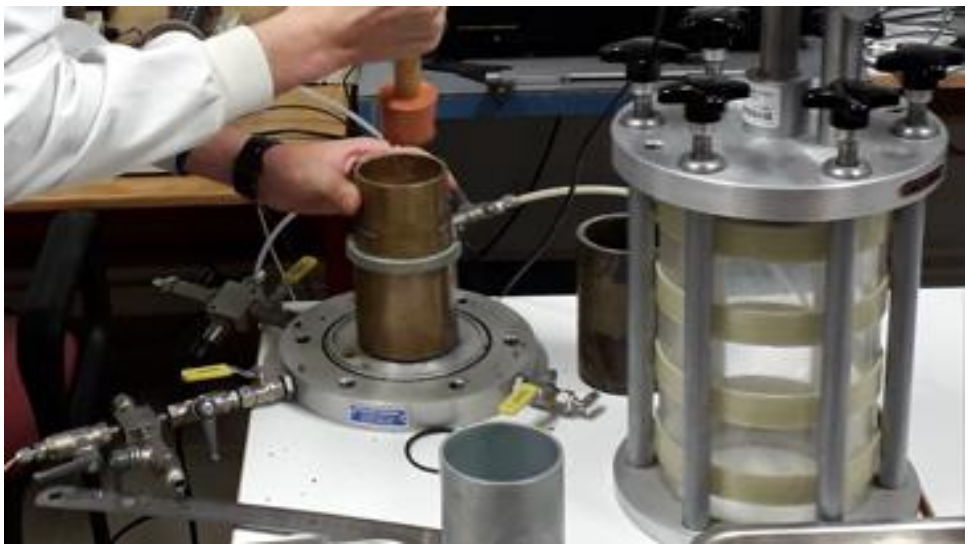

Figure II-28: Compaction mold for triaxial test specimen

To obtain uniform compaction, the soil specimen was dynamically compacted into three layers of equal thickness inside the PVC mold with a Normal Proctor test hammer. The amount of material and the required mixing water content were calculated from the desired final dry density using the standard Proctor curve (NF P 94-093) (Figure II-29).

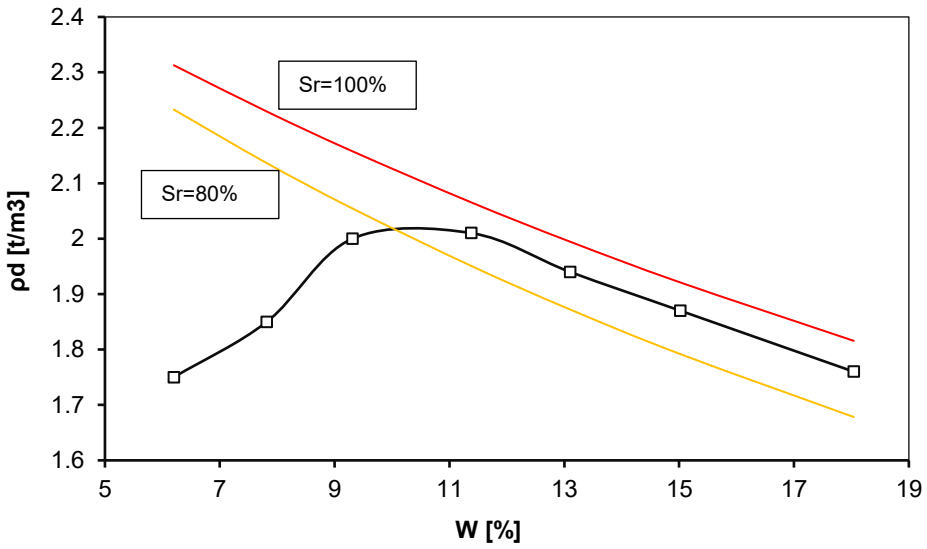

Figure II-29: Normal Proctor Curve

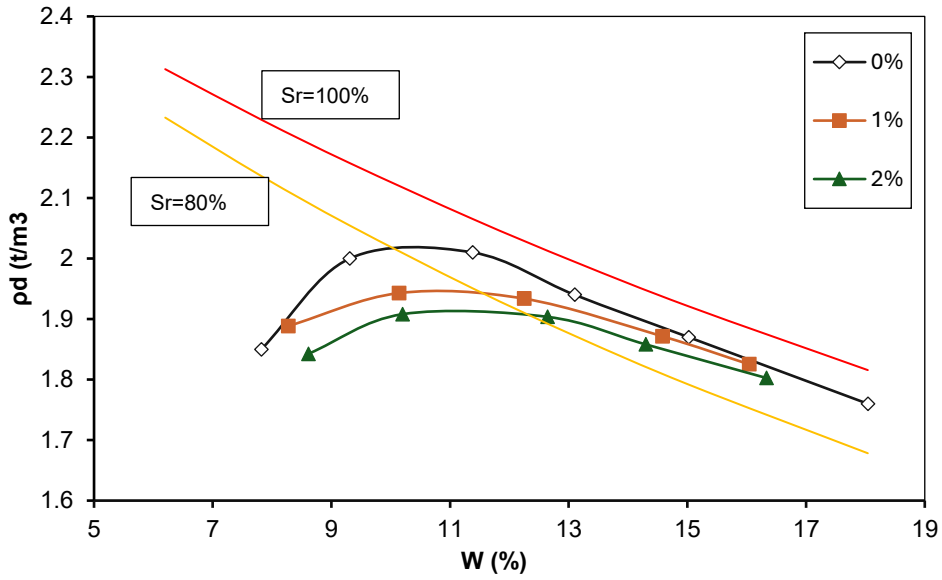

Figure II-30: Normal Proctor test for lime treated soil

In terms of the preparation of the treated specimen, following a 24-hour period of storage, the pre-prepared soil was mixed with a quantity of lime/ cement equal to the target dosage for two to three minutes, or until the soil was visually observed to have a grind whose granularity is stabilized and whose color is uniform. Following this, the soil was once more placed in an airtight bag for a maximum of fifteen minutes (1h for lime treated soil) prior to the compaction

(AFNOR (1994) NF P 94-093). Proctor curve for lime and cement treated soil are presented in Figure II-30 and Figure II-31 respectively.

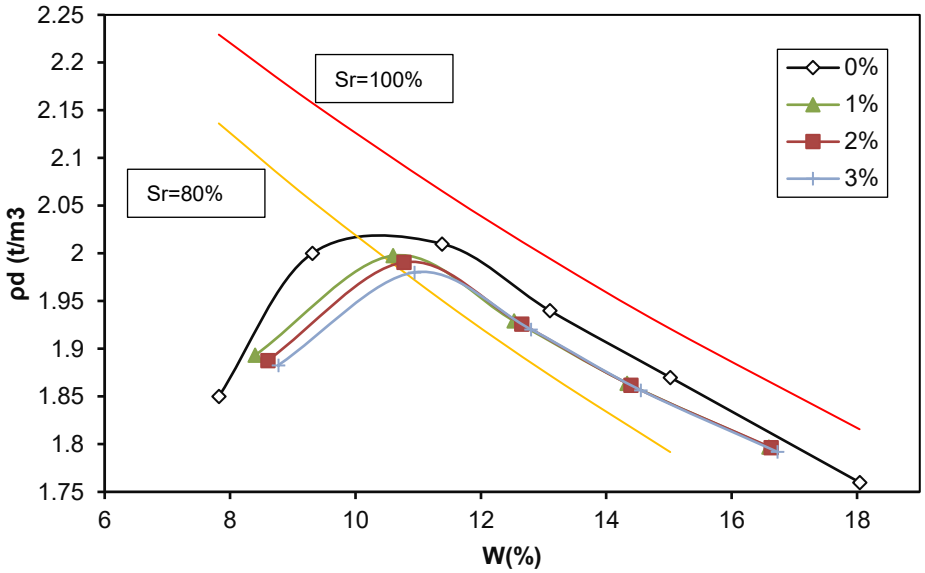

Figure II-31: Normal Proctor test for cement treated soil

The specimens were then covered with plastic film to prevent water evaporation and to preserve the compaction's water content, and they were stored at an ambient temperature of roughly 20°c until the test day. Figure II-32 and II-33 illustrate the storage of HET and triaxial specimens, respectively.

The specimens prepared to carry out the two test (HET, Crumb test) have the same characteristics.

Figure II-32: Storage of HET specimen

Figure II-33: Storage of triaxial specimen

II.7.2 Saturation

Just prior to the test, the specimen is pierced longitudinally in a central pattern with a metal drill bit, replicating the erosion process by letting a controlled flow of concentrated water through the hole. As per the intended starting shear stress, the diameter of the hole is established first. The molten paraffin has been poured into the hole to check the initial hole diameter (Figure II.34).

Figure II-34: Drilling the hole and checking the initial hole diameter

Following hole drilling, the central component was put into the erosion cell and firmly secured with eight tie beams. O-rings are used at the points of contact between the bases and the PVC

tube in order to prevent any water leaks and ensure the watertightness of the cell. This makes it possible for water to pass only through the pre-made hole.

Only HET tests undergo the saturation phase, which is carried out with a low hydraulic gradient of about 0.5. Its duration can last up to 24 hours. To avoid particle movement, this phase must be carried out with caution and at a slow pace (Figure II-35).

Figure II-35: Saturation

After setting up the entire erosion cell on a balance, a mild gradient was applied. The system's overall mass change was noted. Figure II-36 shows that the change of specimen mass stabilized after a certain interval of time, indicating the beginning of saturation.

Following a 24-hour period, the specimen is removed from the cell and recovered from the PVC mold. Multiple samples are then collected from various sections of the specimen to quantify the water content and subsequently determine the saturation degree. The results are summarized in Table II-5.

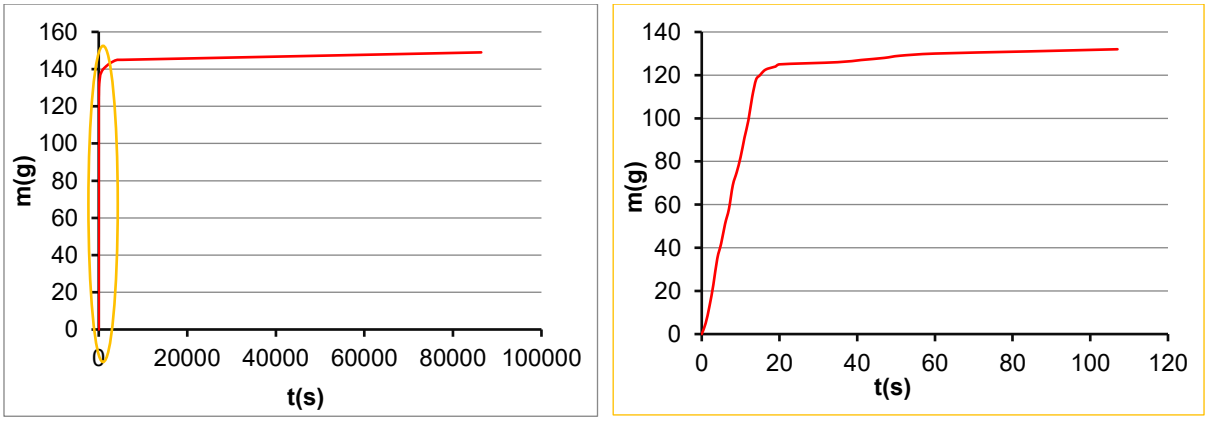

Figure II-36: Mass evolution of the specimen as a function of time

Table II-5: Saturation degree verification in deferent part of the specimen

Sample	m_t	mh	ms	w	Sr
Test 1 (Horizontally)					
Inlet	17.53	84.29	75.61	14.94	1
Middle	17.8	78.98	71.43	14.08	0.94
Outlet	17.72	64.37	58.81	13.53	0.90
Top	17.67	65.74	59.97	13.64	0.91
Test 2 (Horizontally)					
Top 1	17.71	64.5	58.9	13.60	0.91
Top 2	17.81	73.69	66.61	14.51	0.97
Top 3	17.55	77.37	69.73	14.64	0.98
Inlet	17.41	76.53	69.16	14.24	0.95
Middle	17.83	72.69	66.09	13.68	0.91
Outlet	17.65	81.45	74.07	13.08	0.87
Bottom 1	17.85	84.35	76.43	13.52	0.90
Bottom 2	17.51	80.5	72.73	14.07	0.94
Bottom 3	17.79	63.77	57.8	14.92	0.99
Test 3 (3h) (Horizontally)					
Top1	17.72	57.71	52.22	15.91	1
Top 2	17.65	61.53	56.23	13.74	0.92
Top 3	17.41	70.71	64.23	13.84	0.92
Inlet	17.66	63.83	58.02	14.40	0.96
Middle	17.82	59.78	54.55	14.24	0.95
Outlet	17.81	57.69	52.96	13.46	0.90
Bottom 1	17.68	72.75	65.51	15.14	1
Bottom 2	17.53	64	58.29	14.01	0.93
Bottom 3	17.86	62.89	57.12	14.70	0.98
Test 4 (vertically)					
Top1	17.71	70.35	63.92	13.91	0.93
Top 2	17.53	65.37	59.54	13.88	0.93
Top 3	17.52	74.94	67.93	13.91	0.93
Inlet	17.54	81.33	73.67	13.65	0.91
Middle	17.46	76.07	69.01	13.70	0.91

Outlet	17.77	84.18	76.39	13.29	0.89
Bottom 1	17.5	77.69	70.3	14.00	0.93
Bottom 2	17.46	80.04	72.29	14.13	0.94
Bottom 3	17.78	75.98	68.79	14.10	0.94
Test 5 (Horizontally)					
Top1	17.72	70.64	64.21	13.83	0.92
Top 2	17.64	76.57	69.49	13.65	0.91
Top 3	17.42	70.19	64.02	13.24	0.88
Inlet	17.65	86.2	78.29	13.04	0.87
Middle	17.82	93.31	84.6	13.04	0.87
Outlet	17.79	62.2	56.87	13.64	0.91
Bottom 1	17.7	65.96	60.18	13.61	0.91
Bottom 2	17.52	75.34	68.16	14.18	0.95
Bottom 3	17.87	62.56	56.13	16.81	1

II.7.3 Hydraulic loading

Following the saturation, the sample is subjected to hydraulic stress by first applying a gradient of order 1, which is subsequently increased in steps of 1 until the hydraulic rupture gradient is reached.

The soil hole is directly connected to the outflow pipe of the column. Upstream of the soil sample, there is a layer of gravel with a thickness of 5 cm and a diameter of 10 mm. This layer of gravel is placed there to facilitate the spreading of flow, as shown in Figure II-37. Outlet eroded particles mass and flow rate were continuously monitored.

Figure II-37: A layer of gravel

8 hydraulic gradient increments were employed consecutively. The hydraulic gradient value was increased every 15 minutes, as shown in Table II-6, which presents the experimental schedule. The increase in hole diameter resulting from erosion tests was determined by analysing the cumulative eroded mass. Additionally, the visual evolution of the wall shape was examined after the test.

Table II-6: Test procedure (hydraulic loads)

Hydraulic load (gradient)	1	2	3	4	5	6	7	8
Test duration (s)	900	1800	2700	3600	4500	5400	6300	7200

II.7.4 Measurement of final hole volume

Once the test is over, the specimen has been taken out of the erosion cell and molten paraffin has been poured into the enlarged hole, the sample is cut to remove the intact "candle", which represents the shape of the hole in the test specimen after erosion (Figure II-38). The volume of the "candle" can be measured using the ‘‘Water Displacement Method’’, and this measurement allows one to calculate the final average diameter of the eroded hole.

Figure II-38: The extracted candle

III CHAPTER 3. ASSESSMENT OF SOIL'S STABILITY TOWARDS INTERNAL EROSION

III.1 Introduction

This chapter examined the soil's erosivity. To evaluate its dispersiveness, chemical analyses including SAR, PS and cations exchange were conducted, alongside verification of particle size criteria. The soil was thoroughly analyzed employing a double hydrometer test in conjunction with Crumb tests. A parametric study was conducted using the Hole Erosion Test (HET) to empirically examine the initiation and progression of internal erosion in soil, focusing on the effects of compaction degree and hole diameter.

III.2 Soil chemical tests (cations)

The concentration of various ions is identified through the chemical analysis of soil pore water. This is significant due to the correlation between the electrolyte concentration in the soil pore water and the exchangeable ions present. Elevated salt concentrations raise the dispersiveness of the soil (Bhuvaneshwari et al. 2007).

The Sodium Absorption Ratio (SAR) and Percent Sodium (PS) are two metrics commonly employed to assess chemical compatibility (Mitchell et al. 2005) and (Lashkaripour and Soloki 2003). The "Sodium Adsorption Ratio" (SAR) is the ratio of sodium concentration to the square root of half the sum of calcium and magnesium concentrations. PS and SAR are derived from the subsequent equations:

$$TDS = Ca^{2+} + Mg^{2+} + Na^{+} + K^{+} \quad \text{(III.1)}$$

$$PS = \frac{Na^{+}}{TDS} \times 100 \quad \text{(III.2)}$$

$$SAR = \frac{Na^{+}}{\sqrt{\frac{Ca^{2+} + Mg^{2+}}{2}}} \quad \text{(III.3)}$$

The soil samples underwent acid digestion, after which the extracts were utilized for chemical analysis. The concentrations of Ca2+, Mg2+, Na+, and K+ were ascertained by atomic absorption spectroscopy. The values of SAR and PS were juxtaposed with the Sherard Curve (Sherard et al. 1976). Soils with a sodium adsorption ratio of 13 or above may exhibit elevated dispersion of organic matter and clay particles, diminished saturated hydraulic conductivity and

aeration, and an overall degradation of soil structure (NRCS, U. 2007). The erosivity of the soil diminished as the sodium adsorption ratio of the pore water increased (Lim 2006).

In comparison, the values of SAR and PS were found to be low, indicating that the soil is categorized as non-dispersive. The results of the chemical analysis are presented in Table 2.

Table III-1: Chemical analyses of Soil

Eliments	**Na^+**	**K^+**	**Ca^{++}**	**Mg^{++}**	**TDS**	**PS%**	**SAR**
Concentration(mg/L)	190	27	395	37	649	29.27	-
Exchangeable Cations [meq/L]	8.26	0.69	9.85	1.52	-	-	**3.47<13**

III.3 Double hydrometer test

The method outlined in the standard (ASTM D 4221–99. 2005) involves comparing the grain size of the soil's fine fraction through two distinct approaches. The first approach entails conducting a particle size analysis via sedimentation utilizing Sodium Hexametaphosphate as a dispersing agent and employing a mechanical agitator (Figure III-1). The second approach involves performing the same test without the use of a dispersing agent or an agitator.

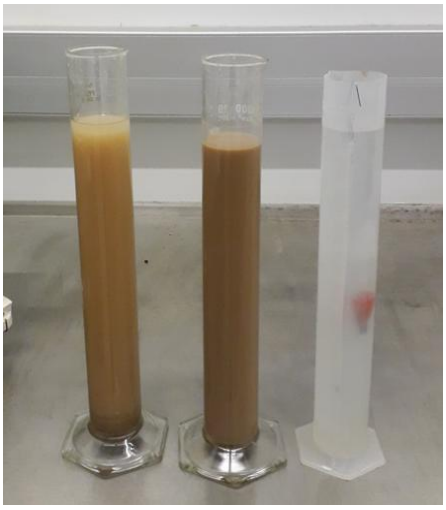

Figure III-1: Double hydrometer test

The test consists of analyzing the dispersion rate D determined by the ratio between the percentages of fines less than 5 microns without dispersant (A) and with dispersant (B), according to the following formula:

$$D = \frac{A}{B} = \frac{\%<5\mu m\ without\ dispersant}{\%<5\mu m\ with\ dispersant} \times 100 \qquad \text{(III.4)}$$

This approach was originally inspired by (Sail 2012), which was followed by (Bhuvaneshwariet al. 2007) providing the first description of the test procedure.

The findings of the double hydrometer test are illustrated in Figure III-2. The differentiation between these two curves illustrates the inherent dispersion propensity of the examined soil. (A) is determined to be 42 and (B) is determined to be 16. The calculated dispersion rate (D) indicates that Biskra soil exhibits a dispersion rate of approximately 38 percent. Therefore, it signifies that the degree of dispersion of this soil is within the intermediate range.

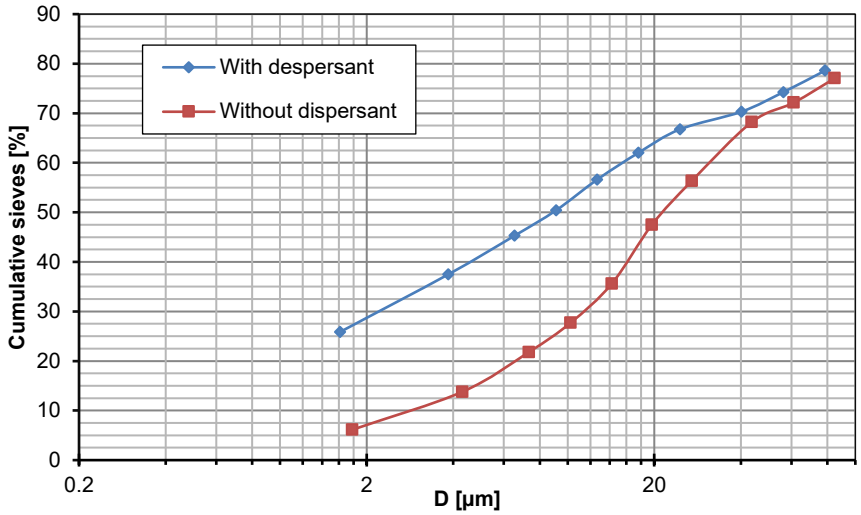

Figure III-2: Double hydrometer test

III.4 Verification of criteria for soil instability with respect to internal erosion phenomena (particle size criteria)

III.4.1 Initiation of internal erosion

The existing particle size criteria are determined by the shape of the particle size distribution curve of the tested material and its particle sizes (Sail 2012). The particle size distribution curve of the soil was utilized to verify these requirements, and the results are described in Table III-2. Based on these observations, it was determined that the soil is unstable.

Table III-2: particle size criteria results

Criterion	Istomina (1957)	Terzaghi	Kenney and Lau (1984, 1985)	Lubochkov (1965)	Sail (2012)	BURENKOVA (1993)
Stability	**Unstable**	**Stable**	**Unstable**	**Stable**	**Unstable**	**Unstable**

III.5 Specimen preparation for HET test and Crumb test

On the wet side of the standard Proctor curve, the specimens are compacted to a final dry density of 95% and 90% of the maximum dry density. As discussed in the previous chapter, an initial hole measuring 10, 7, and 4 mm in diameter is made using metal wicks in the specimen's center to simulate pipe erosion for the HET test. Table III-3 provides a summary of the specimens' characteristics.

Table III-3: Characteristics of specimens

Specimen	**d10-95**	**d7-95**	**d7-90**	**d4-95**	**d4-90**
ρd [t/m3]	1.92	1.92	1.82	1.92	1.82
w [%]	13.6	13.6	16.4	13.6	16.4
Initial hole diameter [mm]	10	7	7	4	4

III.6 Immersion test (Crumb test)

Numerous studies have focused only on clay soils, consisting of colloidal particles with a maximum diameter of 3 mm, utilizing cylindrical specimens of 15 mm in diameter and 20 mm in height ((Pham 2008) and (Haghighi 2012)). This study utilized specimens measuring 10 cm in diameter and 20 cm in height to assess the effects of clay proportion in the soil (10%), dry density, compaction water content, and degree of saturation on the initiation of dispersion phenomena. According to the results of this configuration, the specimen compacted to 95% of the optimum dry density totally disintegrates after 7 hours, whereas the specimen compacted to 90% disintegrates after 12 hours (Figure III-3).

It should be mentioned that in both situations, the specimen is submerged in water for the first few minutes before the particles begin to separate from the solid bulk. When compared to the tests conducted by (Elandaloussi 2019), the separation of larger flocs was observed after approximately one hour of immersion, and the turbidity effect —a halo of suspended particles surrounding the sample— was absent. However, it was observed when the specimens were completely dispersed, indicating that the behavior of submerged soil in water tends to both slaking and dispersion.

The results indicate that the degree of compaction (dry density and water content) affects the dispersive nature of Biskra's soil. Dispersion occurs more rapidly in specimens with high dry

density and low water content compared to those with low dry density and high-water content, where the soil is in contact with water. This process typically occurs within a few minutes (Haghighi 2013; Pham 2008; Tarog 2000).

In the instance of Biskra soil, the dispersion of the specimen requires significantly more time, potentially attributable to water content and the electromagnetic and electrostatic interparticle forces, which are affected by the dry density. Furthermore, soil structure and fabric, together with pore-water chemistry, particle size distribution, and clay mineralogy appear to affect the slaking process during the dispersion test, as noted by (Paaswell 1973).

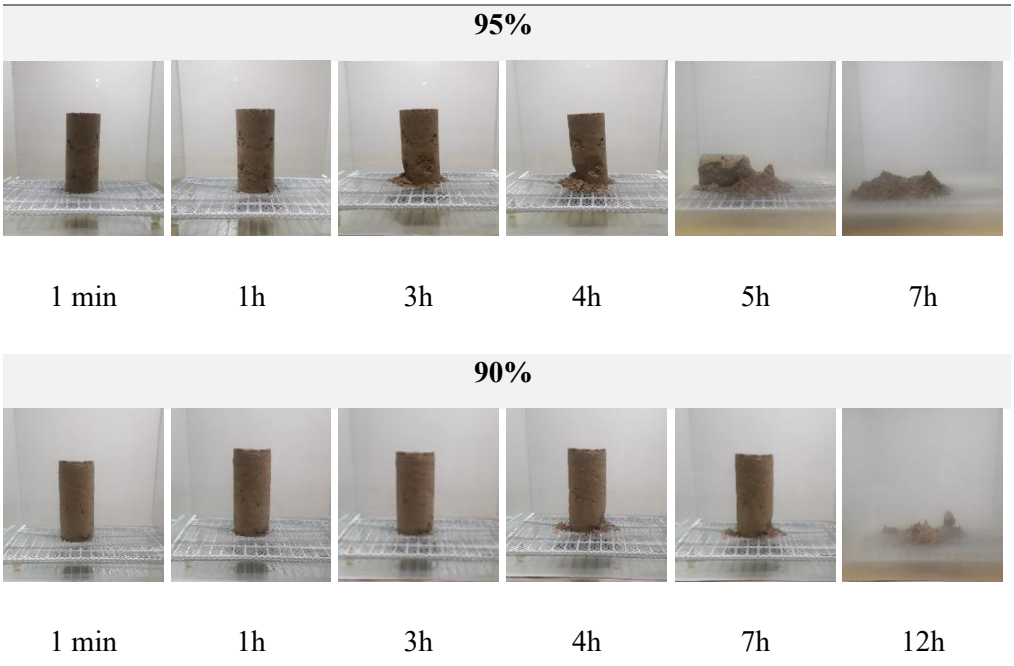

Figure III-3: Evolution of soil samples over time during immersion in water

III.7 Hole Erosion Test (HET)

Internal erosion is assessed by monitoring hydraulic parameters, specifically the pressure differentials between the upstream and downstream regions of the sample and the flow through the hole. The findings establish the empirical erosion law of the material, which may be articulated as follows:

The erosion rate, pertaining to soil erodibility, is defined by (Wan and Fell. 2004) as:

$$\dot{\varepsilon}_t = c_e(\tau_t - \tau_c) \qquad \text{(III.5)}$$

Where,

$\dot{\varepsilon}_t$: is the erosion rate [kg/s/m^2],

c_e: is the coefficient of soil erosion obtained from the slope of the erosion curve [s/m],

τ_t: is the hydraulic shear stress along the hole at time t [N/m^2],

τ_c: is the minimum hydraulic shear stress for the initiation of erosion, also referred to as the critical shear stress [N/m^2].

The erosion rate $\dot{\varepsilon}$ [kg/s/m^2] is expressed by the eroded soil mass m_t [kg] per unit area of the hole at time t [s]:

$$\dot{\varepsilon}_t = m_t/(a_t \times t) \qquad \text{(III.6)}$$

Several prior studies assessed the erosion rate by estimating the instantaneous hole diameter. (Lim 2006) utilized pipeline flow theory to estimate flow rate via the "Moody diagram", although this does not ensure a consistently turbulent or laminar flow regime. (Mehenni et al. 2016) proposed a general theoretical model, treating the hole as ellipsoidal; however, this remains unrealistic. (Haghighi 2013), attempted to estimate the instantaneous diameter using turbidity measurements, but they inaccurately employed grain solid density instead of dry density, since the eroded mass is a part of the specimen which is compacted to a given dry density.

This study calculates the erosion rate by utilizing the eroded mass corresponding to each applied shear stress, which is associated with the hydraulic gradient observed across the hole, without making any assumptions on flow laws. The erosion rate may be articulated as follows:

$$\dot{\varepsilon}_t = \frac{m_t}{2\pi r_t l\, t} \qquad \text{(III.7)}$$

The hydraulic shear stress along the hole can be expressed as:

$$\tau = \rho_w g s_t \frac{\phi_t}{4} = \rho_w g i_t \frac{r_t}{2} \qquad \text{(III.8)}$$

Where:

ρ_w: The density of the eroding fluid [10^3 kg/m^3],

g: The gravitational acceleration [9.81 m/s^2],

i_t: The hydraulic gradient across the soil sample at time t and

r_t: The average diameter of the erosion hole assumed to remain circular at time t.

Consequently, the diameter of the hole is determined as follows:

$$v_t = \pi\, r_t^2\, l = v_i + \Delta v \qquad \text{(III.9)}$$

$$\pi\, r_t^2\, l = \pi\, r_i^2\, l + \frac{m_t}{\rho_d} \qquad \text{(III.10)}$$

$$r_t = \sqrt{\frac{m_t}{\rho_d \pi L} + r_i^2} \qquad \text{(III.11)}$$

$$\phi_t = 2r_t \qquad \text{(III.12)}$$

Where:

v_t: the volume of the hole at time t.

v_i: the volume of the hole.

Δv: the volume variation.

r_t and r_i: the hole rayon at time t and the initial hole diameter respectively.

Validation of the calculation method (results)

Figure III-4 illustrates the final diameter derived from the measured eroded mass in comparison to the final eroded diameter obtained at the end of the tests from the extracted candles.

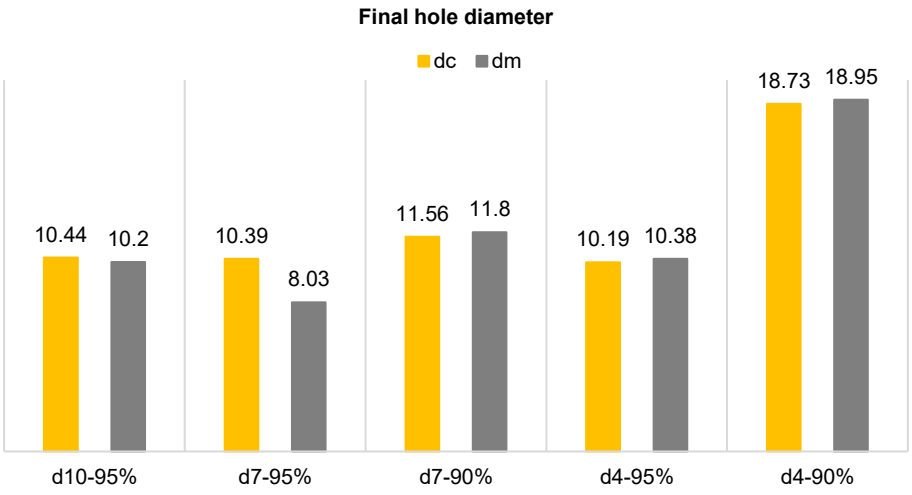

Figure III-4: comparison of the calculated and measured final diameters

The minor variations may result from inaccurate mass calculations and hole diameter measurements at both the beginning and ending of the test. The results indicated the method's effectiveness in predicting the hole diameter during the test by utilizing the mass of eroded soil particles.

III.8 HET results

A parametric study was conducted to assess the effect of compaction degree and initial diameter of the hole on the onset of piping erosion. This section will describe and show the initiation and development of the internal erosion mechanism under horizontal unidirectional flow conditions.

III.8.1 Eroded particles mass

Figure III-5 illustrates the relationship between the mass of eroded particles and the hydraulic gradient. This mass is clearly influenced by the level of compaction and the initial diameter of the hole. In the cases of (d10-95, d7-95, and d4-95) and (d7-90 and d4-90), where the groups exhibit identical dry density and compaction water content but a diminishing hole diameter, the findings indicate that soil instability or erodibility escalates with the reduction of hole diameter. This phenomenon results in heightened pressure, consequently increasing the water flow shear stress at the water-soil interface. The instances of (d7-95, d7-90) and (d4-95, d4-90) illustrate that soil erosion instability increases as the degree of compaction diminishes, specifically characterized by reduced density and elevated water content during compaction. The results indicate that the soil is unstable towards internal erosion or piping due to significant particle departure. The mass of eroded particles is inversely related to both the degree of compaction and the diameter of the hole.

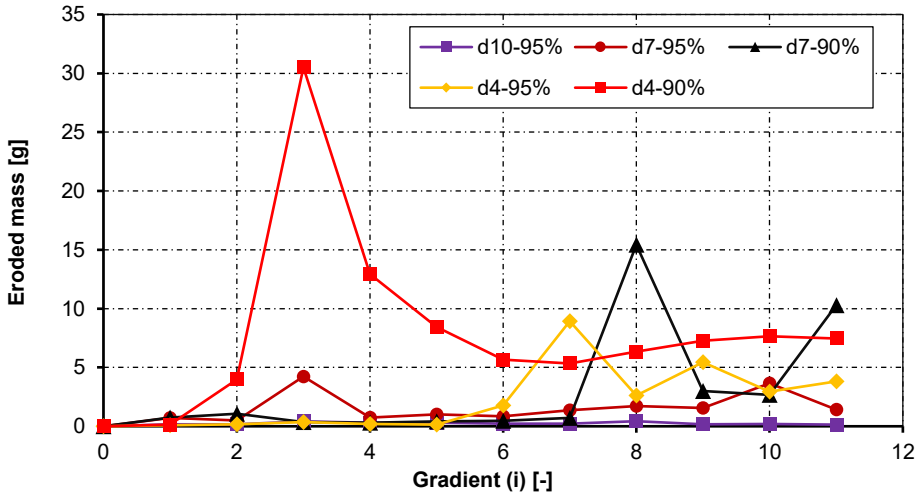

Figure III-5: eroded mass evolution

III.8.2 Cumulative eroded mass

Figure III-6 illustrates the progression of cumulative eroded mass as a function of hydraulic gradient. It exhibits a quasi-linear relationship for soil d10-95% and d7-95%, whereas the variations in other cases are non-linear. The ultimate cumulative eroded mass is affected by compaction conditions and the initial hole diameter, with the highest values observed during the HET test conducted on the specimen d4-90%. This specimen is characterized by lower density, higher compaction water content, and smaller initial diameter, rendering it the most unfavorable case regarding soil's resistance to piping erosion.

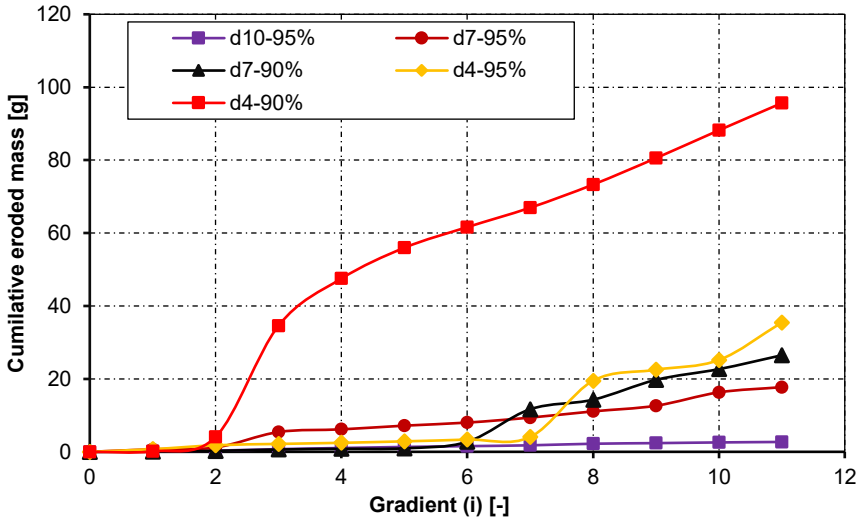

Figure III-6: Evolution of the cumulative mass of the eroded particles soil

III.8.3 The outflow

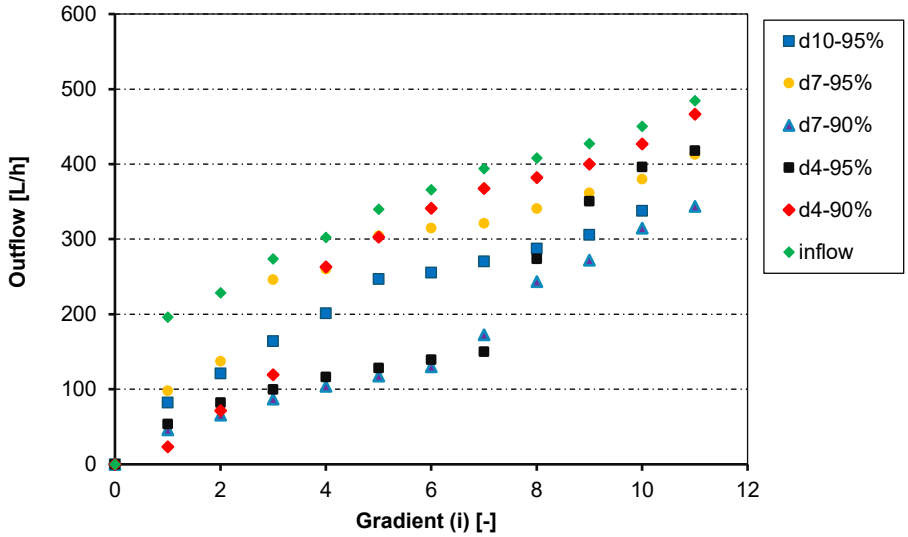

Figure III-7: Evolution of the outflow during HET test

The outflow rate is contingent upon the instantaneous diameter of the hole, as illustrated in Figure III-7. In the case of the d4-90% test, deemed the most adverse scenario, the initial flow rate was 23 L/h. Subsequently, with increasing hydraulic loading, shear stress intensified, resulting in raised particle detachment and an expansion of the hole diameter, ultimately leading to a flow rate of 459 L/h. The flow rate appears to be influenced by both the initial hole diameter and the cumulative mass of eroded particles (instantaneous diameter). In essence, an increase in the cumulative mass of eroded particles correlates with a heightened outflow rate.

III.8.4 Evolution of the hole's diameter

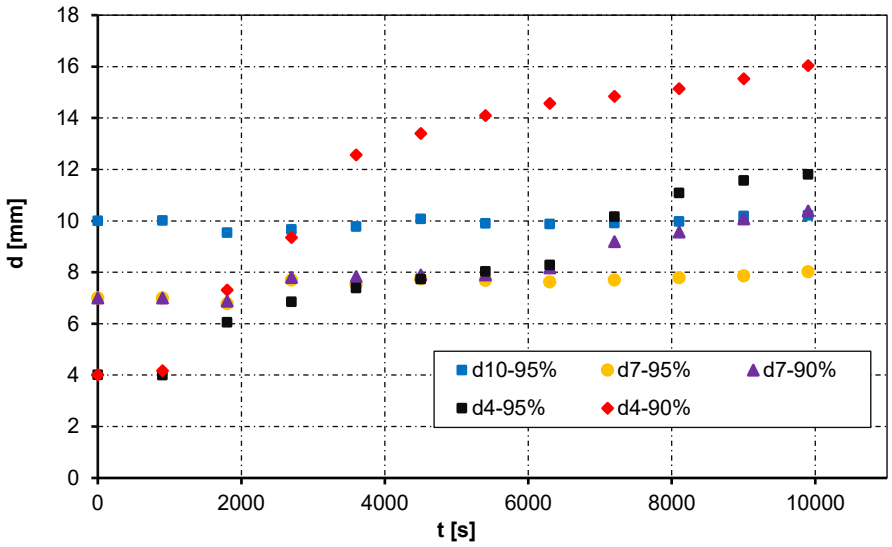

Figure III-8: Evolution of the hole's diameter during HET test

The instantaneous diameter is computed using equation (III-12). As illustrated in Figure III-8, the variation of the calculated instantaneous diameter is plotted against time. The specimens most impacted by diameter variation from the beginning to the end of the test are those with an initial diameter of 4 mm, with a notable difference observed in specimen (d4-90%).

III.8.5 The erosion rate

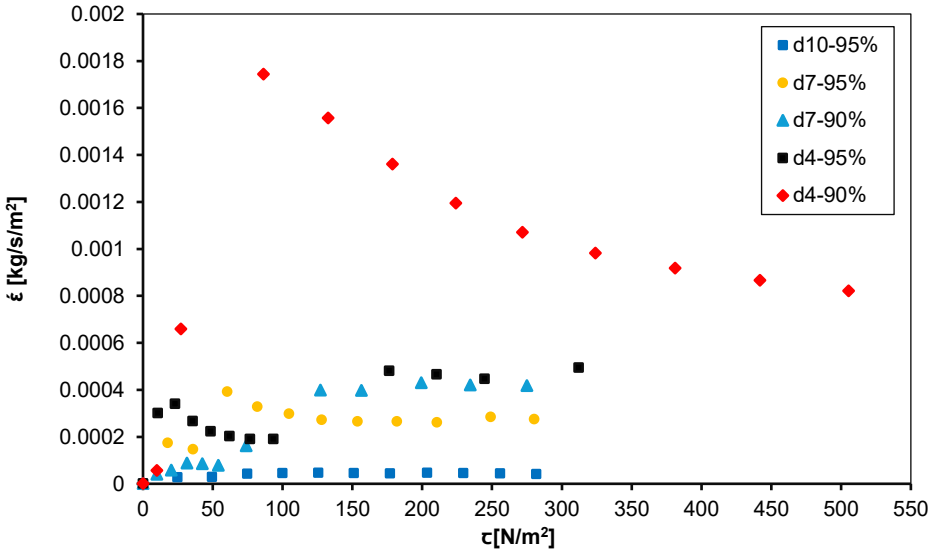

Figure III-9: Erosion curves

The results of the Hole Erosion Test across many scenarios are illustrated in Figure III-9, where the erosion rate έ is plotted against the shear stress τ at the interface.

Repeatable testing and varying pressure drop (shear stress) were employed to gather experimental data points for each scenario. The data demonstrate a linear fit consistent with the erosion rule (2) for the (d10-95%) range; however, this is not evident in other situations, particularly (d4-90%). No critical shear stress was detected, as similarly observed in the procedures described in references (Wan and Fell 2004) and (Bonelli and Brivois 2008).

The variable parameters include the initial diameter and the degree of compaction. Experimental data for various specimens may be easily differentiated, and HET facilitates the distinction among the different cases.

As compaction degree is increased, the erosion rate decreases, and the erosion coefficient (c_e) tends to decrease, thus the texture becomes more resistant to erosion and vice versa. However, as the initial diameter is decreased, the erosion rate usually tends to increase. The highest erosion rate values were recorded in case of specimen (d4-90%), which considered the most unfavourable case of this soil erosion resistance.

As the degree of compaction increases, the erosion rate decreases, and the erosion coefficient (c_e) generally drops, resulting in a texture that exhibits greater resistance to erosion, and vice versa. Conversely, a reduction in the initial diameter typically leads to an increase in the erosion

rate. The maximum erosion rate values were observed in specimen (d4-90%), which represents the most unfavorable scenario for this soil's erosion resistance.

III.8.6 Estimation of final hole diameter

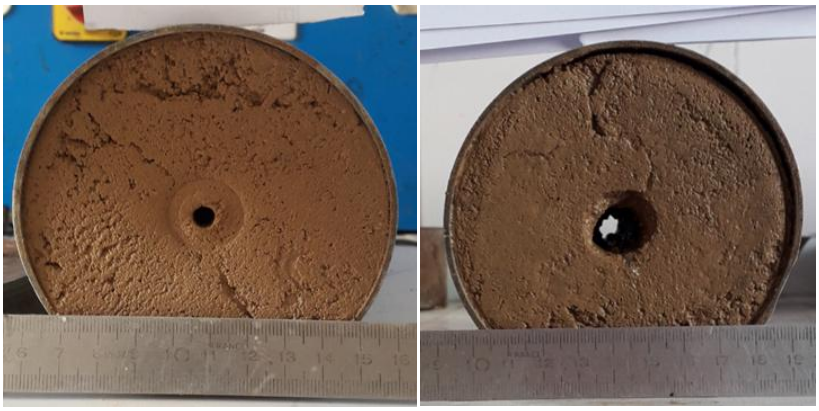

Figure III-10: Hole's diameter before and after HET test (d4-90%)

Using melted paraffin, the diameter of the hole is measured after the test is finished, and the volume of the extracted paraffin that is removed from the hole is used to calculate the average hole diameter in the current work.

Figure III-11: Extracted candle (d4-90%)

The extracted paraffin took over the shape of the eroded hole, which appeared to be irregular. In the case of the d4-90% test, the diameter of the latter measured about three times the initial diameter; in general, the upstream part of the hole had a slightly larger diameter than the downstream part (Figure III-11).

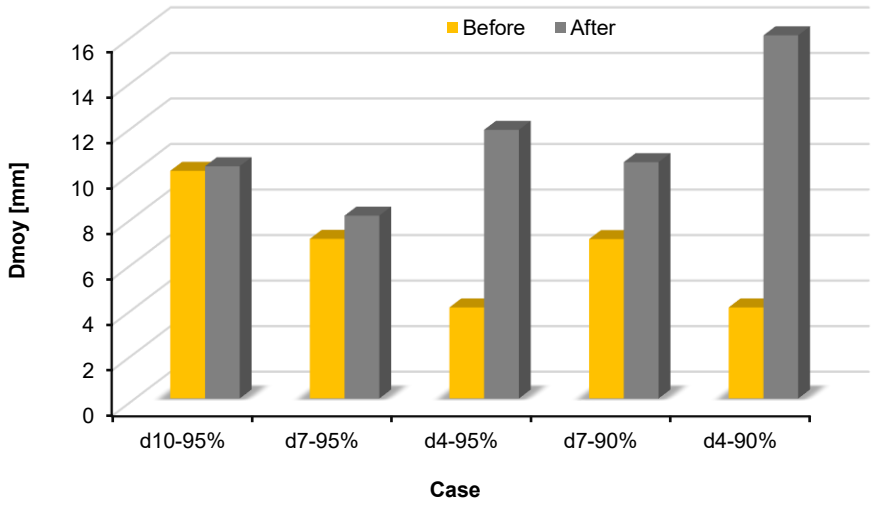

Figure III-12: Final versus initial hole's diameter

The final hole diameter is inversely proportional to the initial diameter and the degree of compaction, as illustrated in Figure III-12. The smaller initial hole diameter and the degree of compaction, the larger the final hole diameter.

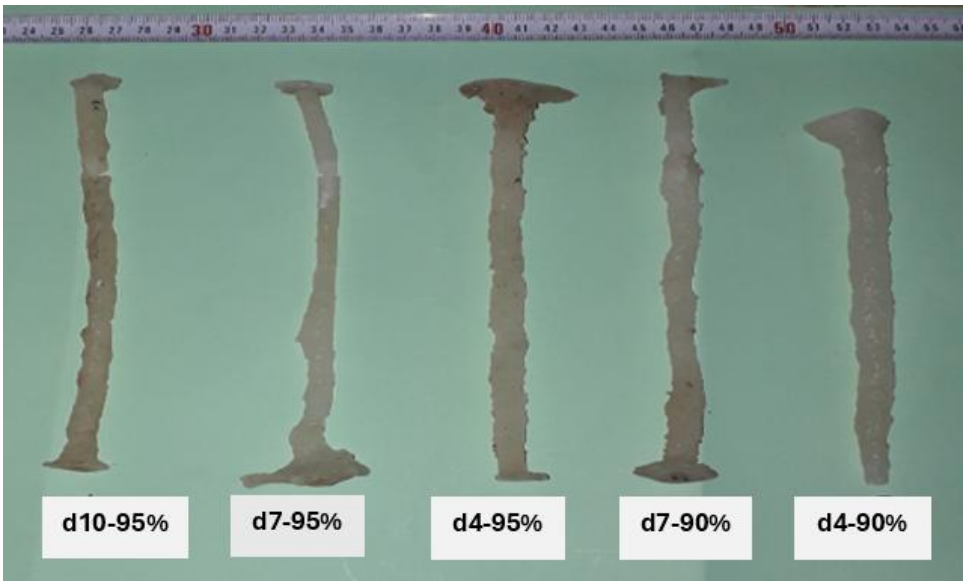

Figure III-13: Final initial hole's diameter

A comparison of the final diameter (Figure III-13) to the initial diameter for each case serves to quantify the soil's erodibility. The alteration in final diameter for specimens with an initial diameter of 4 mm is clearly greater than that for specimens with initial diameters of 7 and 10 mm. For specimens with identical initial diameters but varying degrees of compaction, the final hole diameter is larger when the degree of compaction is reduced.

III.9 Repeatability tests

In experimental activity, verifying the repeatability of tests is crucial for validating both the testing apparatus and the corresponding experimental methodology. Ensuring the reliability of experimental data. It helps determine the reliability of a measurement or experiment. If the results are consistent across multiple trials, it increases confidence in their accuracy and validity.

In order to verify the consistency of the results, five tests are presented below that were carried out on a d4-90% specimen under the same conditions. The test results are compared during the hydraulic loading phases, then at the time of hydraulic fracturing.

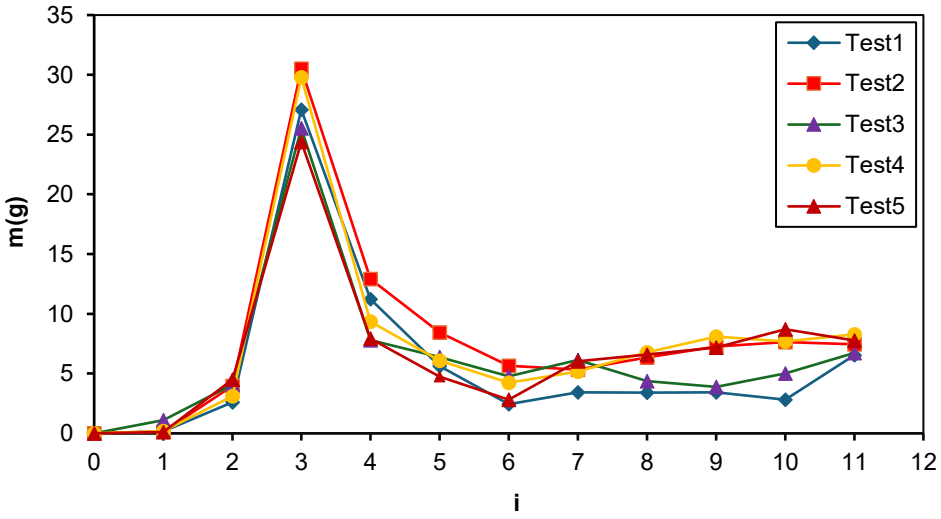

Figure III-14: eroded mass

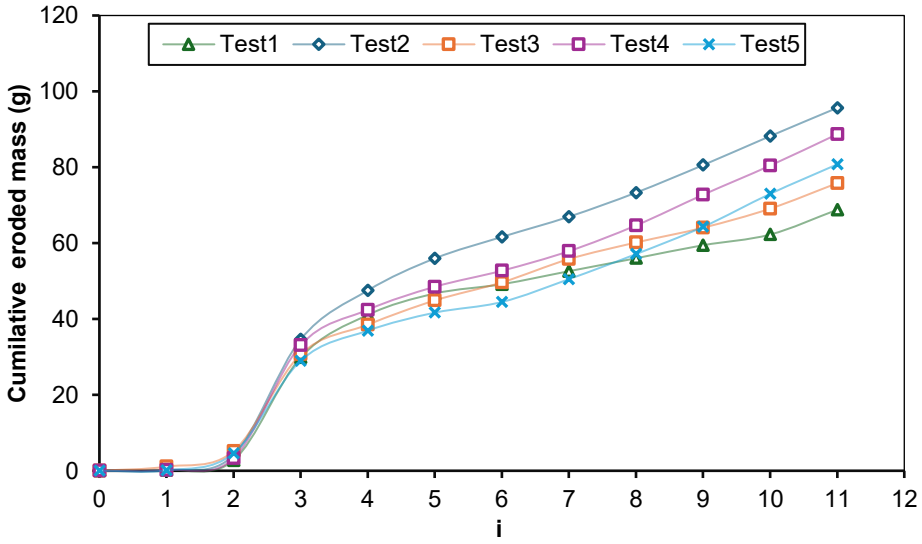

Figure III-15: Evolution of the cumulative mass of the eroded particles

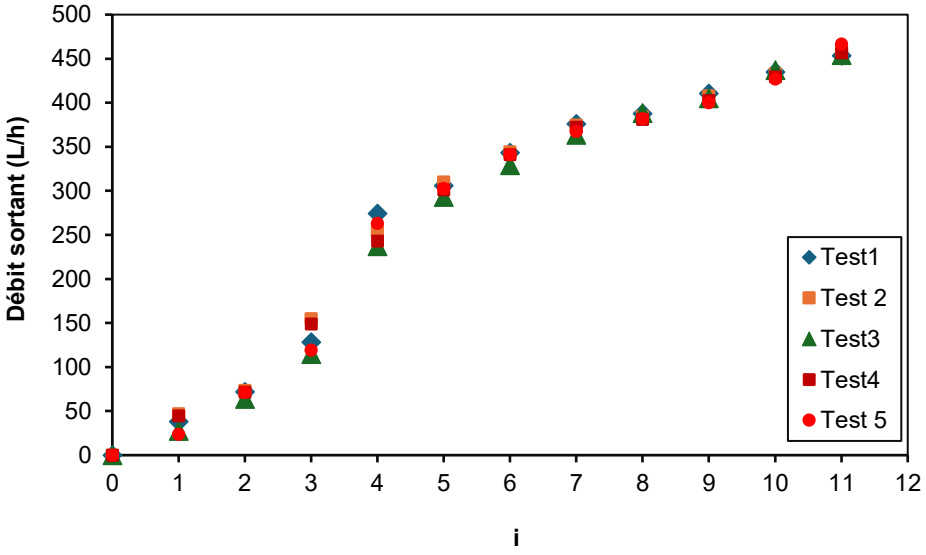

Figure III-16: Evolution of outflow

It should also be noted that the HET repeatability tests proved to be quite satisfactory with a similar aspect and fluctuation from one test to another for the same configuration.

Figure III-14 shows the comparison in terms of eroded mass, an initial rapid phase followed by a decrease and then stabilization. The influence of the hole's diameter on water pressure and shear stress is highlighted as a key factor in controlling the erosion process. The cumulative eroded mass data suggests a consistent erosion rate after a certain point, all tests show an increasing trend in eroded mass over the test, indicating ongoing erosion (Figure III-15). The same thing is observed for outflow curves (Figure III-16).

III.10 Conclusion

This study aimed to assess the hydraulic properties (erosivity and dispersity) of a representative coarse soil and its suitability for hydraulic earthworks. The results indicated that the soil exhibited instability concerning internal erosion phenomena.

The soil was categorized as non-dispersive based on chemical analyses that revealed low SAR and PS values; nevertheless, upon confirmation of the instability particle size requirements, it was determined that the soil is dispersive and so unstable with respect to erosion.

In order to go deeper into the investigation, the soil was tested using a double hydrometer, which revealed that the degree of dispersion was in the intermediate range. Additionally, tests using crumb revealed that the soil completely disintegrates when submerged in water; the duration of this process is determined by the compaction conditions.

HET tests indicated a correlation between the initial diameter of the hole and the degree of compaction, which affects the initiation and development of internal erosion.

The results are more significant with specimens with a 4mm (d4) diameter hole, and the soil compacted to a dry density of 90% of the Normal Proctor curve (opt90).

The obtained results provide more data for future studies on the behavior of compacted coarse soils, regarding the lack of understanding about this type of soil in terms of its behavior to the phenomenon of erosion.

The results collected contribute further data for future research on the behavior of compacted coarse soils, addressing the existing knowledge gap concerning their response to erosion phenomena.

Future research will focus on this scenario (selected as the most unfavorable) to enhance soil resistance to erosion, employing various methods to stabilize the soil.

IV CHAPTER 4. THE INFLUENCE OF CEMENT AND LIME TREATMENT ON THE HYDRAULIC BEHAVIOR OF THE SOIL

IV.1 Introduction

The objective of this section is to examine the efficacy of cement/lime treatment in stabilizing soil containing a specific quantity of clay, deemed unsuitable, against piping erosion. To ascertain the appropriate dosage and curing duration, an experimental program utilizing the HET test is conducted on both untreated and treated soil, incorporating 1%, 2%, and 3% of cement / 1% and 2% of lime relative to the weight of the dry fine soil component, over varying periods of 1, 7, and 28 days. Subsequently supplemented with Crumb tests, hydraulic conductivity and triaxial tests to investigate the progression of the soil's mechanical properties.

Furthermore, microstructure characterization analyses have been carried out as Thermo-Gravimetric Analysis (TGA), particularly Mercury Intrusion Porosity (MIP) and scanning electron microscopy (SEM).

IV.2 HET erosion Tests

HET tests were performed for each untreated and treated soil to investigate the influence of cement and lime treatment on the hydraulic behavior of the soil. A series of tests were conducted on specimens subjected to various dosages after 1, 7, and 28 days of curing to determine the appropriate dosage and curing time for better soil stability against piping erosion.

IV.2.1 Untreated soil

This part will delineate and illustrate the initiation and advancement of internal erosion mechanisms in untreated soil, focusing on the most unfavorable scenario outlined in chapter 3, wherein a horizontal unidirectional flow is induced by elevating the hydraulic head.

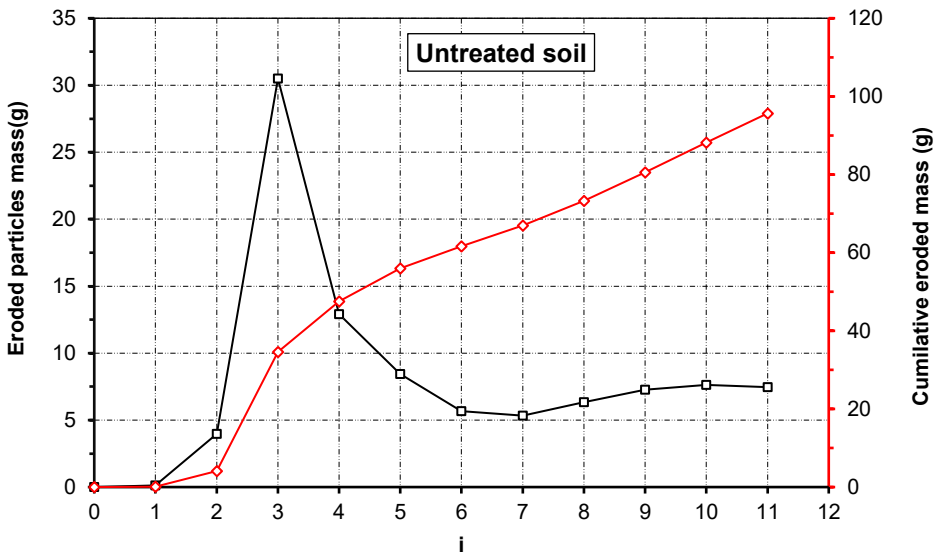

Figure IV-1: Evolution of eroded particles and cumulative eroded mass during the charging phase on untreated soil

The evolution of eroded particle mass and cumulative eroded mass with the increase of hydraulic gradient (i) is illustrated in Figure IV-1. Applying a hydraulic gradient of 1 results in a minor change in the mass of eroded particles, indicating that the untreated soil's internal erosion begins with a low hydraulic load. Then, as the hydraulic head increases, both this mass and the cumulative mass continue to rise.

A significant departure of eroded particles in which the mass reaches a highest value of 30,5 g is observed while the application of gradient 3 magnifies the cumulative eroded mass to 34,6 g. Beyond that and from gradient 4, a drop of eroded mass is observed; this decrease goes to a lower value of 5.33 g at gradient 7. Gradient 8 sees a slight increase to 6,34 g, but at higher gradients, it sustains a value of roughly 7,5 g. The widening of the hole's diameter during the departure of eroded particles influences the water pressure in the hole, leading to a decrease in water flow shear stress, which in turn causes the soil particles to detach. Returning to the cumulative eroded mass, we see an increase at a quasi-fixed rate of about 7 g from gradient 4 until the end of the test.

IV.2.2 Treated soil

IV.2.2.1 Eroded particles mass

IV.2.2.1.1 Lime treatment

Figure IV-2 presents the HET tests for 1%-1 day. At the hydraulic head of gradient 5, the soil begins to erode, reaching a maximum value of 19.34 g. In the case of (1% -7 days), the first

departure of soil's particles was observed at gradient 6. Then, as the hydraulic load increases, it gradually rises at a slow pace. The soil exhibited good erosion stability after 28 days of curing (1%-28 days); however, the application of hydraulic load at gradients of 6, 10, and 11 resulted in the departure of some particulates.

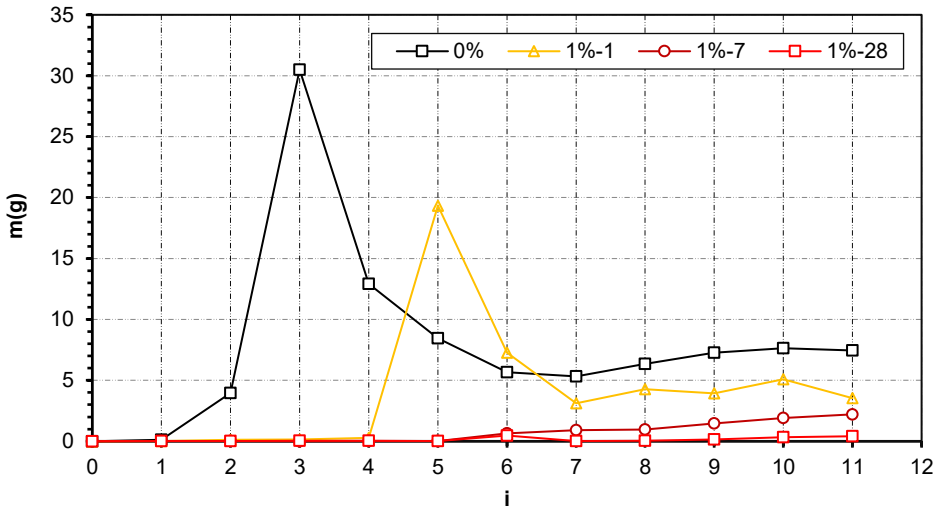

Figure IV-2: Evolution of eroded particles mass during the charging phase on 1% lime treated soil

Due to the results shown by 1% lime-treated soil, it was necessary to examine its behavior after the addition of 2% lime. The soil reached optimum stability only after 24 hours of curing as well as after 7 days (Figure IV-3).

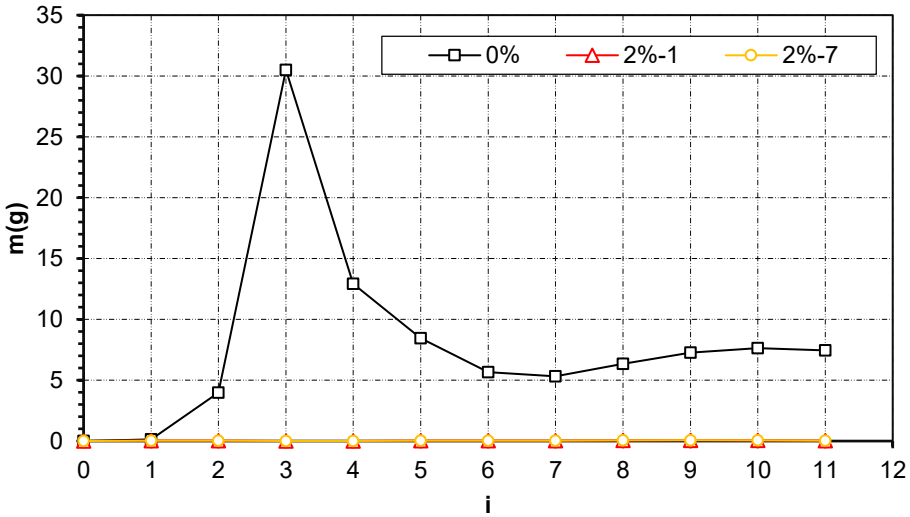

Figure IV-3: Evolution of eroded particles mass during the charging phase on 2% lime treated soil

IV.2.2.1.2 Cement Treated soil

To investigate the impact of cement treatment on hydraulic behavior, HET tests are conducted on specimens treated with varying cement dosages of 1, 2, and 3%, and curing times of 1, 7, and 28 j.

Soil treated with 1% cement has enhanced stability and erosion resistance compared to untreated soil, which experiences particle erosion under minimal hydraulic load at a hydraulic gradient of 1.

In test (1%-1) illustrated in (Figure IV-4), erosion of the soil initiates at a hydraulic gradient of 2, achieving a peak mass of 34.93 g, which exceeds that of untreated soil. This phenomenon occurs because the pipe remains constricted, resulting in a heightened hydraulic load that produces increased shear stress at a gradient of 6. A similar trend is observed in the test (1%-7), but with a reduced mass compared to (1%-1), as the soil exhibits enhanced stability following 7 days of treatment. Subsequently, there is a decline in the mass of eroded particles at subsequent gradients, approximately 4 g, attributed to the significant mass loss leading to an expansion of the hole's diameter, thereby reducing pressure and shear stress. It is noted that the soil maintains stability up to a gradient of 4 in test (1%-7). After 28 days of curing time, the soil resists the erosion phenomenon up to a gradient of 5, however remains unstable.

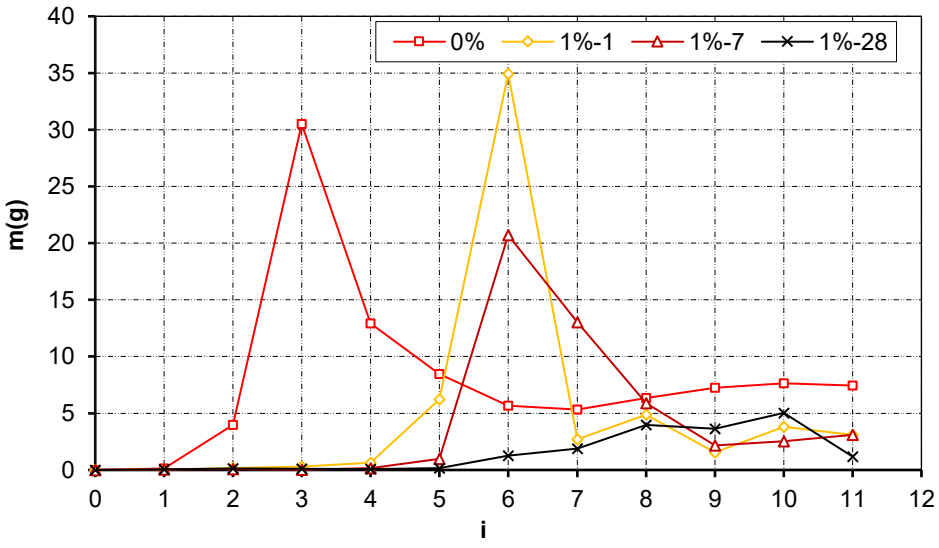

Figure IV4: Evolution of eroded particles mass during the charging phase on 1% cement treated soil

The 2% tests depicted in Figure IV.5 indicate that the soil is stable under low gradients but becomes unstable under elevated hydraulic loads. The soil has superior stability and erosion resistance relative to soil treated with 1% cement. The greatest mass of eroded particles is 4.9

g, observed when the hydraulic head attains a gradient of 10 after 24 hours of cure time. The soil remains inadequately stable against erosion even after 28 days of curing time.

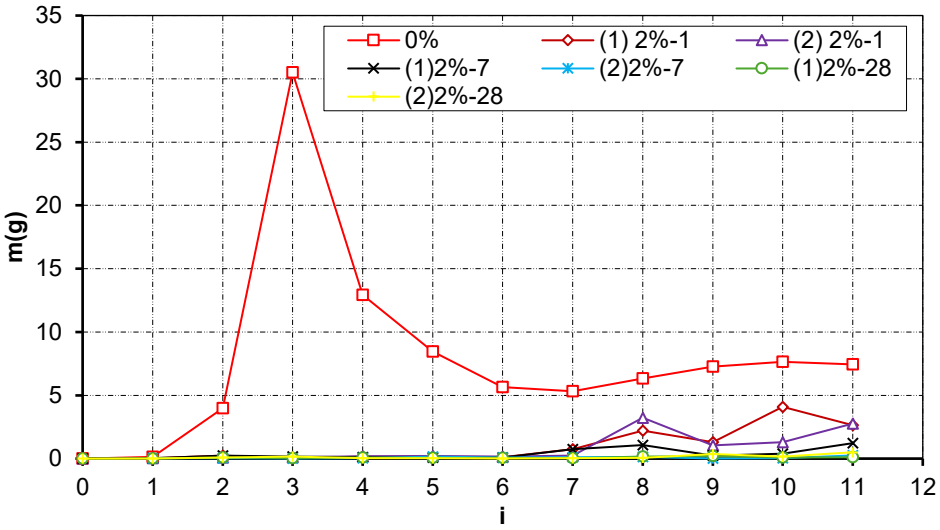

Figure IV.5: Evolution of eroded particles mass during the charging phase on 2% cement treated soil

The latest tests are on a soil treated with 3% cement (Figure IV-6). Only after 24 hours and 7 days of curing time, the soil exhibit great stability, with a very low eroded particle mass that does not exceed 0.01 g, corresponding to a hydraulic gradient of 11. According to these results, 3% of cement is chosen as the adequate dosage.

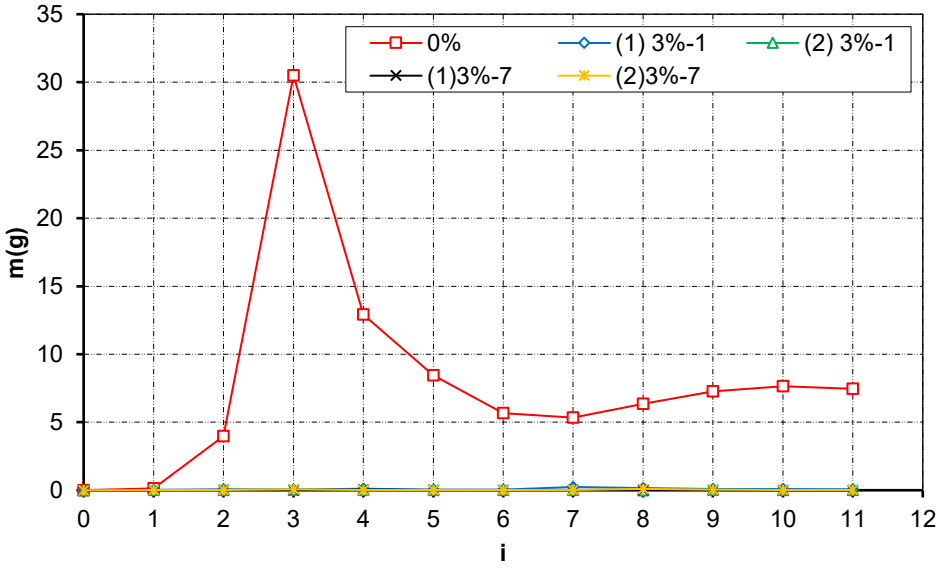

Figure IV-6: Evolution of eroded particles mass during the charging phase on 3% cement treated soil

IV.2.2.2 The cumulative mass of the eroded particles

Figures IV-7 and IV.8 illustrate the progression of the eroded particles' cumulative mass in relation to the hydraulic gradient. The curve of the untreated soil envelops all the other curves with a cumulative mass at the end of the test of 95 g.

Figure IV-7 shows that the incorporation of lime resulted in a significant decrease of the cumulative mass; the lowest value of (0.39 g) was recorded after 7 days of treatment with 2% of lime. It is concluded that 2% lime was the optimal dosage for stabilizing the examined soil.

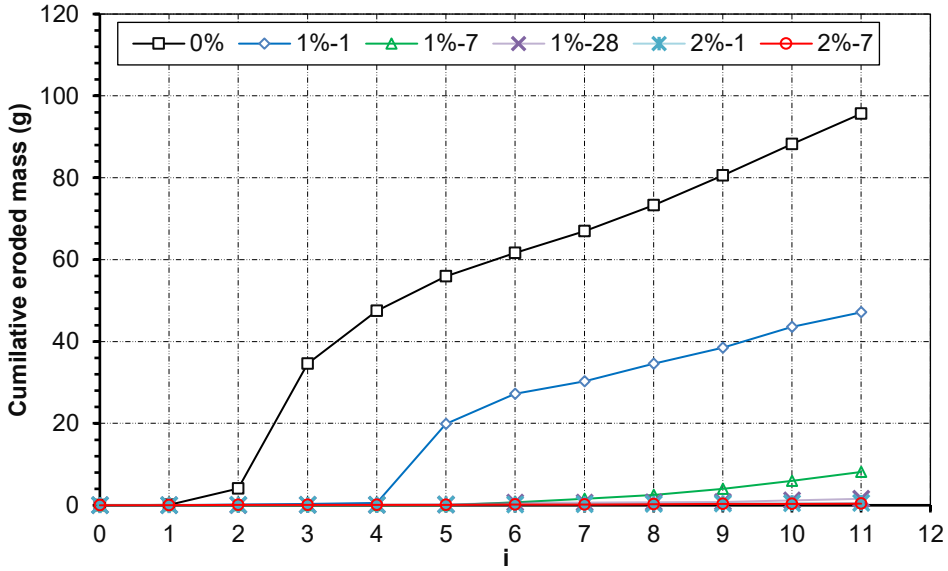

Figure IV-7: Evolution of the cumulative mass of the eroded particles (soil+lime)

A similar observation is noted for soil treated with cement, where the reduction in cumulative mass of eroded particles is directly related to both cement dosage and curing duration. The minimum value (0.18 g) was observed after 7 days of treatment with 3% cement. The best dosage for stabilizing the investigated soil was determined to be 3% cement.

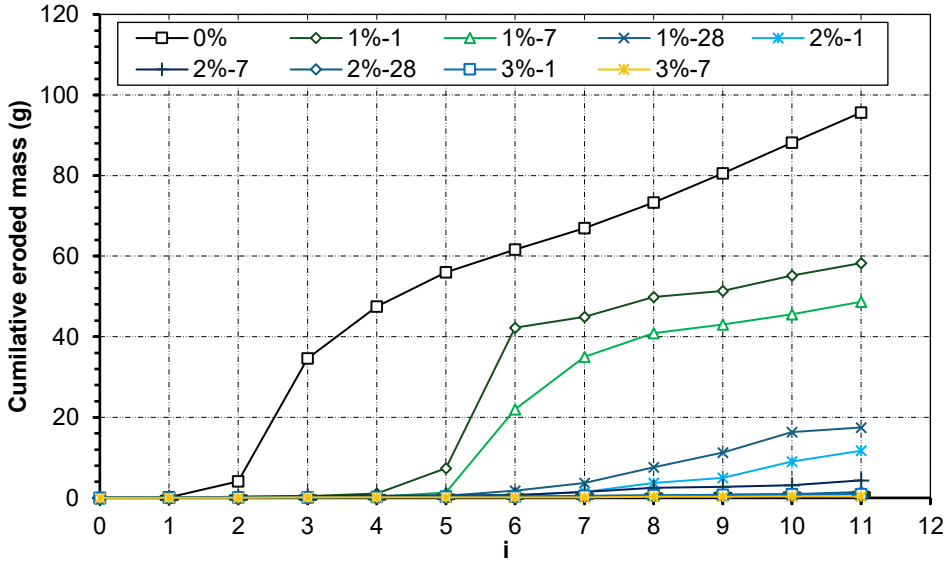

Figure IV-8: Evolution of the cumulative mass of the eroded particles (soil+cement)

Particle agglomeration and adhesion necessitate greater shear stresses for detachment from a surface in contact with water flow, hence reducing the erodibility of treated soil relative to untreated soil. The initial effects of incorporating cement or lime primarily induce clay particle flocculation, which may enhance the early strength of the treated samples, subsequently leading to pozzolanic reactions that establish bonds between soil particles and inhibit their separation (Lemaire 2013; Indraratna 1991). Consequently, it is essential to exert supplementary hydraulic shear stress to disrupt these connections and facilitate the detachment of smaller agglomerates or individual soil particles.

IV.2.2.3 The outflow

IV.2.2.3.1 Untreated soil

Regarding the untreated soil (Figure IV-9), the outflow was at 47 L/h in the beginning of the experiment; then, under the increase in hydraulic loads, the shear stress augments, resulting in particle detachment and consequently in enlargement of the hole diameter, which leads to a larger outflow that ends up at 459 L/h. This ultimately depends on the cumulative eroded particle mass, or weight. In other words, a rise in cumulative eroded particle mass is associated with a greater outflow.

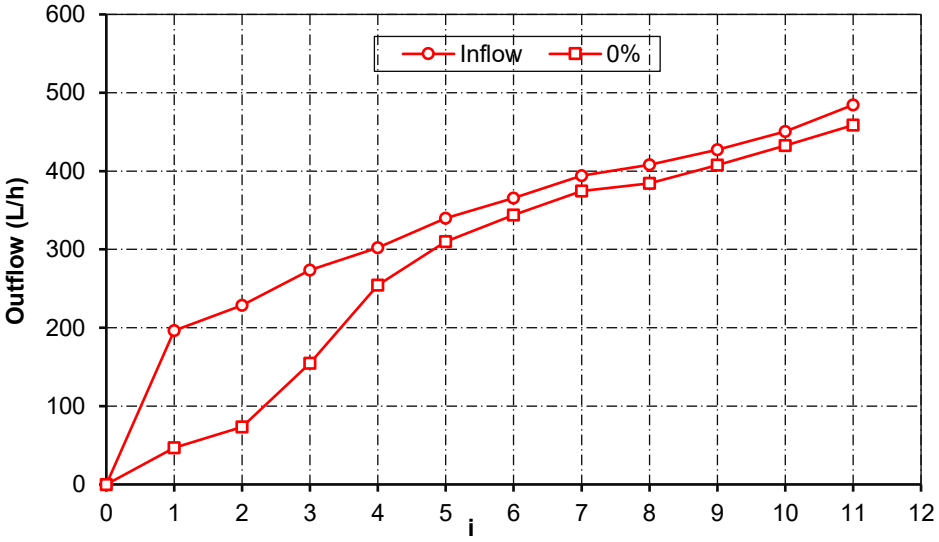

Figure IV-9: Evolution of the outflow during the charging phase on untreated soil

IV.2.2.3.2 Lime treated

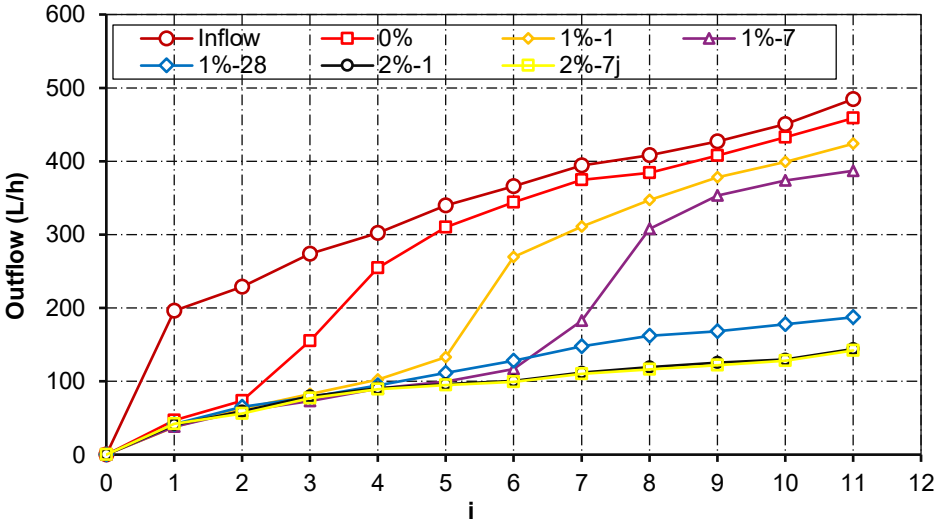

Figure IV-10: Evolution of the outflow during the charging phase on 1/2% treated soil

The graphs show the relationship between outflow (L/h) and curing time (days) for different lime dosages. Overall, the graph suggests that increasing lime dosage and curing time both contribute to lower outflow rates. The specific relationship between these factors depends on the specific lime dosage and curing time.

The outflow curves illustrated in Figure IV-10 indicate a reduction in outflow relative to the hydraulic gradient, affected by elevated lime doses and curing time. It depends on the instantaneous diameter of the hole. The untreated soil has considerable particle mass loss; hence, the hole's diameter progressively enlarges with the increase in hydraulic load, leading to

heightened water outflow. Conversely, the treated soil, owing to its enhanced resistance, restricts both particle detachment and outflow. Consequently, the outflow progressively diminishes with an increase in dosage and curing duration.

IV.2.2.3.3 Cement treated

Post-treatment, figures IV-11, 12, and 13 indicate a reduction in outflow as a function of the hydraulic gradient, influenced by elevated cement doses and extended curing time. The outflow is dependent on the current diameter of the hole. In the erosion test, the untreated soil experiences substantial particle mass loss; hence, the hole's diameter progressively enlarges with the increase in hydraulic load, leading to high water outflow. Conversely, the treated soil, due to its enhanced resistance, restricts both particle detachment and outflow. Consequently, as the dosage and treatment duration increase, the outflow progressively diminishes.

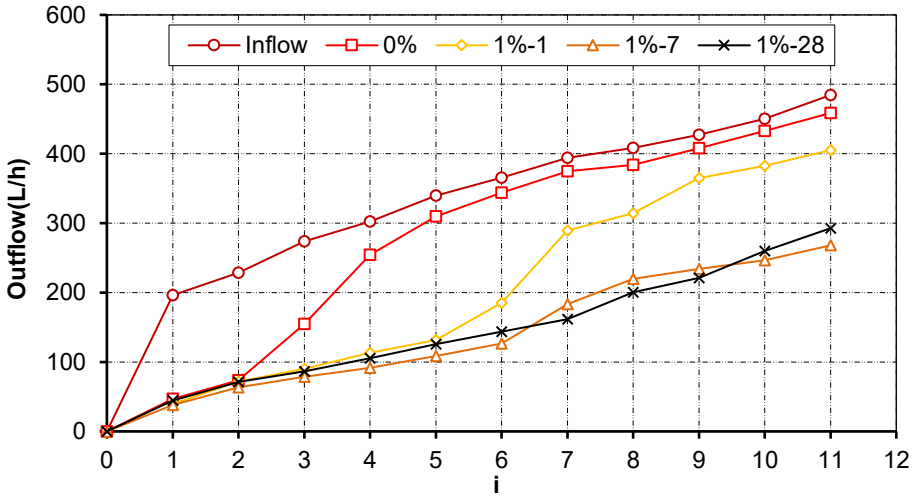

Figures IV-11: Evolution of the outflow during the charging phase on 1% cement treated soil

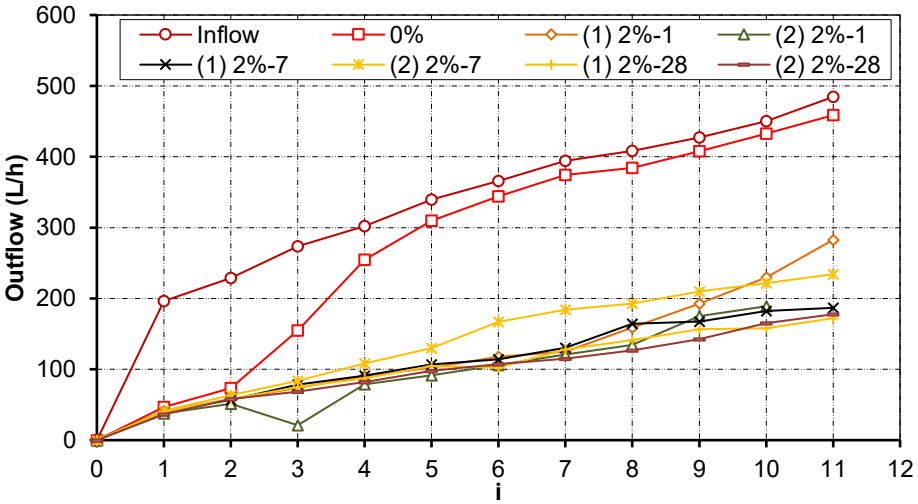

Figures IV-12: Evolution of the outflow during the charging phase on 2% cement treated soil

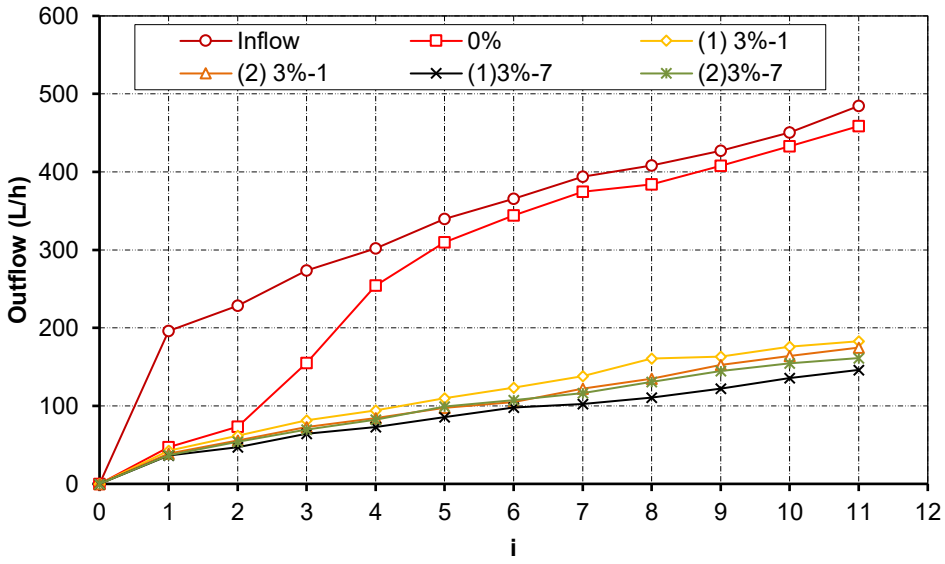

Figures IV-13: Evolution of the outflow during the charging phase on 3% cement treated soil

IV.2.2.4 The hole's final diameter

The final diameter of the hole, which is derived from the mean diameter of the extracted paraffine and is shown in Figure IV.14 as (D0) and Figure IV-15 (a, b, c), can also be used to assess the soil's resistance to piping erosion. Figure IV.14 and Figure IV-15 (d) show that the final diameter of the untreated soil is 16 mm. This diameter decreases as the dosage of cement or lime is increased and the curing time is extended, reaching a low value of 4,02 mm (Figure IV-15 (e)) and 4,04 mm (Figure IV-15 (f)), which correspond to the case of soil treated with 3% cement and 2% lime after 7 days, respectively.

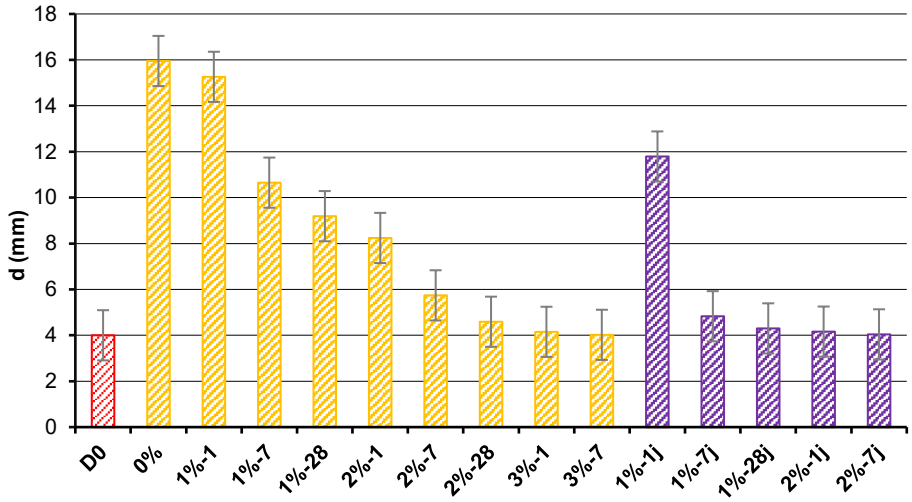

Figure IV-14: Evolution of the final hole diameter size compared with the initial one

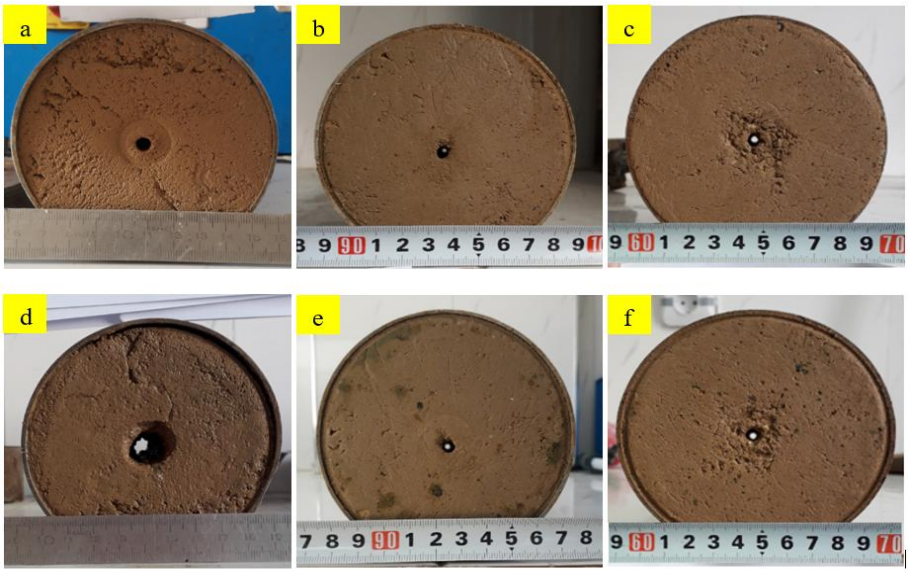

Figure IV-15: Initial and final hole diameter: (a) untreated soil before test, (b) 2% lime treated soil before test, (c) 3% cement treated soil before test, (d) untreated soil after test, (e) 2% lime treated soil after test, (f) 3% cement treated soil after test

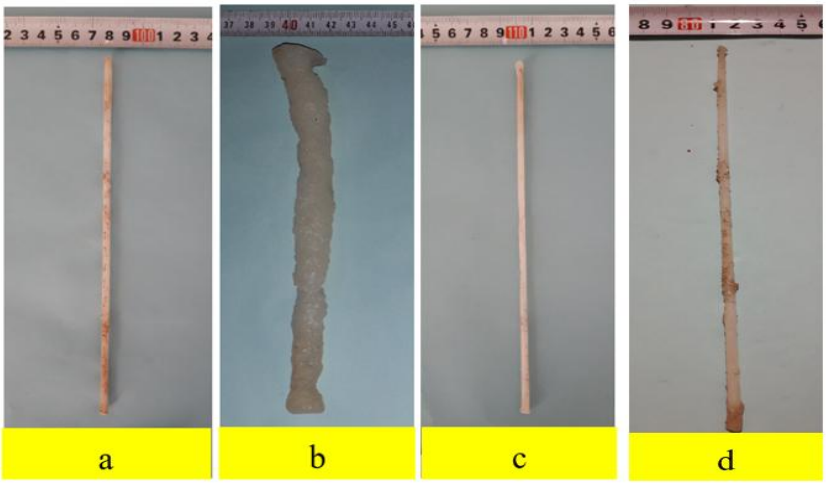

Figure IV-16: Shape of extracted paraffin: (a) before test, (b) after test for untreated soil, (c) after test for 3%-7 cement treated soil, (d) after test for 2%-7 lime treated soil

Additional photographs depicting the final diameter and configuration of the extracted paraffin are presented in the annexe.

IV.3 Immersion test (crumb test)

The immerged specimen created with untreated soil withstands only 12 hours until the full collapse (Figure IV-17 a). It should be emphasized that the detachment of the particles from the solid mass began from the first minutes of the specimen being immersed in water. After approximately one hour of immersion, the disintegration of larger flocs was noted, devoid of the turbidity effect characterized by a halo of suspended particles surrounding the sample, in

contrast to the experiments conducted by Elandaloussi (2015); however, this effect was observed after five hours, when the specimen was fully dispersed.

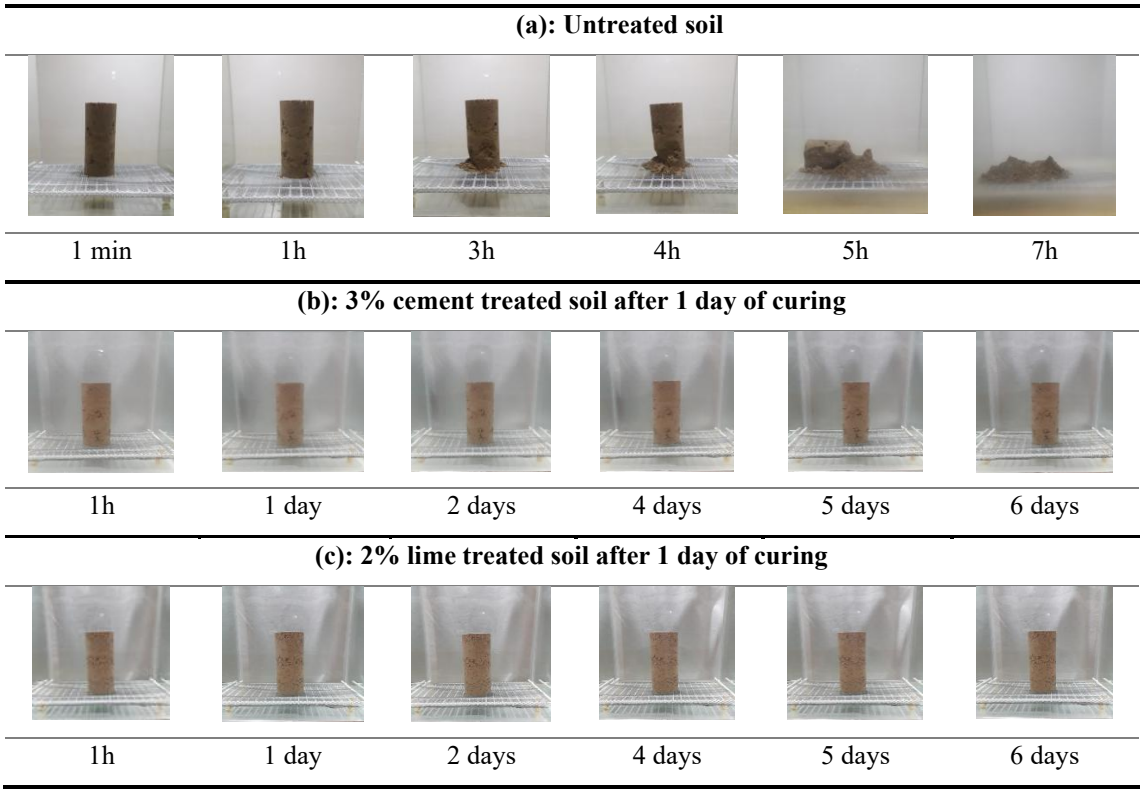

Figure IV-17: Shape of immerged sample: (a) untreated soil, (b) 3% cement treated soil, (c) 2% lime treated soil

Conversely, the samples treated with 3% cement and 2% lime remain manifestly unflawed after only 24 h of curing, maintaining their original form throughout 6 days of immersion (Figure IV-17 (b, c)), with minimal, if any, detachment of agglomerate mass. This corroborates the findings regarding the treated soil's resistance to erosion. More photos about other scenarios are illustrated in the annexe.

IV.3.1 Emitted particles

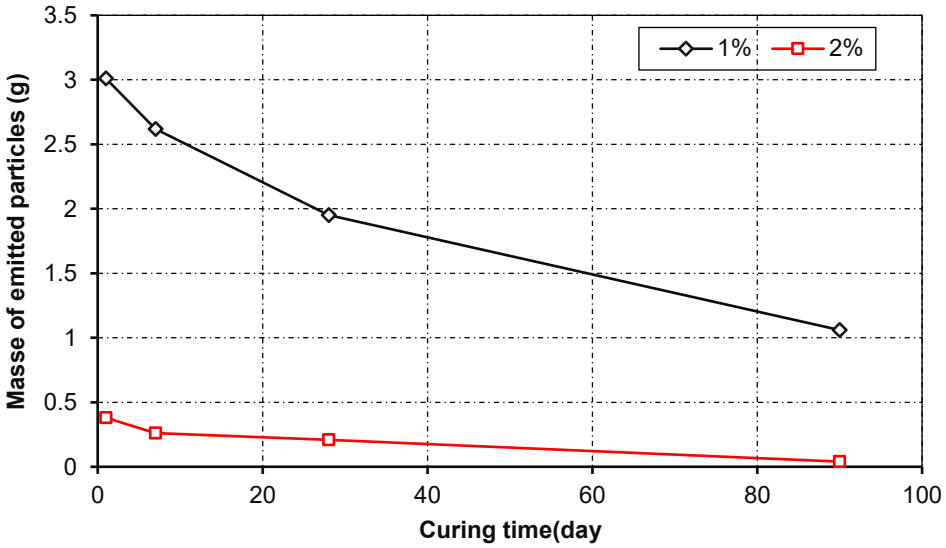

Figure IV-18: Mass of emitted particles during 6 days of immersion in water of lime treated sample

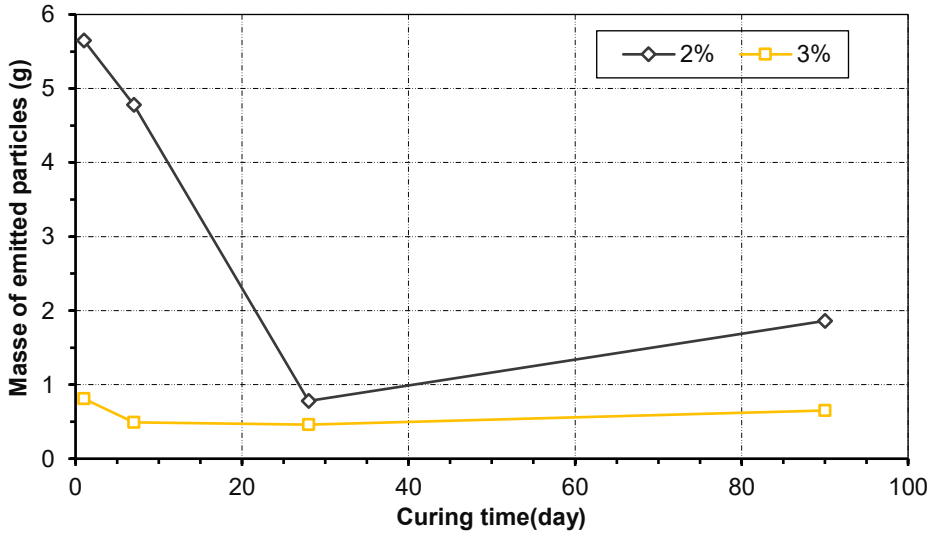

Figure IV-19: Mass of emitted particles during 6 days of immersion in water of cement treated sample

The results indicate the treatment's effectiveness after one day, demonstrating the mitigation of the soil's dispersive nature and its erosion susceptibility, thereby confirming that initial chemical reactions were responsible for reducing erosion at a short curing duration.

With a very low detachment of agglomerates mass even negligible (Figure IV-18) and (Figure IV-19), this confirms the obtained results of treated soil insensitivity against erosion.

IV.4 Triaxial tests (CU)

Triaxial tests evaluate the enhancement of mechanical properties in compacted soil pre- and post-treatment, providing a better understanding of cement and lime action on the mechanical characteristics of the soil. The subsequent results were derived from consolidated undrained (CU) tests conducted within the normally consolidated domain on both natural soil and soil treated with 3% cement and 2% lime. These proportions were selected as optimal for effective soil stabilization against erosion, and then the improvement in mechanical properties is evaluated.

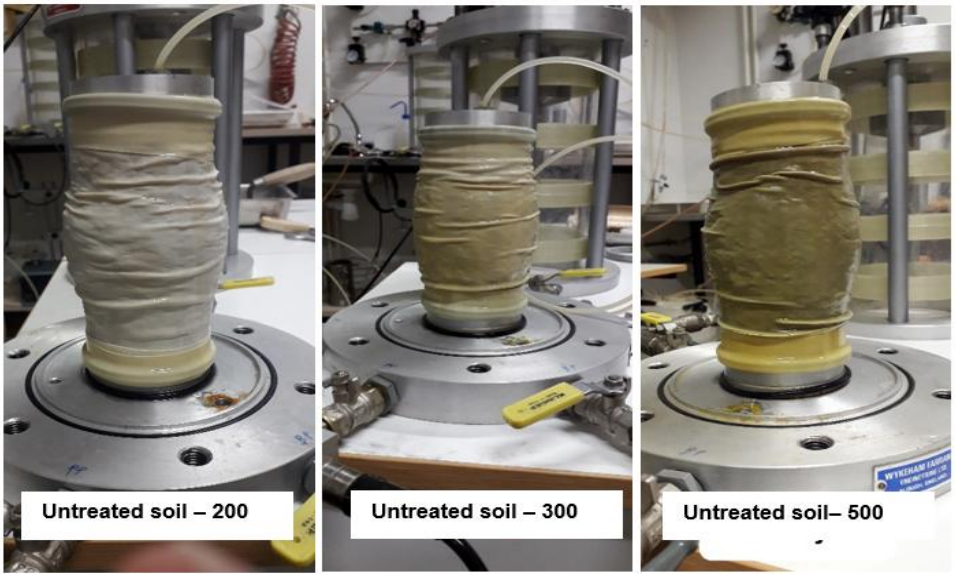

Figure IV-20: Untreated specimen after test

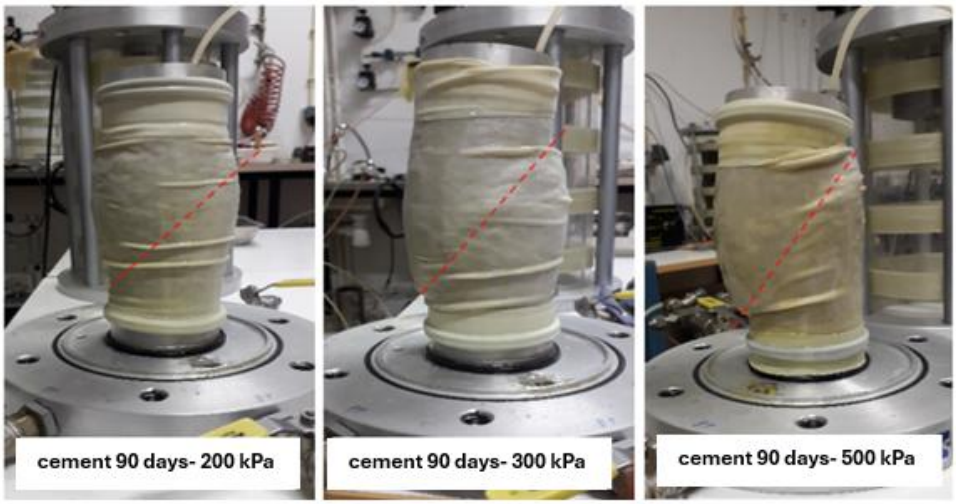

Figure IV-21: Cement treated specimen after test (3%-90 days)

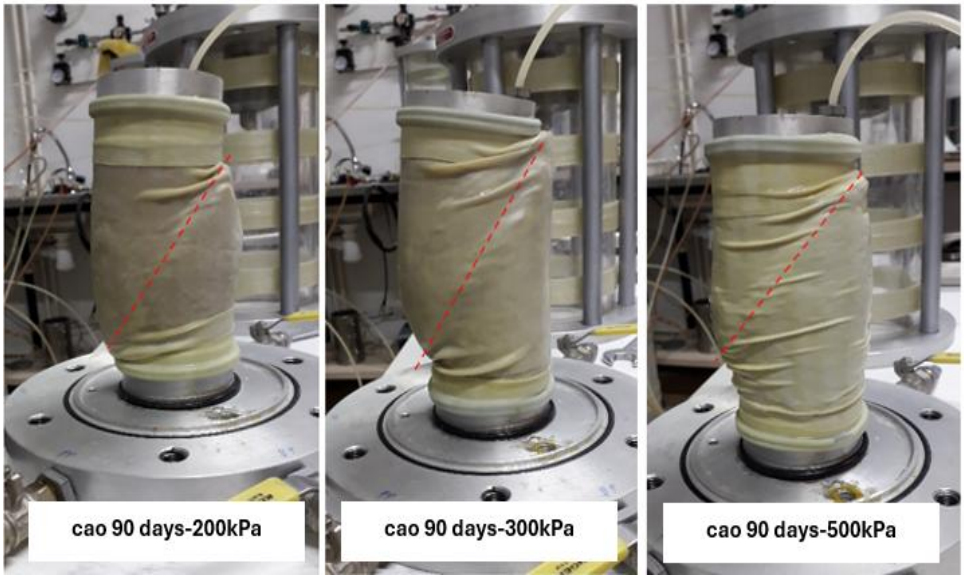

Figure IV-22: Lime treated specimen after test (2%-90 days)

Figures IV-20 depict specimens subjected to the triaxial test for untreated soil, while Figures IV-21 and IV-22 illustrate specimens subjected to the triaxial test for soil treated with 3% cement and 2% lime, respectively, after 90 days of curing, where a shear plane is observable. Further specimens with varying curing durations related to cement-treated soil and lime-treated soil, respectively are presented in the annexe.

IV.4.1 Cement treated soil

When comparing the treated specimens to the untreated ones (Figure IV-23, Figure IV-24), it is observed that the deviator stress increases progressively with both confinement stress and curing time, resulting in enhanced shear strength of the soil. The deviator stress values recorded for specimens cured for seven days surpass those reported by Sariosseiri and Muhunthan [49] for specimens treated with 5% cement.

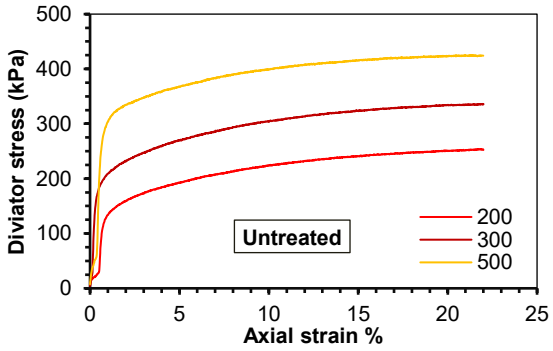

Figure IV-23: Variation of deviator stress versus axial strain (untreated soil)

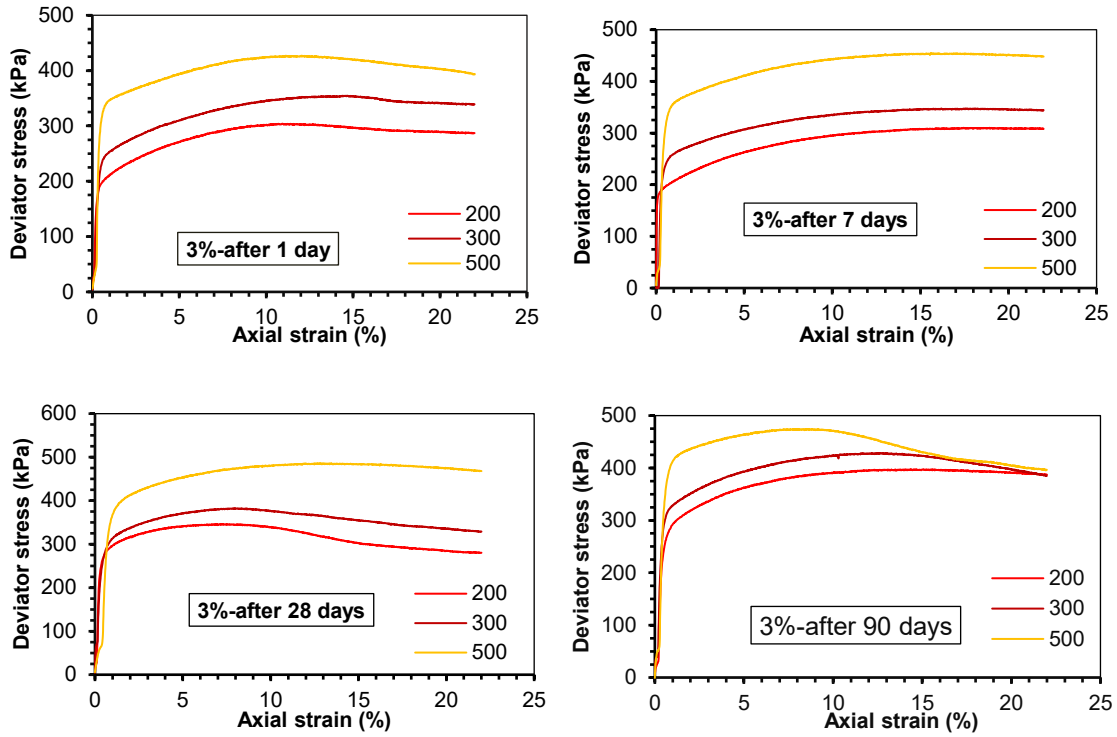

Figure IV-24: Variation of deviator stress versus axial strain (soil+cement)

The parameters of untreated soil were determined as c'= 3.23 kPa for effective cohesion and φ'= 32.26° for the friction angle (Figure IV-25). The friction angle decreases to 30.93° after 24 hours of cement treatment; on the 7th day, it drops to 13.48° and stabilizes around 15° after 28 days of curing. Simultaneously, the soil attains an additional cohesiveness of 17.81 kPa after 24 hours, with considerable increases in cohesion reaching 101.33, 103.75, and 117.79 kPa on the 7th, 28th, and 90th days of curing, respectively. The cohesion value (c') is increased by a factor of 31 after 7 days.

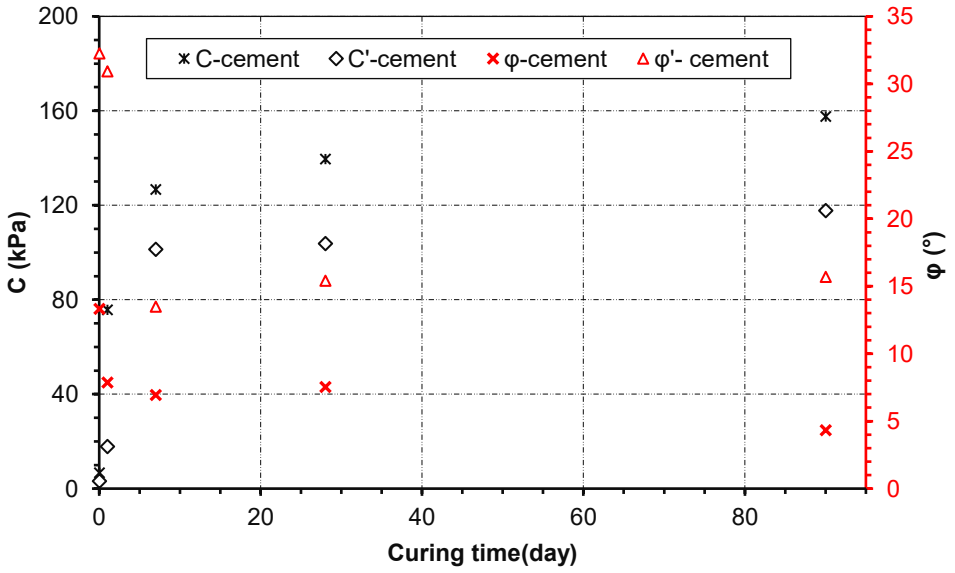

Figure IV-25: Evolution of cohesion and friction angle versus curing time (soil+cement)

Cement hydration rapidly produces calcium hydroxide and elevates pH, creating an alkaline environment. In our study this is confirmed by pH tests (Figure IV-26) as described in standard ASTM D6276. The results Are depicted in Figure IV-27.

Figure IV-26: pH test

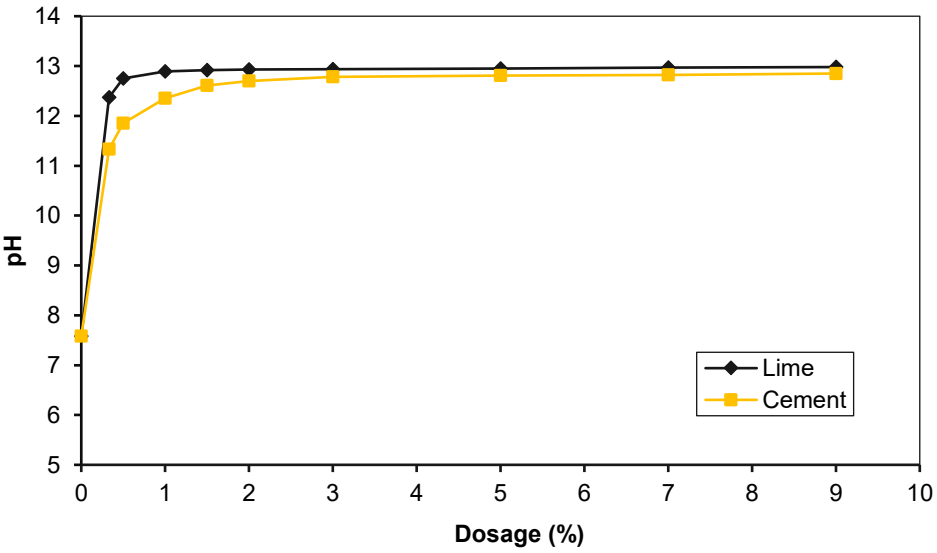

Figure IV-26: pH test curve

Subsequently, pozzolanic reactions occur between calcium hydroxide, siliceous and aluminous components from clays, and water. This process results in a new configuration of soil particles due to the formation of cohesive bonds, which arise from the cementitious connections between calcium silicate hydrate (C-S-H) and calcium aluminate hydrate (C-A-H). Consequently, cohesion increases over curing time, leading to a heightened threshold for shear stress resistance. These findings are confirmed by the TGA analysis presented in the subsequent section. (Yi et all. 2015; Sharma and Sivapullaiah 2016).

The significant improvement in shear strength is attributed to the development of internal cementitious bonding leading to better cohesion (Lemaire et al. 2013). The soil's enhanced

stability shows the beneficial effects of cement addition, which can effectively stabilize and reinforce a dispersed soil by stimulating flocculation in the short term and through its pozzolanic properties in the long term (Jauberthie et al 2010).

IV.4.2 Lime treated soil

Notably, during the same curing duration, the soil treated with lime exhibits superior shear strength compared to that treated with cement (Figure IV-28). The friction angle diminished to 28.92° following 24 hours of lime treatment; on the 7th day, it measured 23.51°, and on the 28th day, it was 20.2°, with a further reduction to 7.7° observed after 90 days. The soil's cohesion attained 66.81 kPa after 24 hours, whereas on the 7th, 28th, and 90th days, the effective cohesion measured 81.47, 115.86, and 174.39 kPa, respectively (Figure IV-29).

The extent of measured cohesion values is significantly above the restrictions encountered on dikes and other hydraulic structures (Herrier et al. 2013).

The lime addition increases the shear strength by both the flocculation process and the formation of cementitious compounds through pozzolanic reactions such as hydrated calcium silicates or hydrated calcium aluminates (C–S–H and C–A–H) which is formed from the dissolution of silica and/or alumina present in the soil, increasing the soil cohesion and its resistance (Locat et al. 1990; Little 1995; Bell 1996; Boardman et al. 2001; Muller 2005; Maubec 2010; Le Runigo et al. 2011; Pomakhina et al. 2012).

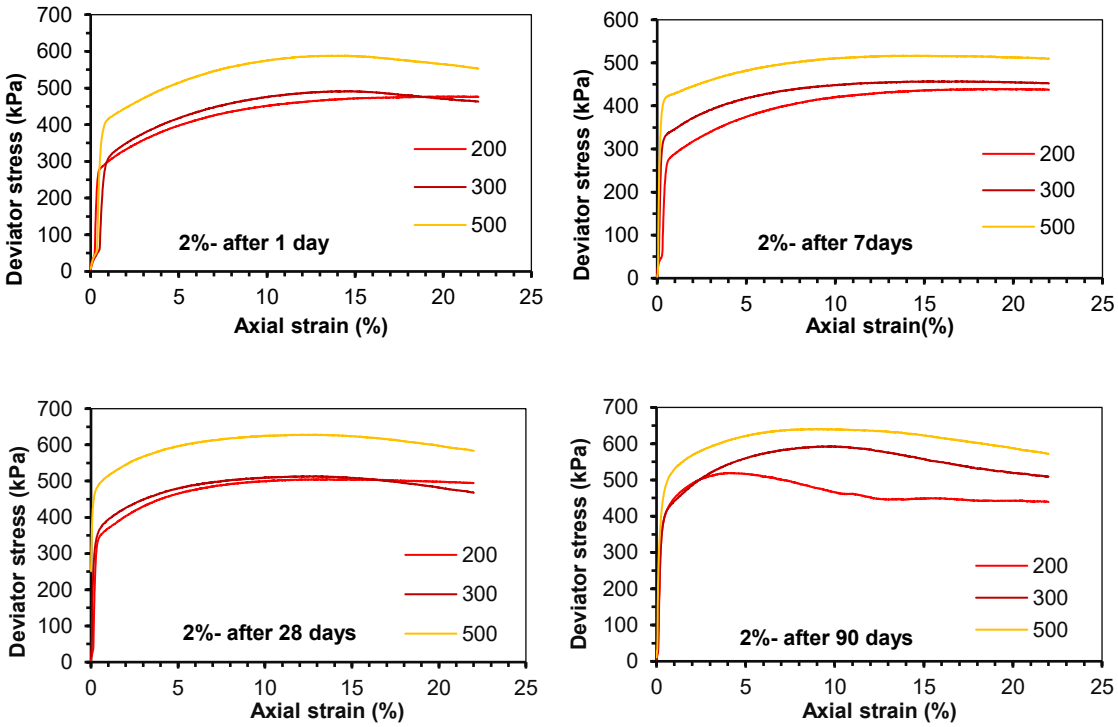

Figure IV-27: Variation of deviator stress versus axial strain (soil+lime)

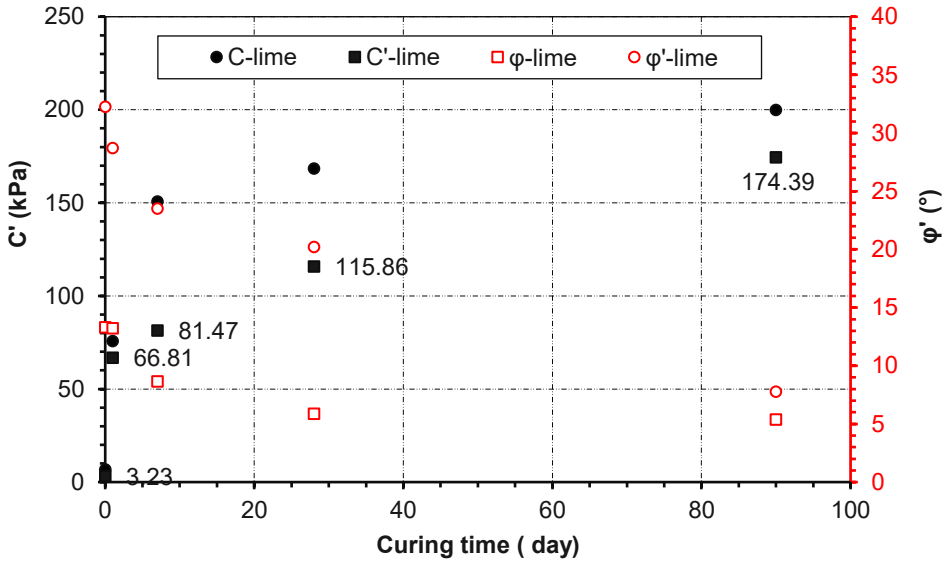

Figure IV-28: Evolution of cohesion and friction angle versus curing time (soil+lime)

IV.5 Microstructure Evolution

IV.5.1 Thermogravimetric Analysis (TGA)

Thermogravimetric Analysis (TGA) is a technique used to evaluate the changes in weight of the sample with heat flow. The substance nature will be designated based on the change in weight (%) and the derivative (D.W.) of this later (%/C°).

The TGA curves for natural and treated soil after 28 days are illustrated in Figure IV-30 and Figure IV-31, depicting the variation in weight and its derivative (D.W.) versus the temperature change. From ambient temperature to 100 °C, the weight loss indicated by the peak in the D.W. curve corresponds to moisture loss. A peak is noted in the temperature range of 115-150 °C, signifying the presence and decomposition of calcium silicate hydrate (CSH) and calcium aluminate hydrate (CAH) (Sharma et al. 2012; Peethamparan et al. 2009).

These changes reflect the preliminary formation of gelatinous products and their later reconfiguration into crystalline minerals. The 410°C peak indicates the dehydroxylation of calcium hydroxide (Ca(OH)2), whereas the temperature range of 700 to 750°C signifies the decomposition of products resulting from the carbonation of calcium hydroxide (Ca(OH)2). The minimal peaks between 450 and 550 correspond to the dehydration of clay minerals and the gelatinous hydration products (Kolias et al. 2005; Macphee et al. 1993).

The weight loss rate between 650 and 750 °C is important. This indicates the abundant presence of calcite CaCO3 in the soil. Matschei et al (2007) disclosed that most, if not all, of this calcite

is reactive and controls the lime distribution, alumina, and sulfate, thereby altering the hydration products mineralogy. Thus, two main functions are attributed to calcite, the first as an active participant in the hydration process, which may explain the optimum stabilization of soil with the addition of low lime or cement content, and the second as an inert filler.

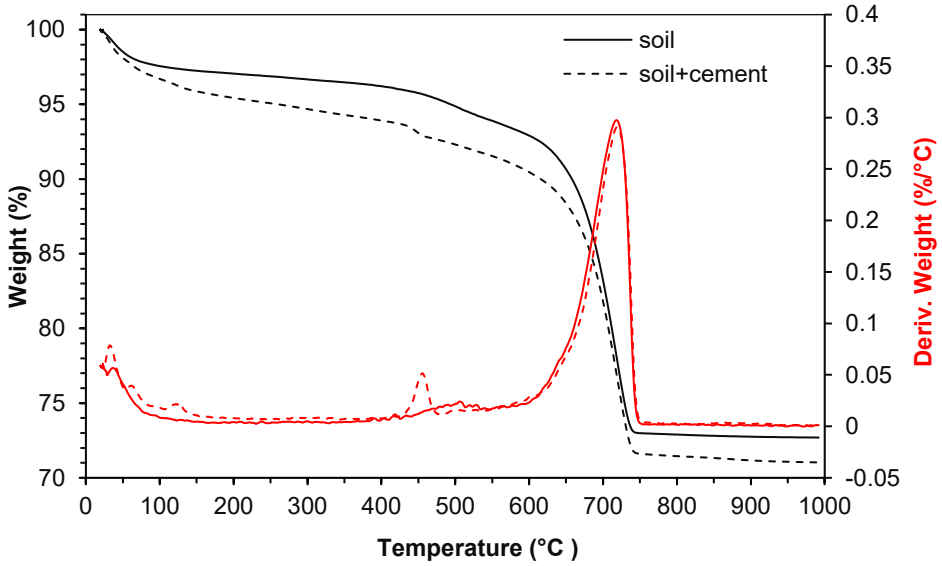

Figure IV-29: TG and DTG curves of soil and (soil+cement)

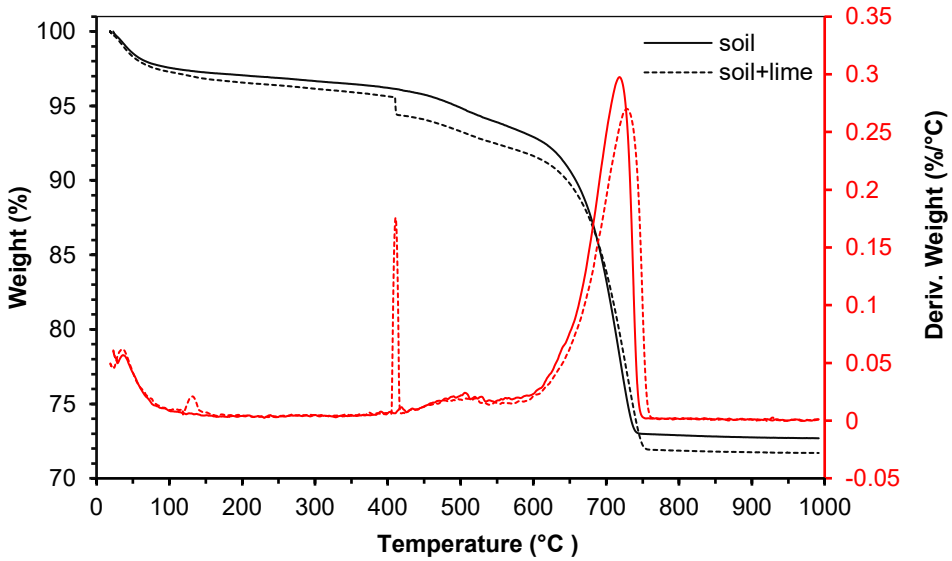

Figure IV-30: TG and DTG curves of soil and (soil+lime)

IV.5.2 SEM Examination

SEM examinations of both natural as well as stabilized soil are presented in Figure IV-32. It demonstrates that they are dissimilar in their microstructure morphology. At low magnification (Figure IV-32 a), untreated soil shows a group of agglomerates of different configurations and

sizes from a few hundred microns to a millimeter. A few numbers of macrospores (inter-aggregate) pores are observed between the agglomerates, resulting from compaction (Nguyen 2015). At a higher magnification (Figure IV-32 b), a tidy association is clearly visible between clay and quartz particles; clay particles form a film that covers the sand grains and connects them tightly. pores around 2 µm can be observed.

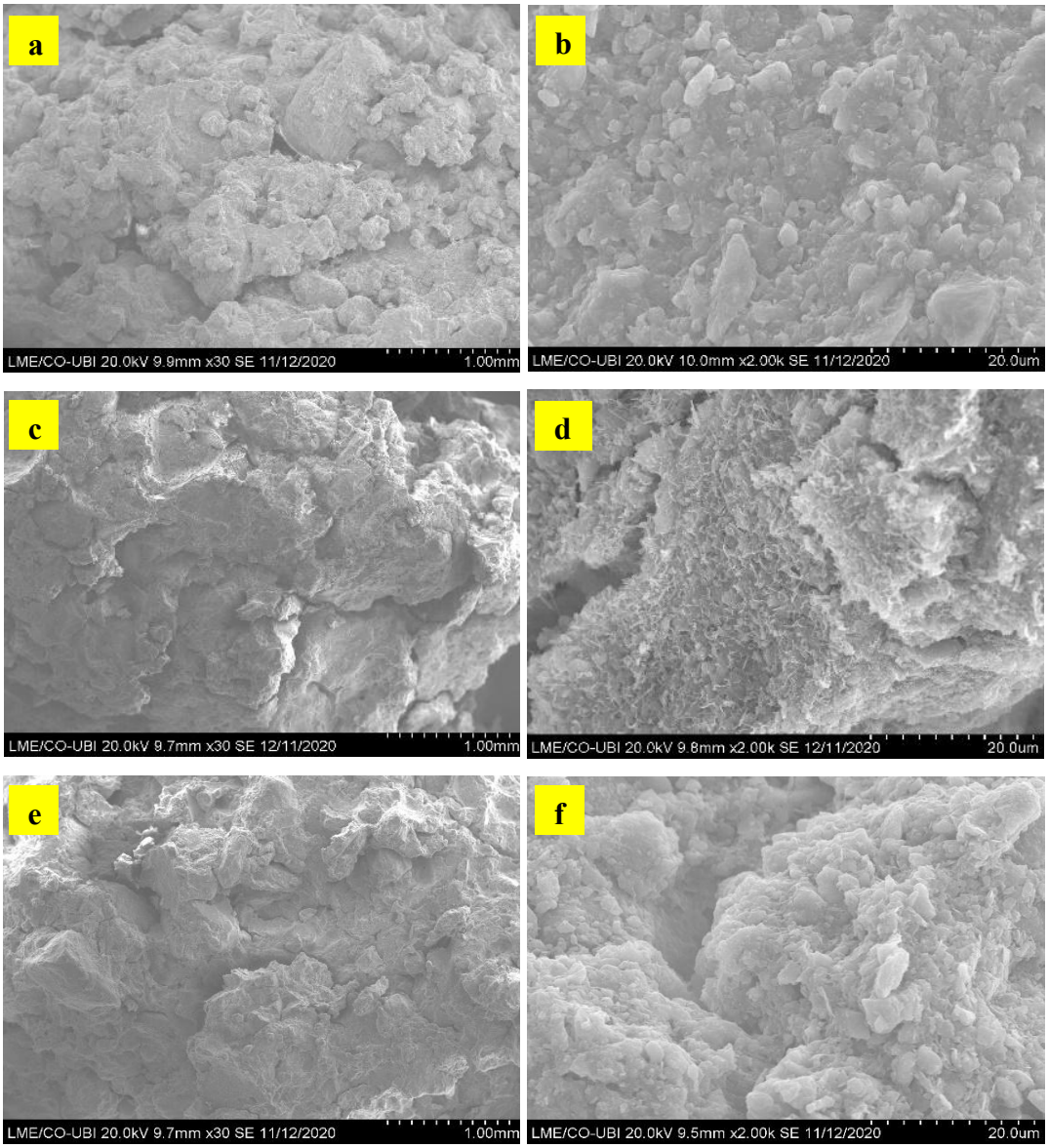

Figure IV-31: SEM pictures. (a) untreated soil 1 mm, (b) untreated soil 20 µm, (c) cement treated soil 1 mm, (d) cement treated soil 20 µm, (e) lime treated soil 1 mm, (f) lime treated soil 20 µm

At low magnification observation of the cement stabilized specimen (Figure IV-32 c), The soil texture is tighter compared with that of the untreated one. A few numbers of pores around 10 µm can be observed. At high magnification (Figure IV-32 d), the pictures show a gel enveloping the agglomerates. EDX analysis of this gel confirms the presence of silicon, calcium, and

aluminum, which constitute the C-(A)-S-H molecule. Featuring micropores approximately 0.1μm in size.

Figure IV-32e illustrates the examination of lime-treated soil at low magnification. A range of agglomerates of various sizes has been identified. At elevated magnification (Figure IV-32f), a granular structure with cementitious gel (CSH) is observed, lime addition forms a film that coats quartz particles. Intra-agglomerates micropores can be seen in this microstructure scan.

IV.5.3 Mercury Intrusion Porosimetry (MIP)

Mercury intrusion porosimetry tests were conducted on both natural and treated samples (incorporating cement and lime) across various curing durations. The findings are depicted in Figure IV-33 and Figure IV-34. The differential mercury intrusion curves presented in (Figure IV-33a) and (Figure IV-34a) demonstrate a trimodal pore size distribution for both untreated and treated soil, comprising a small pore class below 0.9 μm, a medium pore class ranging from 0.9 μm to 10 μm, and a large pore class exceeding 10 μm. According to Lemaire et al. (2013), the small pore diameter class is attributed to intra-agglomerate micropores, while the other classes correspond to inter-agglomerate macropores.

The untreated soil exhibits a predominant pore size family of approximately 3 μm, which governs permeability alongside macropores. The treatment led to a notable increase in the volume of small pores, which progressively decreases with extended curing time due to the deposition of secondary compounds. Nonetheless, the quantity of medium pores diminishes, with the peak shifting to around 6 μm and disappearing after 90 days, which correlates with the development of gelatinous and crystalline hydration products. Furthermore, there is a minor increase in the large pores class on the first day of treatment; however, this amount diminishes over the curing period, returning to levels comparable to untreated soil due to the filling of pores by hydration products.

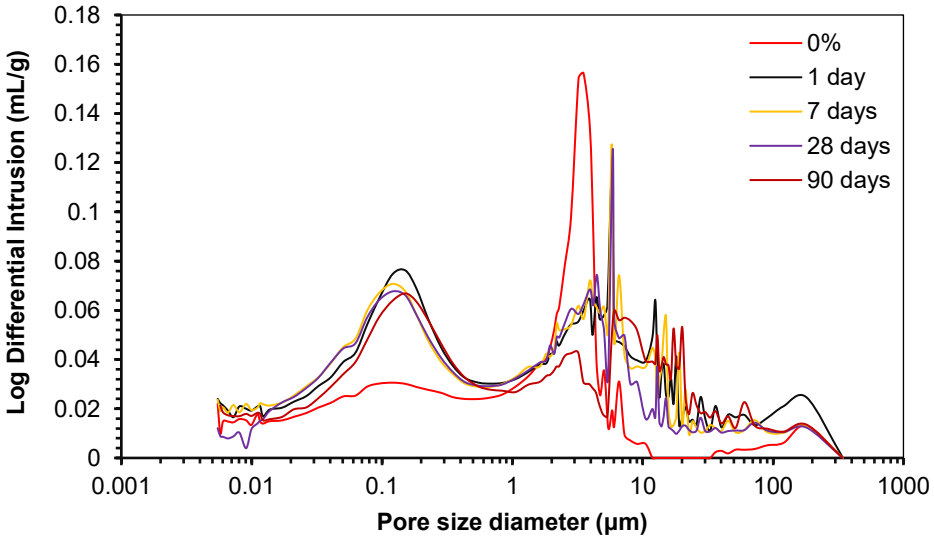

(a)

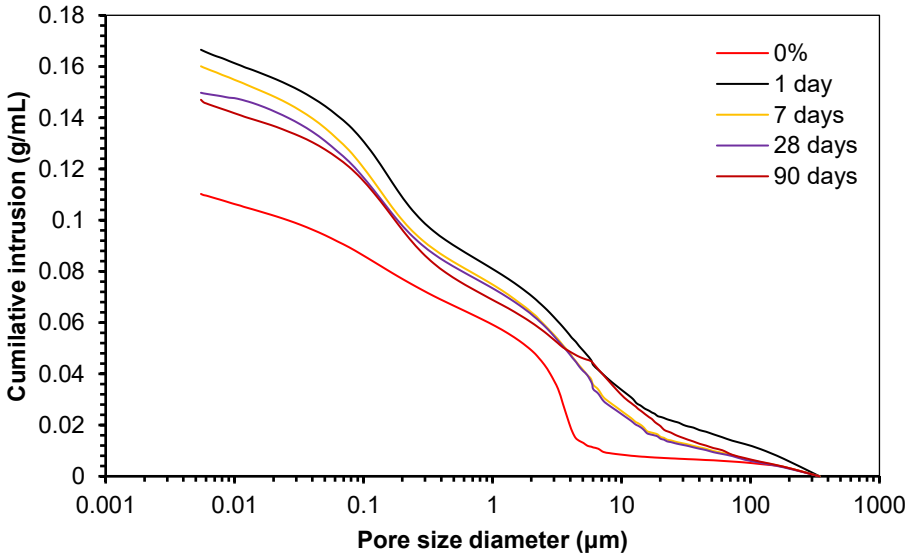

(b)

Figure IV-32: Pore size distribution of untreated and 3% cement stabilized soil

The cumulative mercury intrusion curves, depicted as a function of pore size diameter in Figure IV-48b and Figure IV-49b, indicate that on the first day of curing, the pore volume increases, particularly pronounced in the pore range below 0.9 µm, thereby confirming the variation in dry density following cement incorporation. The volume diminishes gradually over the cure duration.

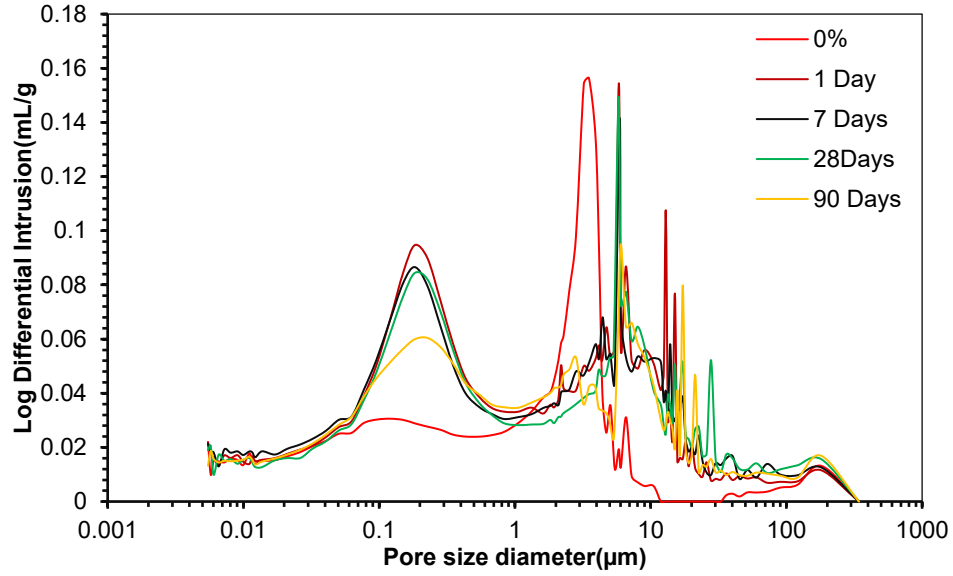

(a)

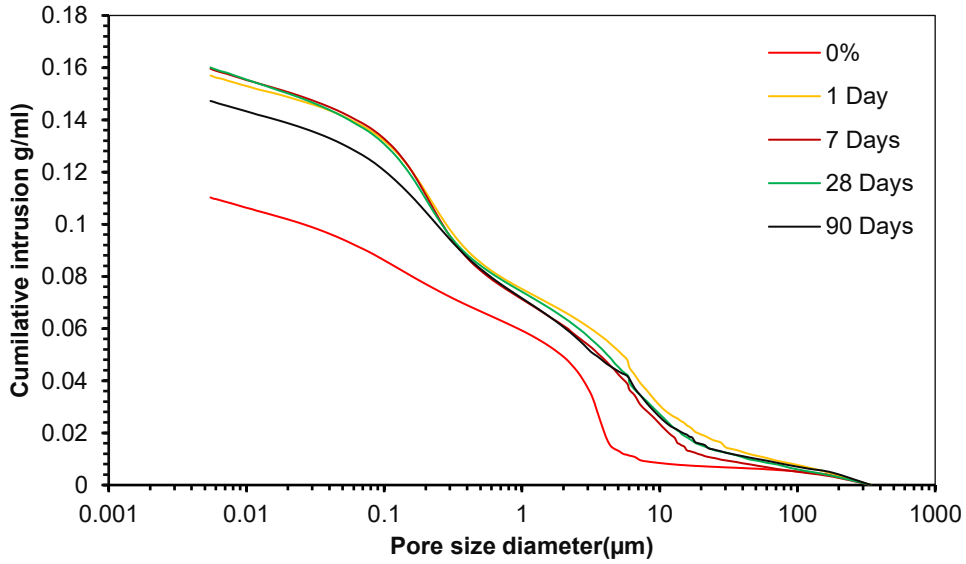

(b)

Figure IV-33: Pore size distribution of untreated and 2% lime treated soil

IV.6 Permeability

This section aims to investigate the impact of cement and lime treatment on soil permeability and its fluctuation over the curing time.

The permeability of untreated soil is measured, revealing an extremely low permeability coefficient. Following separate treatment with cement and lime, the permeability coefficient exhibited a slight increase, however remained comparable to that of the untreated sample; these findings are corroborated by MIP tests conducted before and after treatment.

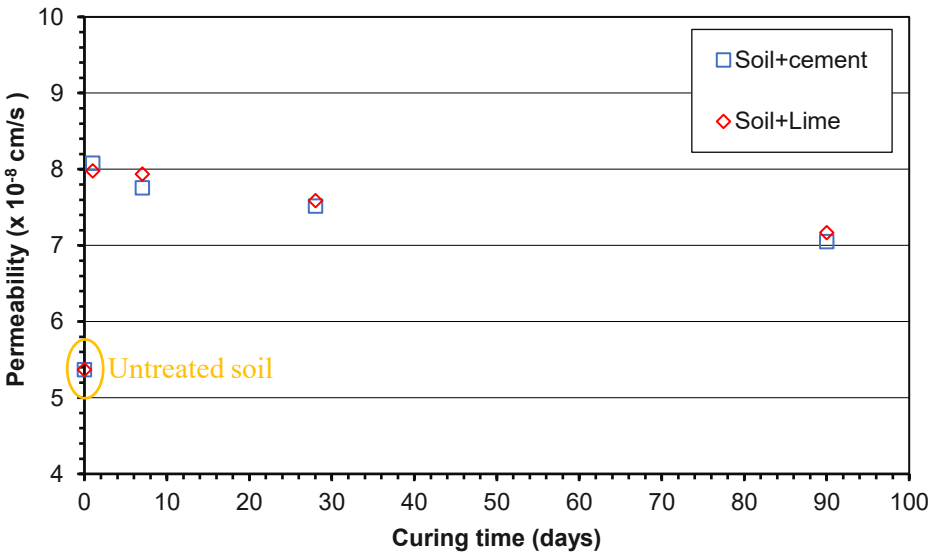

Figure IV-34: hydraulic conductivity

The hydraulic conductivity plots for natural and stabilized soil with cement and lime separately, shown in Figure IV-35, clearly indicate that the permeability of cement-stabilized soil is almost the same of the lime-stabilized soil, although cement-stabilized soil is slightly less permeable. The closeness in hydraulic conductivity values at both cement and lime treatment suggests that the tortuosity or the pore connectivity developed in the stabilized system is similar. Initially After 24 hours of treatment, the hydraulic conductivity values for the cement and lime stabilized soils are a little higher than untreated soil but decrease over the curing time. This effect is the result of the pozzolanic reactions of lime and cement addition at later ages. Stocker (1975) reported that only 0.5% Ca(OH)2 is sufficient to produce a unit layer of reaction product and eliminate swelling. Subsequently, the process becomes diffusion dependent, as Ca2+ ions have to diffuse through the reaction product. As the solubility of calcium hydroxide is low, either formed due to the hydration of Portland cement or supplied by the hydrated lime, Stocker's observation suggests that by increasing the stabilizer dosage, the gain in the long-term properties may not be significantly different. permeability results are supported by MIP results presented in the previous part. The obtained results are attributed to the formation of a new category of pores as a result of the hydration of lime and cement and the pozzolanic reaction products over curing time.

As a conclusion, the hydraulic conductivities of cement and lime-stabilized soil slightly exceed those of natural soil at all cure durations. The permeability of cement-stabilized soil is typically slightly lower than that of lime-stabilized soil; however, after one day of curing, the permeability of cement-treated soil was marginally higher than that of lime-treated soil. The

results are attributed to the development of a new category of pores due to the hydration of lime and cement, as well as the pozzolanic reaction products over the curing period.

IV.7 Conclusion

This chapter aims to assess the hydraulic, mechanical, and microstructural characteristics of the soil before and after treatment with cement and lime, along with its applicability in hydraulic earthworks in southern Algeria. The results indicated that the natural soil exhibited instability concerning internal erosion, with an optimal cement dosage for stabilization being 3% (by dry weight of the soil). Nevertheless, only 2% of lime was adequate to attain comparable internal erosion resistance; this dose is quite low compared to other research, which is especially appealing from an economic standpoint regarding cost reduction for the project. While the treatment's efficacy was evident after one day, a duration of seven days was required to achieve optimal coherence toward piping erosion.

Crumb tests highlighted the contribution of cement and lime addition in the annulation of soil's dispersive character in water after only 24 hours due to the flocculation of the soil particles. Moreover, the gain in mechanical strength post treatment was significant and proportional to curing time, which explains the stability of the treated soil towards internal erosion in the HET tests due to the enhanced cohesion between the soil particles. Microstructure results revealed that the obtained enhancement after cement and lime addition seems to be the consequence of a couple of physicochemical interactions, resulting in the formation a new configuration of agglomerates at first, followed by the precipitation of hydrated compounds. Furthermore, the chemical composition of Biskra's soil provided an appropriate medium for the pozzolanic reactions.

Hydraulic conductivities of cement and lime-stabilized soil are slightly higher than natural soil one at all curing times. The permeability of cement-stabilized soil is generally a little lower than the lime-stabilized soil, except after one day of curing time. Cement treated soil's permeability was somewhat higher than lime treated one. The obtained results are attributed to the formation of a new category of pores as a result of the hydration of lime and cement and the pozzolanic reaction products over the curing period.

In conclusion, it was determined that the locally extracted coarse soils in the Biskra region, deemed waste due to their poor hydraulic and mechanical properties, can be valorized through treatment with minimal quantities of cement or lime, resulting in reduced costs and promoting

sustainable development. The obtained results furnish further data for future investigations into the behavior of compacted coarse soils, addressing the insufficient comprehension of this soil type about its behavior to erosion phenomena in both untreated and treated scenarios.

GENERAL CONCLUSIONS

This study focuses on erosion-related issues affecting numerous earth constructions. Hydraulic structures, including earthen dikes and dams, are mainly compromised by two predominant erosion mechanisms: internal erosion and overflowing. In recent decades, these factors have been recognized as the primary causes of breakdowns in such institutions. Other forms of infrastructure, such embankments for transportation networks, may also be impacted by these occurrences. While not explicitly engineered to endure hydraulic loads, they are often exposed to such stresses. Moreover, the foundations of crossing structures, such as bridge piers, are affected by scouring, resulting in a diminished bearing capacity of the supporting soil due to erosion exacerbated by flow turbulence. These damages generally arise during unusual weather conditions.

In general, "erosion" refers to the processes of particle detachment and movement caused by water flow. It may take place on the surface of the structures or inside their body. Furthermore, even in the absence of flow, dispersion describes the suspension of colloidal clay particles in water. Despite their tight relationship, internal erosion, exterior erosion, and dispersion are complicated processes that rely on a wide range of factors. On the one hand, the large number of affecting elements makes evaluating soil erodibility difficult. However, even under the best circumstances, research attempting to correlate the physical and conventional aspects of soil mechanics with their vulnerability to erosion has revealed limited associations. Therefore, using particular testing techniques to determine erosion sensitivity is crucial.

The objective of the work presented in this thesis was to evaluate the relevance of using lime or cement treatment techniques on coarse soil, initially considered unsuitable for the construction of hydraulic structures, to improve its resistance to internal erosion. This objective also aimed to deepen the understanding of the underlying mechanisms leading to the expected improvements.

The aim of this thesis was to assess the efficacy of lime or cement treatment methods on coarse soil, previously deemed inadequate for hydraulic structure construction, to enhance its resistance to internal erosion. This purpose also sought to enhance comprehension of the fundamental mechanisms behind the anticipated improvements.

The literature review facilitated the analysis of several elements. An advanced investigation was performed on the structural composition, material reuse potential, and prevalent concerns observed. Soil erosion was initially discussed in broad terms before being examined in further detail, concentrating on two specific forms of erosion: internal erosion by piping and erosion through dispersion. Focus was directed towards determining the typologies and characteristics that influence their beginning. The last segment of this research concentrated on current treatments utilizing lime or cement, predominantly implemented on fine, clayey, or silty soils.

This soil posed a risk of internal erosion and dispersion, according to the analysis's findings. A stabilization procedure was taken into consideration in order to guarantee its stability and

We developed a specialized testing apparatus to enhance our comprehension of the mechanics of internal erosion via piping in both natural soil and soil treated with lime or cement. This device, including an erosion cell and a loading tank, facilitates accurate monitoring of flow rates and the mass of eroded particles. An exacting experimental protocol was implemented, and the preliminary results acquired are encouraging.

To ensure the representativeness of our results, a soil sample was collected from the site and subjected to a comprehensive characterization, including granulometric, microstructural, and mineralogical analyses.

Following an in-depth review of the scientific literature and experts' recommendations, we selected lime and cement treatments, two classic soil stabilization methods, for our study. A detailed mineralogical characterization of these materials was conducted in the laboratory.

To understand how compaction degree and initial hole diameter affect soil erosion and dispersion, a parametric study was conducted. results revealed the hydraulic behaviours of the soil:

-The HET tests indicated that the soil is unstable towards internal erosion and smaller diameters and lower dry densities are associated with increased erosion rates.

-Moreover, Results show that Biskra soil's susceptibility to dispersion is strongly linked to its compaction state. Specimens compacted to higher dry densities and lower water contents exhibit more rapid dispersion, particularly when in contact with water, than those with lower dry densities and higher water contents.

An experimental study, based on HET and Crumb tests, was conducted to quantify the influence of various lime or cement dosages and curing times on the properties of treated soil. The results

demonstrated that lime or cement treatment significantly improves the properties of coarse soil, making it more suitable for use in hydraulic structures.

These improvements are quantified in terms of resistance to internal erosion by piping, resistance to dispersion, and shear strength through triaxial testing, with the aim of correlating these parameters and gaining a better understanding of the underlying mechanisms.

Overall, the behaviour of the soil is affected by curing time, and internal erosion resistance rises as the dose of cement or lime is increased.

The treatment not only eliminated piping erosion but also provided the soil with exceptional resistance to dispersion. The treated samples withstood six days of immersion without showing any signs of degradation.

The examination of triaxial test outcomes reveals an enhancement in shear strength from the initial curing period, ascribed to particle flocculation caused by the binder. This trend continues over time owing to the progressive development of cementation products.

The microstructure results indicated that the observed augmentation with the addition of cement and lime is likely due to several physicochemical interactions, leading to the initial creation of a new agglomeration shape, subsequently followed by the precipitation of hydrated compounds. Moreover, the chemical makeup of Biskra's soil offered a suitable environment for pozzolanic reactions.

The hydraulic conductivities of cement and lime-stabilized soil exceed those of natural soil at all cure durations. The permeability of cement-stabilized soil is often slightly lower than that of lime-stabilized soil, except after one day of curing. The permeability of cement-treated soil was marginally greater than that of lime-treated soil. The results are ascribed to the emergence of a novel category of pores due to the hydration of lime and cement, along with the products of the pozzolanic reaction during the curing period.

Finally, it was established that the locally sourced coarse soils in the Biskra region, considered waste due to their inadequate hydraulic and mechanical properties, can be valorized through treatment with minimal amounts of cement or lime, leading to cost reduction and fostering sustainable development. The results provide further information for future studies on the behavior of compacted coarse soils, addressing the inadequate understanding of this soil type about its response to erosion in both untreated and treated conditions.

Perspectives

The findings of this study offer possibilities for several research approaches, the primary ones being as follows:

- Conduct HET tests following 90 and 365-day cure times.
- Implement elevated hydraulic loads, leading to augmented hydraulic gradients
- Enhance the experimental apparatus by implementing an automated loading system including calibrated hydraulic loads, integrated with pressure sensors and a flow meter.
- Set up a mobile jet erosion device (MoJET) to evaluate the reaction of soil to external erosion.
- Carry out other types of treatments, such as those using lignosulfonates, organic products derived from the transformation of plant-based raw materials, or through bio-cementation.

References

AFNOR (1994) NF P 94-093. Sols : Reconnaissance et essais Détermination des références de compactage d'un matériau. *Essai Proctor normal - Essai Proctor modifié.*

AFNOR XP, P. (1999). 94-011. Soils: Reconnaissance and tests: Description identification denomination of soils: Terminology and classification elements, French Association for Standardization.

AFNOR, N. (1992). P94-057-Sols : reconnaissance et essais-Analyse granulométrique des sols-Méthode par sédimentation. *Association Française de Normalisation, Paris, France*.

AFNOR, N. (1994). 94–074 (1994) Sols : Reconnaissance et essais. *Essais à l'appareil triaxial de révolution. Appareillage, Préparation des éprouvettes et Essais (UU), (CU)*.

AFNOR, N. F. Classification des matériaux utilisables dans la construction des remblais et des couches de forme d'infrastructures routières. NF P1992, 11-300.

Al-Amoudi, O. S. B. (2002). Characterization and chemical stabilization of Al-Qurayyah sabkha soil. *Journal of materials in civil engineering*, *14*(6), 478-484.

Al-Mukhtar, M., Lasledj, A., & Alcover, J. F. (2010). Behaviour and mineralogy changes in lime-treated expansive soil at 20 C. *Applied clay science*, *50*(2), 191-198.

Al-Rawas, A. A., Hago, A. W., & Al-Sarmi, H. (2005). Effect of lime, cement and Sarooj (artificial pozzolan) on the swelling potential of an expansive soil from Oman. *Building and environment*, *40*(5), 681-687.

ANCOLD (1978) Bulletin of the Australian national committee on large dams*, issue no. 51, p 55.*

ASTM D 4221–99. Standard test method for dispersive characteristics of clay soil by double hydrometer. *ASTM International*, 2005.

ASTM D 6572 - 00 (2000). Standard test method for determining dispersive characteristics of clayey soil by the Crumb Test, *Annual Book of ASTM Standards*, vol. 04.08.

ASTM D4221, (2011), "Standard Test Method for Dispersive Characteristics of Clay Soil by Double Hydrometer" *Annual Book of ASTM Standards, Vol. 04.08, ASTM International, West Conshohocken, PA, pp. 1–4.*

ASTM D4647, (2006) e1, "Standard Test Method for Identification and Classification of Dispersive Clay Soils by the Pinhole Test" *Annual Book of ASTM Standards, Vol. 04.08, ASTM International, West Conshohocken, PA, pp. 1–11.*

ASTM STANDARD D 6572-13. Standard test methods for determining dispersive characteristics of clayey soils by the crumb test. *American Society for Testing and Materials, 2013.*

Beguin, R. (2011). *Etude multi-échelle de l'érosion de contact au sein des ouvrages hydrauliques en terre* (Doctoral dissertation, Université de Grenoble).

Bell, F. G. (1996). Lime stabilization of clay minerals and soils. *Engineering geology*, *42*(4), 223-237.

Bellezza, I., & Fratalocchi, E. (2006). Effectiveness of cement on hydraulic conductivity of compacted soil–cement mixtures. *Proceedings of the Institution of Civil Engineers-Ground Improvement*, *10*(2), 77-90.

Belmana, A., Elandaloussi, R., Feia, S., Dadda, A., & Mellas, M. Elaboration of an experimental protocol for erosion behavior improvement of a coarse soil. *ALERT Geomaterials*, 58.

Belmana, A., Mellas, M., & Cavaleiro, V. (2024). Assessment of Coarse Soil's Stability Towards Internal Erosion Case of Biskra's Dam Soil. *Civil And Environmental Engineering*, *20*(1), 332-348.

Bendahmane, F., Marot, D., & Alexis, A. (2008). Experimental parametric study of suffusion and backward erosion. *Journal of geotechnical and geoenvironmental engineering*, *134*(1), 57-67.

Bennabi, A., Herrier, G., & Lesueur, D. (2016). Lime treated soil erodibility investigated by EFA erosion testing.

Bertaina, G. (2009) « Mise en charge hydraulique de remblais d'infrastructures de transport – Rapport de synthese *», Rapport de synthese de l'operation de recherche 11M053, CETE de Lyon, référence du dossier Dossier n°40200-1*, pp. 155

Bhattacharja, S., & Bhatty, J. (2003). Comparative performance of portland cement and lime stabilization of moderate to high plasticity clay soils. *Portl. Cem. Assoc*, *2066*, 60-67.

Bhuvaneshwari, S., Soundra, B., Robinson, R. G., & Gandhi, S. R. (2007, August). Stabilization and microstructural modification of dispersive clayey soils. In *1st International Conference on Soil and Rock Engineering, Srilankan Geotechnical Society, Columbo, Srilanka* (pp. 1-7).

Blai, J. P. (2005). Typologie de l'érosion interne et érosion interne des digues fluviales: une courte revue bibliographique. *Sciences Eaux & Territoires*, (Spécial Ingénieries-EAT-21), 65-70.

Boardman, D. I., Glendinning, S., & Rogers, C. D. F. (2001). Development of stabilisation and solidification in lime–clay mixes. *Geotechnique*, *51*(6), 533-543.

Bonelli, S., & Brivois, O. (2008). The scaling law in the hole erosion test with a constant pressure drop. *International Journal for numerical and analytical methods in geomechanics*, *32*(13), 1573-1595.

Bouzid, T. (2010). Les barrages et la politique hydraulique en Algérie: état, diagnostic et perspectives d'un aménagement durable (Dissertation doctorale). *Université de Mentouri–Constantine*.

Briaud, J. L. (2008). Case histories in soil and rock erosion: Woodrow wilson bridge, brazos river meander, normandy cliffs, and new orleans levees. *Journal of Geotechnical and Geoenvironmental Engineering*, *134*(10), 1425-1447.

Cabane, N. (2004). *Sols traités à la chaux et aux liants hydrauliques: Contribution à l'identification et à l'analyse des éléments perturbateurs de la stabilisation* (Doctoral dissertation, Université Jean Monnet-Saint-Etienne).

Catton, M. D. (1940). Research on the physical relations of Soil & Soil Mechanics. *Highway Research Board Bulletin*, *23*, 831-855.

Chevalier, C., Haghighi, I., Pham, T. L., & Reiffsteck, P. (2010). Two complementary tests for characterizing the soil erosion. In *Scour and Erosion* (pp. 152-161).

Chew, S. H., Kamruzzaman, A. H. M., & Lee, F. H. (2004). Physicochemical and engineering behavior of cement treated clays. *Journal of geotechnical and geoenvironmental engineering*, *130*(7), 696-706.

Choquette, M., Bérubé, M. A., & Locat, J. (1987). Mineralogical and microtextural changes associated with lime stabilization of marine clays from eastern Canada. *Applied clay science*, *2*(3), 215-232.

Coats, A. W., & Redfern, J. P. (1963). Thermogravimetric analysis. A review. *Analyst*, *88*(1053), 906-924.

COMITE TECHNIQUE PERMANENT DES BARRAGES. *Le barrage de Perrégaux, 1998. L'illustration N° 4423 du 10.12.1927, les eaux déchaînées en Oranie* »

Consoli, N. C., Cruz, R. C., Floss, M. F., & Festugato, L. (2010). Parameters controlling tensile and compressive strength of artificially cemented sand. *Journal of Geotechnical and Geoenvironmental Engineering*, *136*(5), 759-763. doi:10.1061/(asce)gt.1943-5606.0000278.

Consoli, N. C., Foppa, D., Festugato, L., & Heineck, K. S. (2007). Key parameters for strength control of artificially cemented soils. *Journal of geotechnical and geoenvironmental engineering*, *133*(2), 197-205.

Craig, R.F. (2004) *"Craig's Soil Mechanics",* CRC Press, 7th edition, 264 pages, London UK

Croft, J. B. (1967). The influence of soil mineralogical composition on cement stabilization. *Geotechnique*, *17*(2), 119-135.

Cuisinier, O. (2002). *Comportement hydromécanique des sols gonflants compactés* (Doctoral dissertation, Institut National Polytechnique de Lorraine-INPL).

Currin, D. D., Allen, J. J., & Little, D. N. (1976). *Validation of soil stabilization index system with manual development* (No. FJSRL-TR-76-0006).

De Vries, G., Koelewijn, A. R., & Hopman, V. (2010). Ijkdijk full scale underseepage erosion (piping) test: evaluation of innovative sensor technology. In *Scour and erosion* (pp. 649-657).

Demmak A., 1982. *Contribution à l'étude de l'érosion et des transports solides en Algérie. Thèse de Doc. Ing. Paris VI*; 323p.

Diamond, S., White, J. L., & Dolch, W. L. (1963). Transformation of clay minerals by calcium hydroxide attack. *Clays and clay minerals*, *12*, 359-379.

Eades, J. L., & Grim, R. E. (1960). Reaction of hydrated lime with pure clay minerals in soil stabilization. *Highway Research Board Bulletin*, (262).

Eid, J., Taibi, S., Lefebvre, A., & Dandjinou, J. E. (2015, May). Le traitement des Sols à la chaux et aux liants hydrauliques-Aspects Physico-Chimiques. In *Rencontres Universitaires de Génie Civil*.

Elandaloussi, R., Bennabi, A., Dupla, J. C., Canou, J., Benamar, A., & Gotteland, P. (2019). Effectiveness of lime treatment of coarse soils against internal erosion. *Geotechnical and Geological Engineering*, *37*, 139-154.

Eskisar, T. (2015). Influence of cement treatment on unconfined compressive strength and compressibility of lean clay with medium plasticity. *Arabian Journal for Science and Engineering*, *40*, 763-772.

Fiche DRM *« le risque rupture de barrage »* - *DIMENC* – 2014

Fry, J. J., Vogel, A., Royet, P., & Courivaud, J. R. (2012). Dam failures by erosion: lessons from ERINOH data bases. *ICSE6 Paris*, 273-280.

Gaagai, A., Boudoukha, A., & Benaabidate, L. (2020). Failure simulation of Babar dam–Algeria and its impact on the valley downstream section. *Journal of Water and Land Development*, (44), 75-89. [CrossRef]

Ghadakpour, M., Choobbasti, A. J., & Kutanaei, S. S. (2020). Experimental study of impact of cement treatment on the shear behavior of loess and clay. *Arabian Journal of Geosciences*, *13*, 1-11.

Haghighi, I. (2012). *Caractérisation des phénomènes d'érosion et de dispersion: développement d'essais et applications pratiques* (Doctoral dissertation, Université Paris-Est).

Haghighi, I., Chevalier, C., Duc, M., Guédon, S., & Reiffsteck, P. (2013). Improvement of hole erosion test and results on reference soils. *Journal of Geotechnical and Geoenvironmental Engineering*, *139*(2), 330-339.

Heize, J. O. (1975). "Turbulence" New York, McGraw-Hill.

Herrier G., Chevalier C., Froumentin M., Cuisinier O., Bonelli S., Fry J.J. (2012a). Lime treated soil as an erosion-resistant material for hydraulic earthen structures. *6th International Conference on Scour and Erosion*, Paris, France, No. 290 pp. 8.

Herrier, G., & Bonelli, S. (2014). Internal erosion resistance of soils treated with lime: An evolutive benefit. *Scour and Erosion*, 73-80.

Hilt, G. H., & Davidson, D. T. (1960). Lime fixation in clayey soils. *Highway Research Board Bulletin*, (262).

Hjulström, F. (1935). *Studies of the morphological activity of rivers as illustrated by the River Fyris* (Doctoral dissertation, The Geological institution of the University of Upsala). No. 25, Chapter 3, 221.

Ho, C. C. (2007). *The erosion behavior of revetment using geotextile* (Doctoral dissertation, Université Joseph-Fourier-Grenoble I).

Holmgren, G. G. S., & Flanagan, C. P. (1977). Factors affecting spontaneous dispersion of soil materials as evidenced by the crumb test. In *Dispersive clays, related piping, and erosion in geotechnical projects*. ASTM International.

Howard, A. K., & Bara, J. P. (1976). *Lime stabilization on Friant-Kern canal*. Earth Sciences Branch, Division of General Research, Engineering and Research Center, US Department of the Interior, Bureau of Reclamation. Report No. REC-ERC-76-20, 1976, Denver CO: 53 p.

ICOLD (1990). "*Dispersive soils in embankment dams: review" Bulletin 77*. International Commission on Large Dams

Indraratna, B., Muttuvel, T., & Khabbaz, H. (2009). Modelling the erosion rate of chemically stabilized soil incorporating tensile force–deformation characteristics. *Canadian Geotechnical Journal*, *46*(1), 57-68.

Indraratna, B., Muttuvel, T., Khabbaz, H., & Armstrong, R. (2008). Predicting the erosion rate of chemically treated soil using a process simulation apparatus for internal crack erosion. *Journal of Geotechnical and Geoenvironmental Engineering*, *134*(6), 837-844.

Indraratna, B., Nutalaya, P., & Kuganenthira, N. (1991). Stabilization of a dispersive soil by blending with fly ash. *Quarterly Journal of Engineering Geology and Hydrogeology*, *24*(3), 275-290.

Ingles, O. G., Lang, J. G., & Richards, B. G. (1968). Pre-equilibrium Observations on the Reconstructed Flagstaff Gully Dam.

Jafer, H. M., Atherton, W., Ruddock, F., & Loffil, E. Comparative study of the performance of Ordinary Portland Cement and a waste material in soft soil stabilisation.

James, K. M., & Kenichi, S. (1976). Fundamentals of soil behavior. *University of California, Berkeley, John Wily and sons, Incl*.

James, K. M., & Kenichi, S. (1976). Fundamentals of soil behavior. *University of California, Berkeley, John Wily and sons, Incl*.

Jauberthie, R., Rendell, F., Rangeard, D., & Molez, L. (2010). Stabilisation of estuarine silt with lime and/or cement. *Applied Clay Science*, *50*(3), 395-400.

Jerez Loaiza, A. (2011) « Étude et suivi de l'érosion des sédiments en contexte immergé » Mémoire de fin d'études, Institut National des Sciences Appliquées, Rennes, France

Kavak, A., & Akyarlı, A. (2007). A field application for lime stabilization. *Environmental geology*, *51*, 987-997.

Kheir, R. B. (2002). *Etude des risques d'érosion hydrique des sols par télédétection et SIG: application à une région représentative du Liban* (Doctoral dissertation, Institut national agronomique Paris-Grignon (1971-2006)).

Khemissa, M., & Mahamedi, A. (2014). Cement and lime mixture stabilization of an expansive overconsolidated clay. *Applied Clay Science*, *95*, 104-110.

Kolias, S., Kasselouri-Rigopoulou, V., & Karahalios, A. (2005). Stabilisation of clayey soils with high calcium fly ash and cement. *Cement and Concrete Composites*, *27*(2), 301-313.

Laouina, A., Nafaa, R., Coelho, C., Chaker, M., Carvalho, T., Boulet, A. N., & Ferreira, A. (2000). Gestion des eaux et des terres et phénomènes de dégradation dans les collines de Ksar El Kebir, Maroc. *Bull. Réseau Erosion*, 256-274.

Lashkaripour, G. R., & Soloki, H. R. (2003, April). Study of Dispersive Soils in Sistain Plain in the East of Iran. In *12th Asian Regional Conference on Soil Mechanics &Geotechnical Engineering, ed. Leung et al, Singapore*.

Le Runigo, B., Ferber, V., Cui, Y. J., Cuisinier, O., & Deneele, D. (2011). Performance of lime-treated silty soil under long-term hydraulic conditions. *Engineering geology*, *118*(1-2), 20-28.

Lemaire, K., Deneele, D., Bonnet, S., & Legret, M. (2013). Effects of lime and cement treatment on the physicochemical, microstructural and mechanical characteristics of a plastic silt. *Engineering Geology*, *166*, 255-261.

Lim, S. S. (2006). *Experimental investigation of erosion in variably saturated clay soils* (Doctoral dissertation, UNSW Sydney).

Little, D. N. (1995). *Stabilization of pavement subgrades and base courses with lime*.

Locat, J., Bérubé, M. A., & Choquette, M. (1990). Laboratory investigations on the lime stabilization of sensitive clays: shear strength development. *Canadian Geotechnical Journal*, *27*(3), 294-304.

Luino, F., Tosatti, G., & Bonaria, V. (2014). Dam failures in the 20th century: nearly 1000 avoidable victims in Italy alone. *Journal of Environmental Science and Engineering*, *3*(1), 19-31.

MacPhee, D. E., Black, C. J., & Taylor, A. H. (1993). Cements incorporating brown coal fly ash from the Latrobe Valley region of Victoria, Australia. *Cement and concrete research*, *23*(3), 507-517.

Matschei, T., Lothenbach, B., & Glasser, F. P. (2007). The role of calcium carbonate in cement hydration. *Cement and concrete research*, *37*(4), 551-558.

Maubec, N. (2010). *Approche multi-échelle du traitement des sols à la chaux-Etudes des interactions avec les argiles* (Doctoral dissertation, Université de Nantes).

MEDDI, M. (1992). *Hydropluviometrie et transport solide dans le bassin versant de l'oued mina (algerie)| Theses. fr* (Doctoral dissertation, Université Louis Pasteur (Strasbourg)(1971-2008)).

Mehenni, A., Cuisinier, O., & Masrouri, F. (2016). Impact of lime, cement, and clay treatments on the internal erosion of compacted soils. *Journal of Materials in Civil Engineering*, *28*(9), 04016071.

MELBOUCI, B. (2017). Etude comparative du traitement du sol marneux a la chaux et au ciment dans les couches de forme des chaussées. *Communication Science and technology*, *18*.

Millogo, Y., & Morel, J. C. (2012). Microstructural characterization and mechanical properties of cement stabilised adobes. *Materials and structures*, *45*, 1311-1318.

MITCHELL, James Kenneth, SOGA, Kenichi, et al. Fundamentals of soil behavior. New York : John Wiley & Sons, 2005.

Morsli, B. (2015). Ruissellement et érosion en zone de montagne, analyse des facteurs conditionnels cas des Monts de Beni Chougrane–Algérie. *Unpublished doctoral thesis). University of Tlemcen, Alegria*.

Müller, C. J. (2005). *Pozzolanic activity of natural clay minerals with respect to environmental geotechnics* (Doctoral dissertation, ETH Zurich).

Nguyen, T. T. H. (2015). *Stabilisation des sols traités à la chaux et leur comportement au gel* (Doctoral dissertation, Université Paris-Est).

Nussbaum, P. J., & Colley, B. E. (1971). *Dam construction and facing with soil-cement* (p. 111). Skokie, IL: Portland Cement Association.

Osula, D. O. A. (1996). A comparative evaluation of cement and lime modification of laterite. *Engineering geology*, *42*(1), 71-81.

Paaswell, R. E. (1973). Causes and mechanisms of cohesive soil erosion: The state of the art. *Special report*, *135*, 52-74.

Pakbaz, M. S., & Alipour, R. (2012). Influence of cement addition on the geotechnical properties of an Iranian clay. *Applied Clay Science*, *67*, 1-4.

Park Y. (2003). Investigation of the ability of filters to stop erosion through cracks in dams. *PhD Thesis*, Virginia Polytechnic Institute and State University, USA.

Peethamparan, S., Olek, J., & Diamond, S. (2009). Mechanism of stabilization of Na-montmorillonite clay with cement kiln dust. *Cement and Concrete research*, *39*(7), 580-589.

Perry, J. P. (1977). Lime treatment of dams constructed with dispersive clay soils. *Transactions of the ASAE*, *20*(6), 1093-1099.

Pham, T. L. (2008). *Erosion et dispersion des sols argileux par un fluide* (Doctoral dissertation, Ecole des Ponts ParisTech).

PHAM, T. L., CHEVALIER, C., DUC, M., REIFFSTECK, P., & GUEDON, S. (2008). Development of a new test to characterize dispersion of soil. In *4th international conference on scour and erosion (ICSE). Tokyo, Japan*.

Pomakhina, E., Deneele, D., Gaillot, A. C., Paris, M., & Ouvrard, G. (2012). 29Si solid state NMR investigation of pozzolanic reaction occurring in lime-treated Ca-bentonite. *Cement and Concrete Research*, *42*(4), 626-632.

Prusinski, J. R., & Bhattacharja, S. (1999). Effectiveness of Portland cement and lime in stabilizing clay soils. *Transportation research record*, *1652*(1), 215-227.

Rajasekaran, G. (2005). Sulphate attack and ettringite formation in the lime and cement stabilized marine clays. *Ocean engineering*, *32*(8-9), 1133-1159.

Ranaivomanana, H., & Razakamanantsoa, A. (2018). Toward a better understanding of the effects of cement treatment on microstructural and hydraulic properties of compacted soils. In *MATEC Web of Conferences* (Vol. 163, p. 06007). EDP Sciences.

Rao, S. N., & Rajasekaran, G. (1996). Reaction products formed in lime-stabilized marine clays. *Journal of geotechnical engineering*, *122*(5), 329-336.

Raudkivi, A. J. (1998). Loose boundary hydraulics, Balkema, Rotterdam, The Netherlands.

Reddi, L. N., & Bonala, M. V. (1997). Critical shear stress and its relationship with cohesion for sand. kaolinite mixtures. *Canadian geotechnical journal*, *34*(1), 26-33.

Rekik, B., Boutouil, M., & Pantet, A. (2009). Geotechnical properties of cement treated sediment: influence of the organic matter and cement contents. *International Journal of Geotechnical Engineering*, *3*(2), 205-214.

Roose, E., ARABI, M., BRAHAMIA, K., CHEBBANI, R., MAZOUR, M., & MORSLI, B. (1996). Érosion en nappe et ruissellement en montagne méditerranéenne algérienne.

Sail, Y. (2012). *Caractérisation exprérimentale de l'érosion de volume de matériaux pulvérulents* (Doctoral dissertation, Ecole centrale de Nantes).

Sanchez, R. L., Strutynsky, A. I., & Silver, M. L. (1983). *Evaluation of the erosion potential of embankment core materials using the laboratory triaxial erosion test procedure*. US Army Engineer Waterways Experiment Station, Geotechnical Laboratory.

Sariosseiri, F., & Muhunthan, B. (2009). Effect of cement treatment on geotechnical properties of some Washington State soils. *Engineering geology*, *104*(1-2), 119-125.

Saussaye, L., BOUTOUIL, M., BARAUD, F., & LELEYTER, L. (2012). Soils treatment with hydraulic binders: physicochemical and geotechnical aspects.

Shan, H. (2010). *Experimental study on incipient motion of non-cohesive and cohesive sediments*. The University of Nebraska-Lincoln.

Sharma, A. K., & Sivapullaiah, P. V. (2016). Ground granulated blast furnace slag amended fly ash as an expansive soil stabilizer. *Soils and Foundations*, *56*(2), 205-212.

Sharma, N. K., Swain, S. K., & Sahoo, U. C. (2012). Stabilization of a clayey soil with fly ash and lime: a micro level investigation. *Geotechnical and geological engineering*, *30*, 1197-1205.

Sherard, J. L., Dunnigan, L. P., & Decker, R. S. (1976). Identification and nature of dispersive soils. *Journal of the Geotechnical Engineering Division*, *102*(4), 287-301.

Sherard, J. L., Dunnigan, L. P., Decker, R. S., & Steele, E. F. (1976). Pinhole test for identifying dispersive soils. *Journal of the Geotechnical Engineering Division*, *102*(1), 69-85.

Shields, A. (1936). Anwendung der Aehnlichkeitsmechanik und der Turbulenzforschung auf die Geschiebebewegung. *PhD Thesis Technical University Berlin*.

Souidi, Z., Hamimed, A., & Donze, F. (2014). Cartographie du risque de dégradation des terres en région semi-aride. Cas des Monts de Beni Chougrane dans le Tell occidental algérien. *Geo-Eco-Trop*, *38*(1), 85-102.

Stocker PT (1975) Diffusion and diffuse cementation in lime and cement stabilised clayey soils chemical aspects. Australian Road Research 5(9) : 6–47.

Tarog, I. (2000). *Perméabilité et érosion interne des mélanges sable-argile: Combustion théorique et expériemntale* (Doctoral dissertation, Lyon, INSA).

Teton Dam Failure Review Group (US). (1977). *Failure of Teton Dam: a report of findings*. Department of the Interior, Bureau of Reclamation, Engineering and Research Center.

TOUAIBIA-LABDANI, B. (2000). *Erosion, transport solide, envasement de barrage* (Doctoral dissertation, INA).

Tran, T. D., Cui, Y. J., Tang, A. M., Audiguier, M., & Cojean, R. (2014). Effects of lime treatment on the microstructure and hydraulic conductivity of Héricourt clay. *Journal of Rock Mechanics and Geotechnical Engineering*, *6*(5), 399-404.

Tran, V. D. (2013). Étude de l'amélioration des sols par traitement à la chaux.

U.S. Department Of Agriculture, Natural Resources Conservation Service. National soil survey handbook, title 430-VI. Available online. Accessed 9/13/2012. ((NRCS, U. (2007). National soil survey handbook, title 430-VI.))

Wan, C. F., & Fell, R. (2002). *Investigation of internal erosion and piping of soils in embankment dams by the soil slot erosion test and the hole erosion test*. University of New South Wales, School of Civil and Environmental Engineering.

Wan, C. F., & Fell, R. (2004). Investigation of rate of erosion of soils in embankment dams. *Journal of geotechnical and geoenvironmental engineering*, *130*(4), 373-380.

Wooltorton, F. L. D. (1955). Engineering pedology and soil stabilization. In *Highway Research Board* (Vol. 108, pp. 29-57).

Yi, Y., Gu, L., & Liu, S. (2015). Microstructural and mechanical properties of marine soft clay stabilized by lime-activated ground granulated blastfurnace slag. *Applied Clay Science*, *103*, 71-76.

Annexe

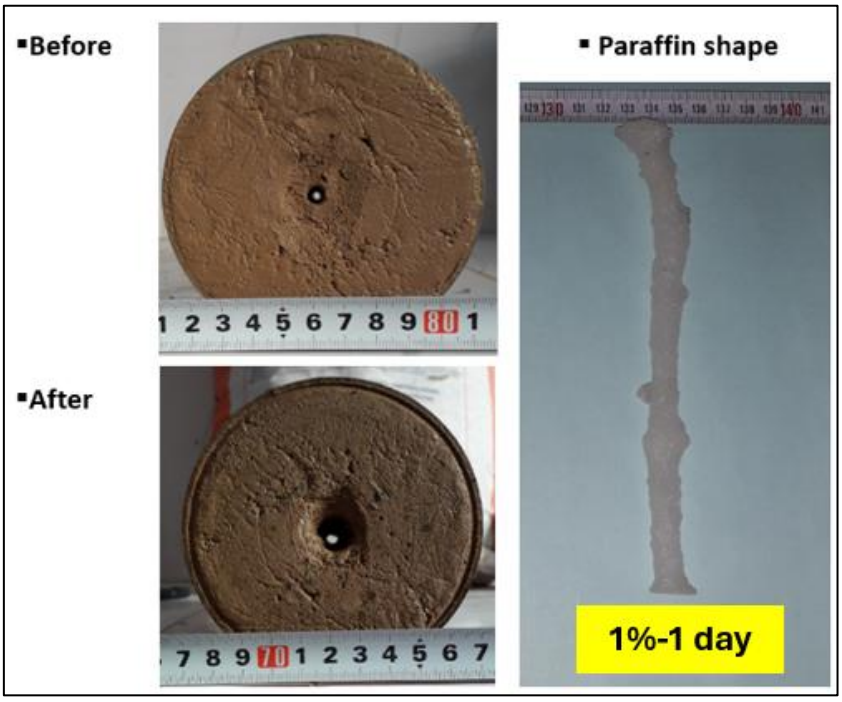

Figure 1: Shape of extracted paraffin (1%-1day lime)

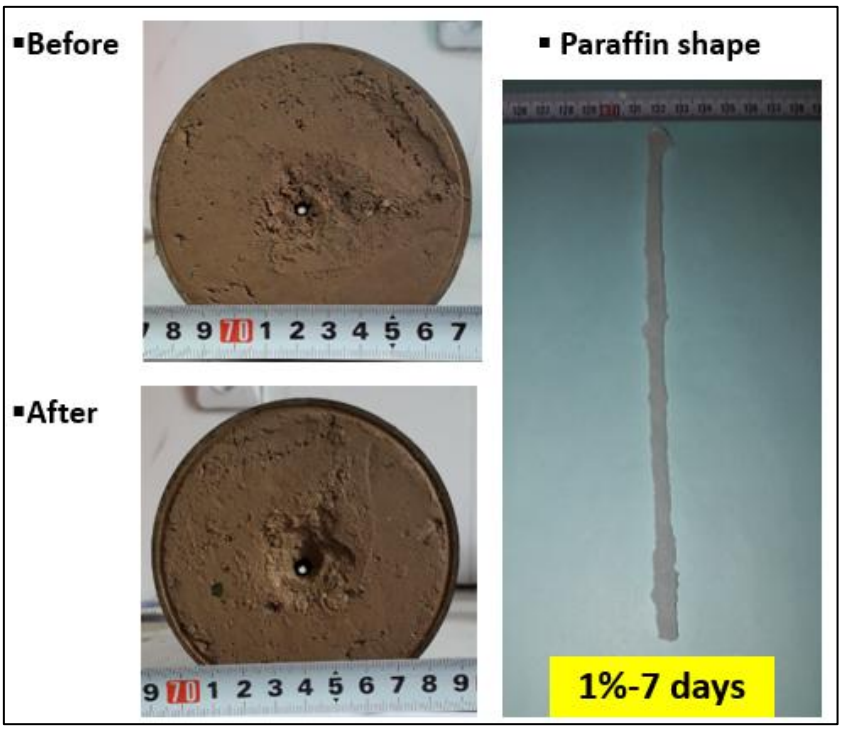

Figure 2: Shape of extracted paraffin (1%-7 day lime)

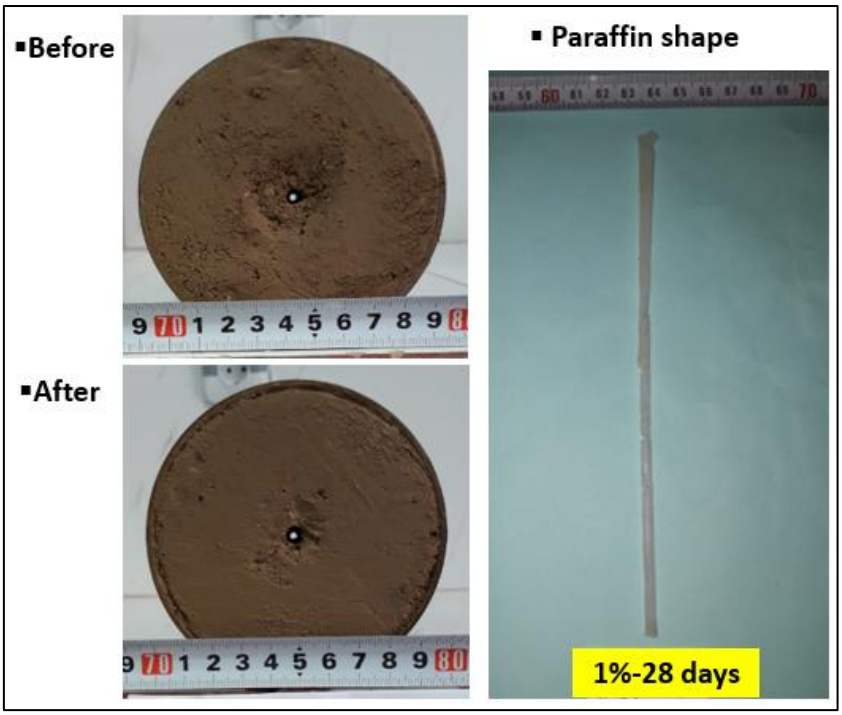

Figure 2: Shape of extracted paraffin (1%-28 day lime)

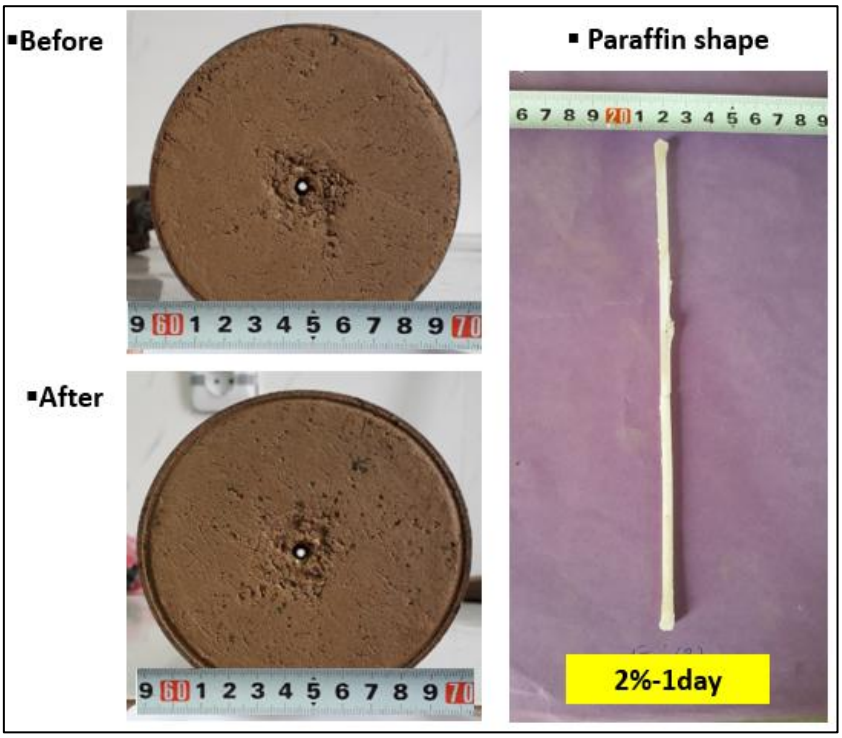

Figure 4: Shape of extracted paraffin (2%-1day lime)

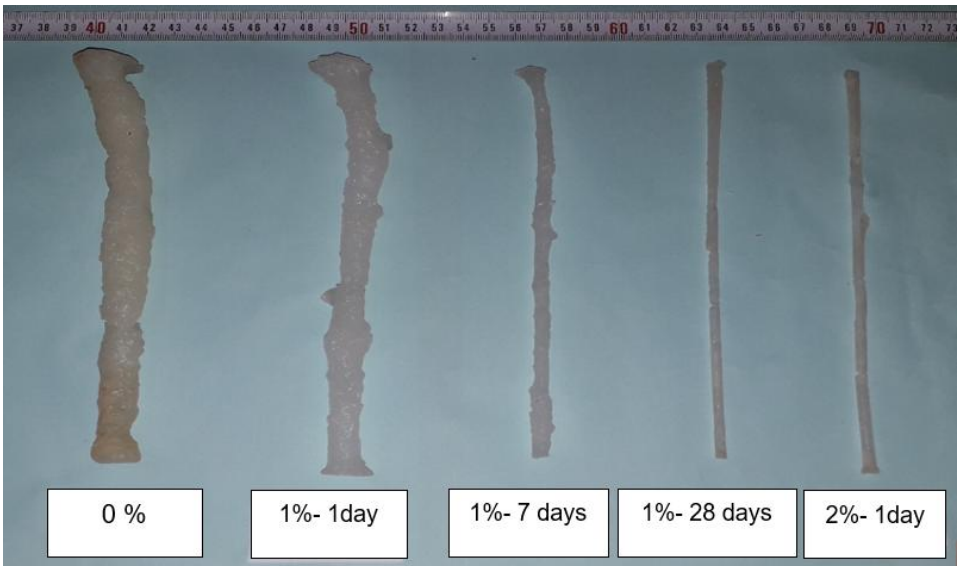

Figure 5: Shape of extracted paraffin for untreated and treated soil

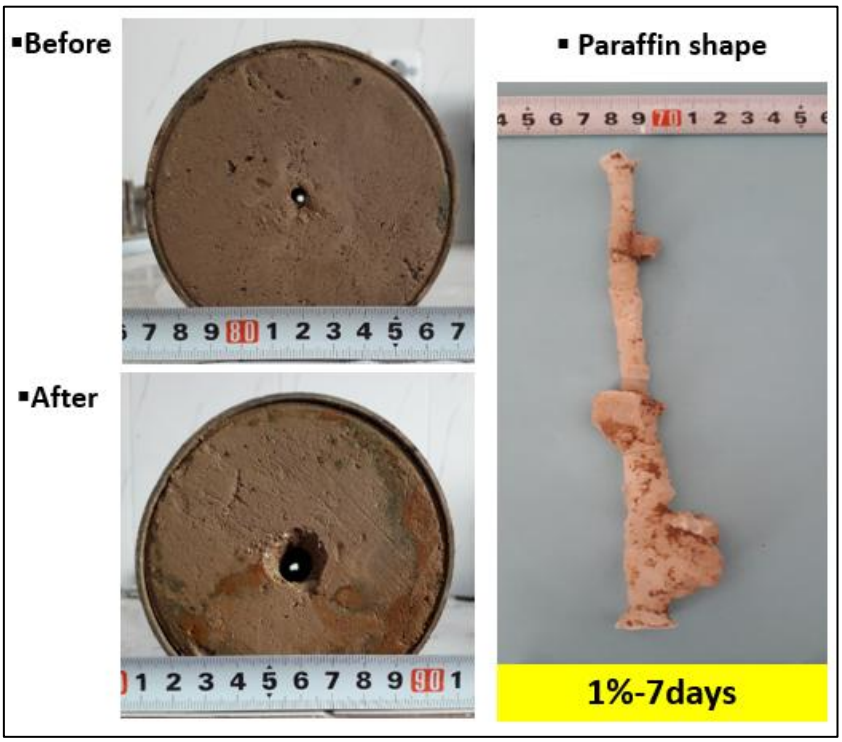

Figure 6: Shape of extracted paraffin (1%-7days cement)

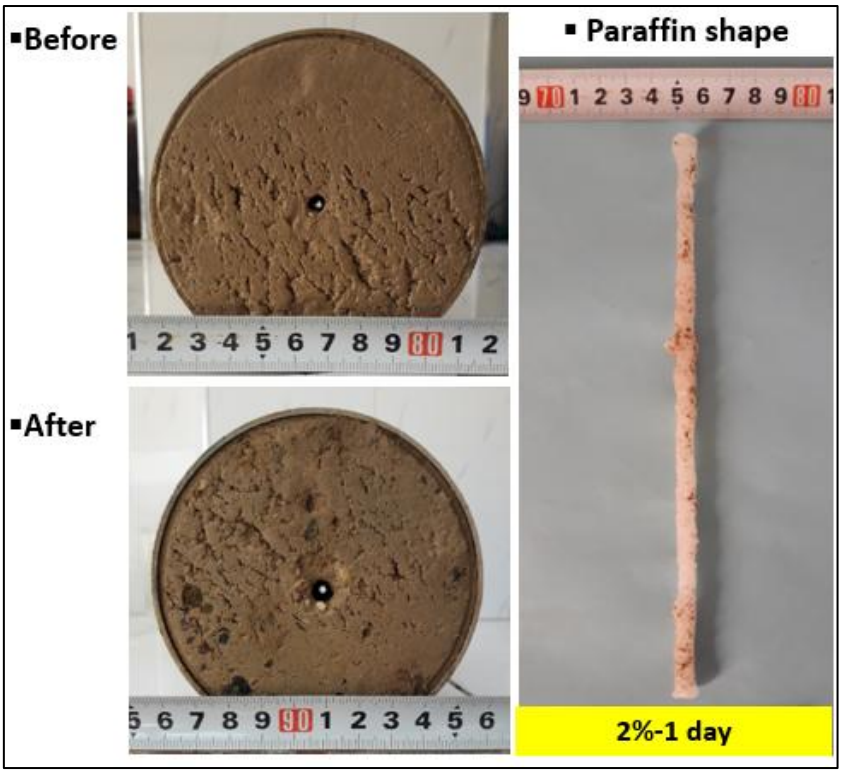

Figure 7: Shape of extracted paraffin (2%-1day cement)

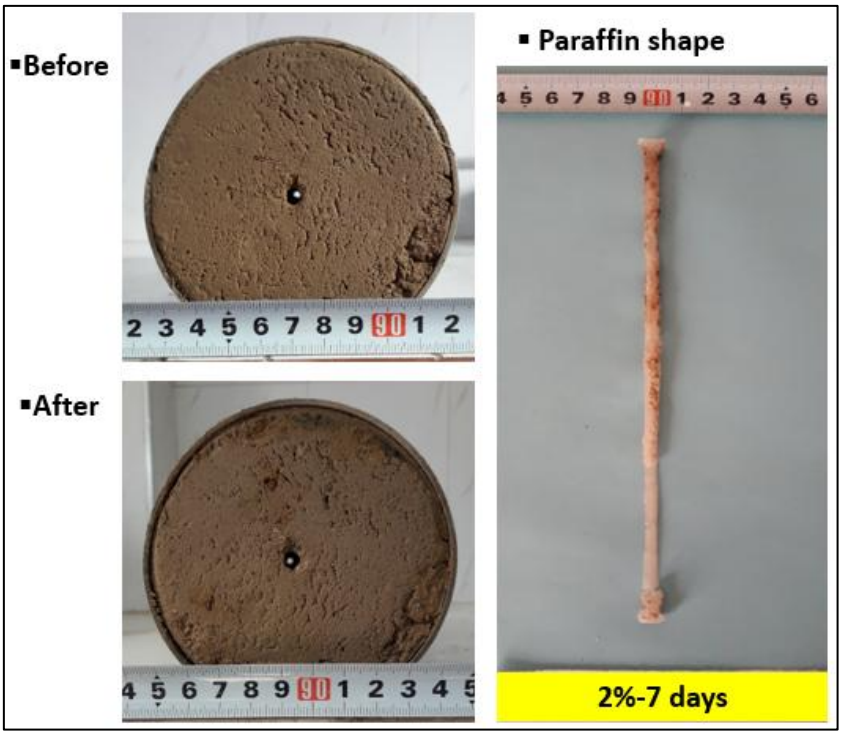

Figure 8: Shape of extracted paraffin (2%-7day cement)

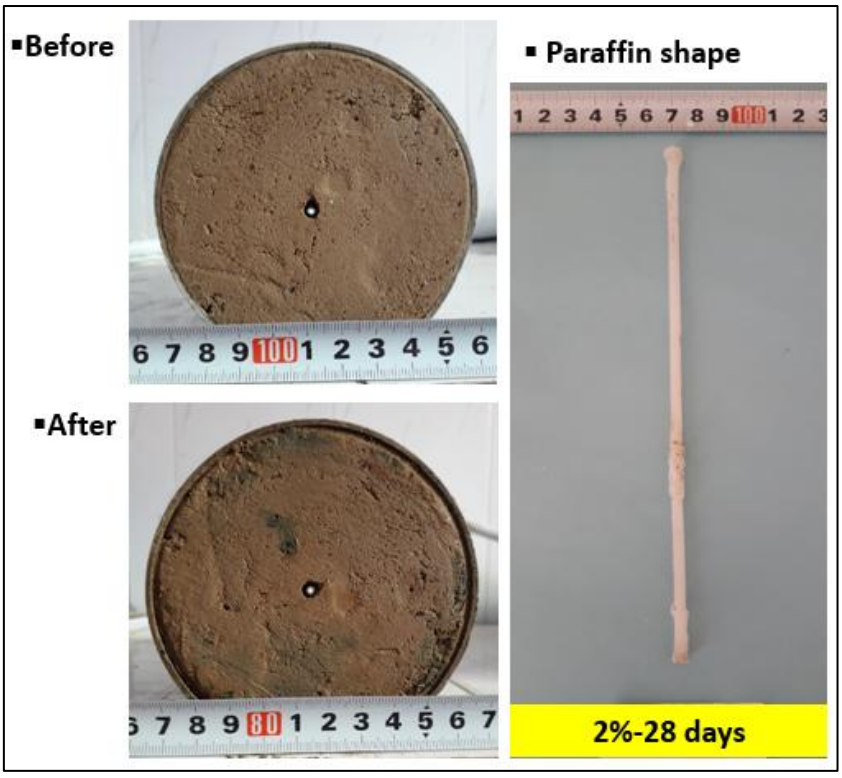

Figure 9: Shape of extracted paraffin (2%-28 days cement)

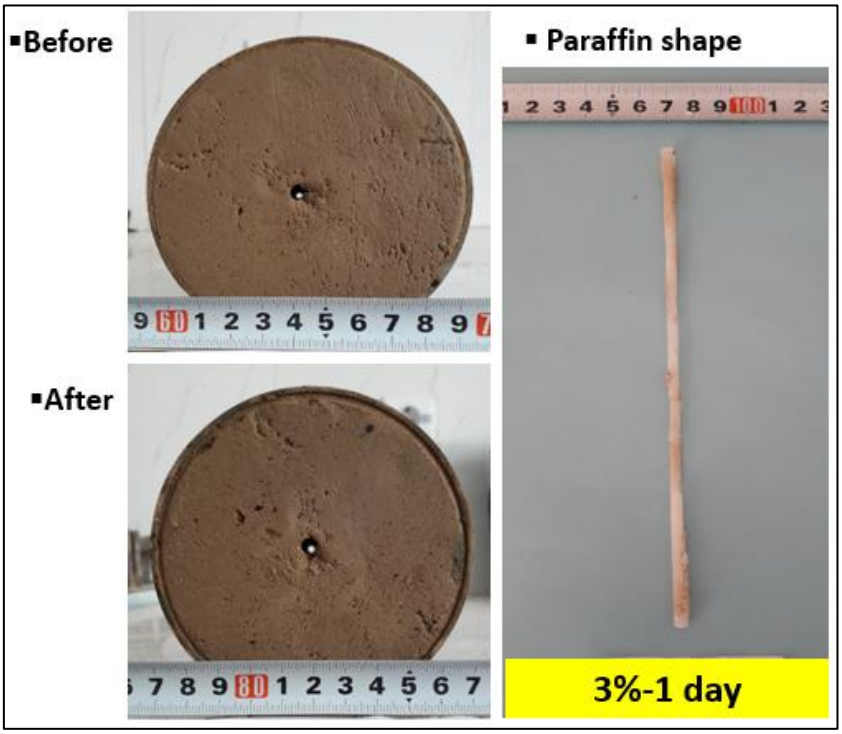

Figure 10: Shape of extracted paraffin (3%-1 day cement)

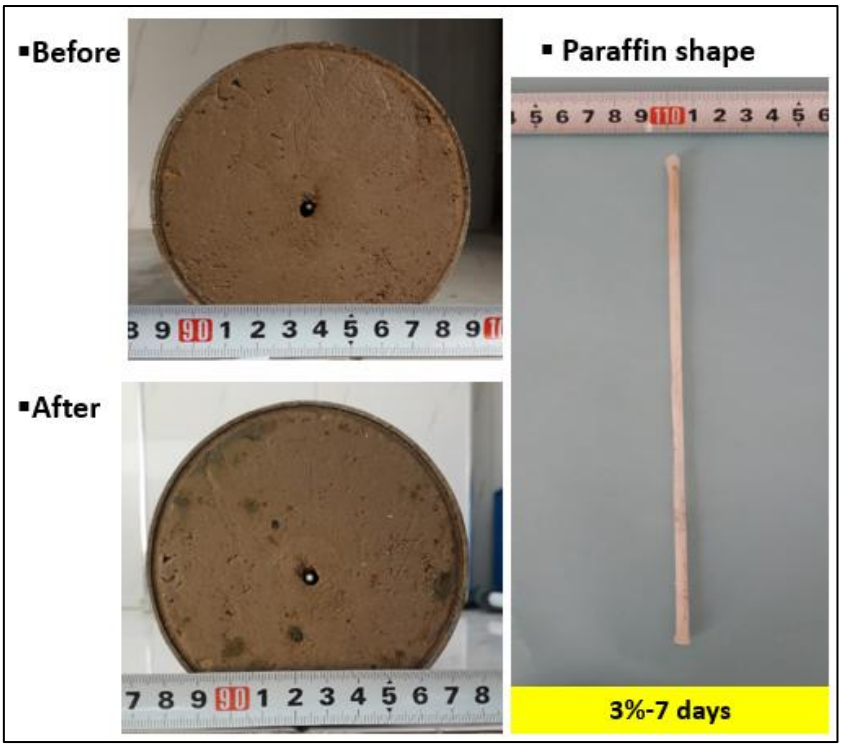

Figure 11: Shape of extracted paraffin (3%-7 days cement)

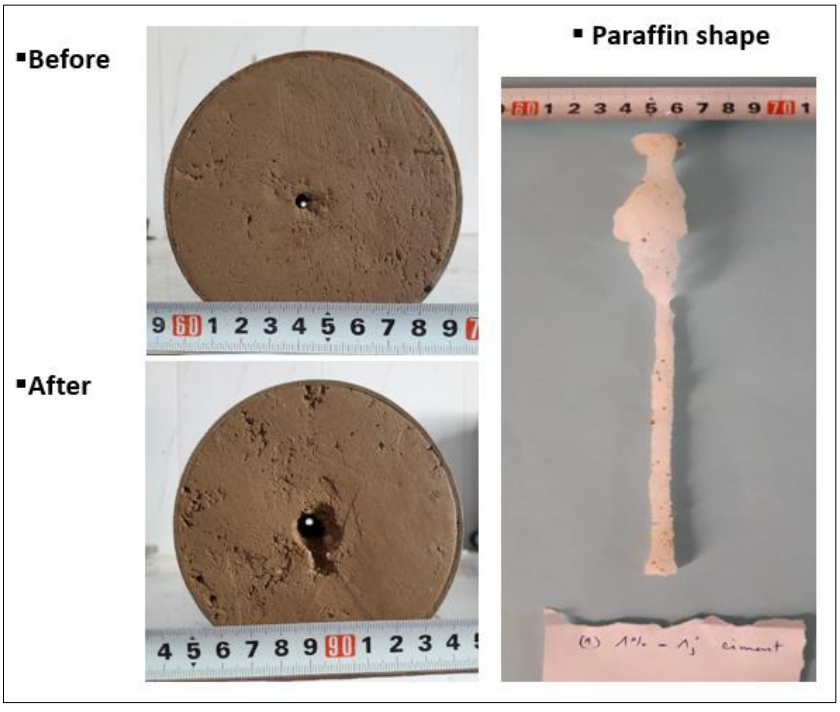

Figure 12: Shape of extracted paraffin (1%-1day cement)

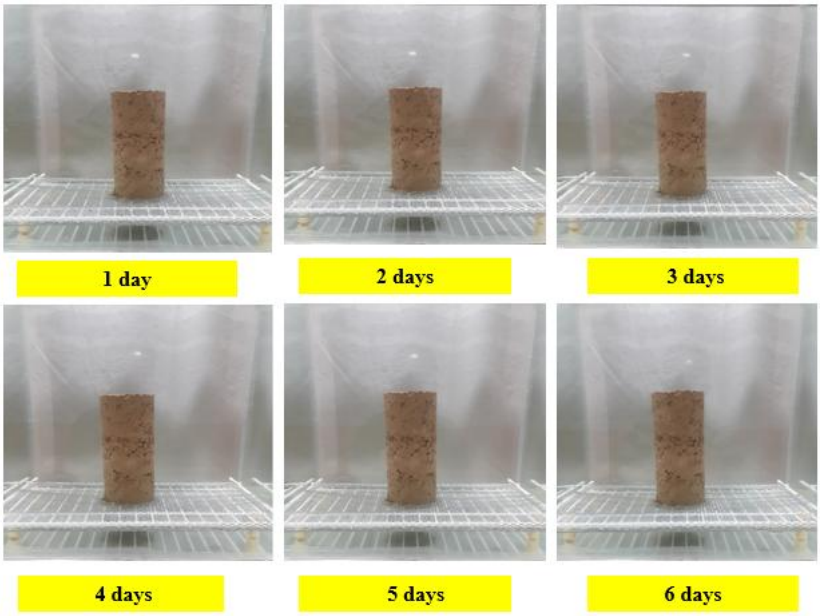

Figure 13: Shape of immerged sample (lime 1%- 1 days)

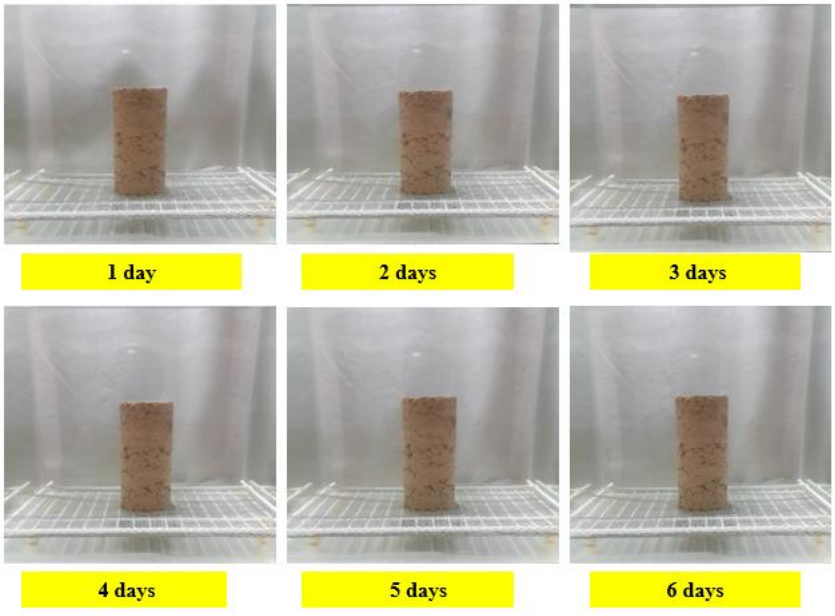

Figure 14: Shape of immerged sample (lime 1%- 7 days)

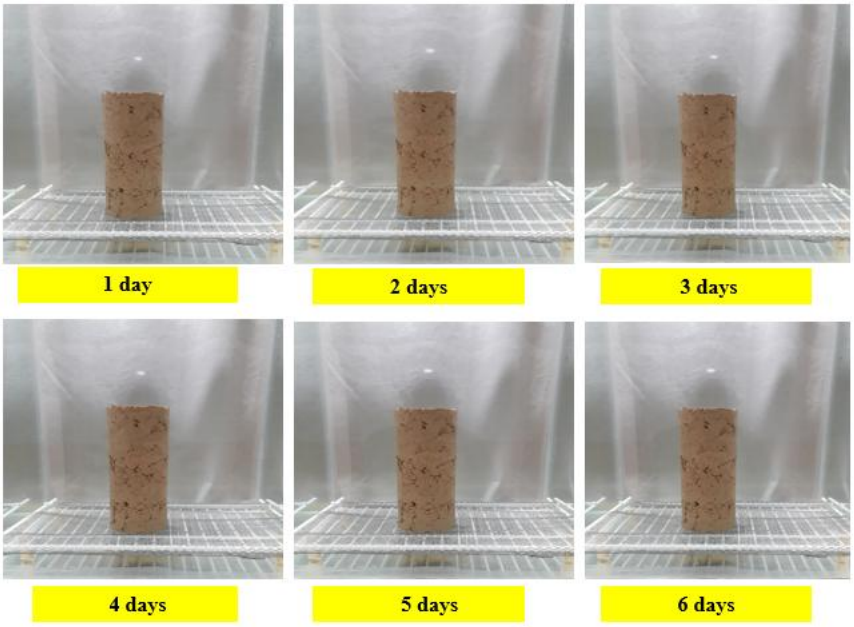

Figure 15: Shape of immerged sample (lime 1%- 28 days)

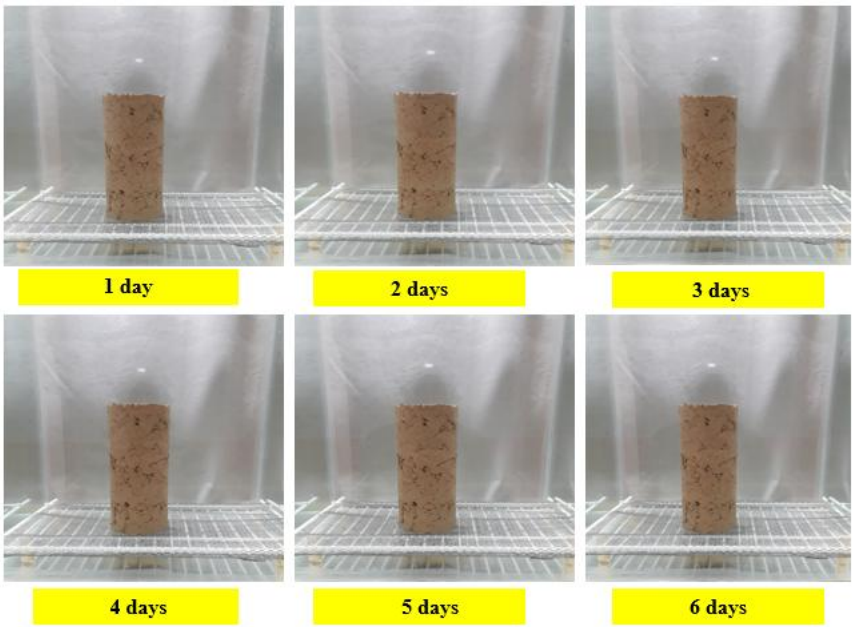

Figure 16: Shape of immerged sample (lime 1%- 90 days)

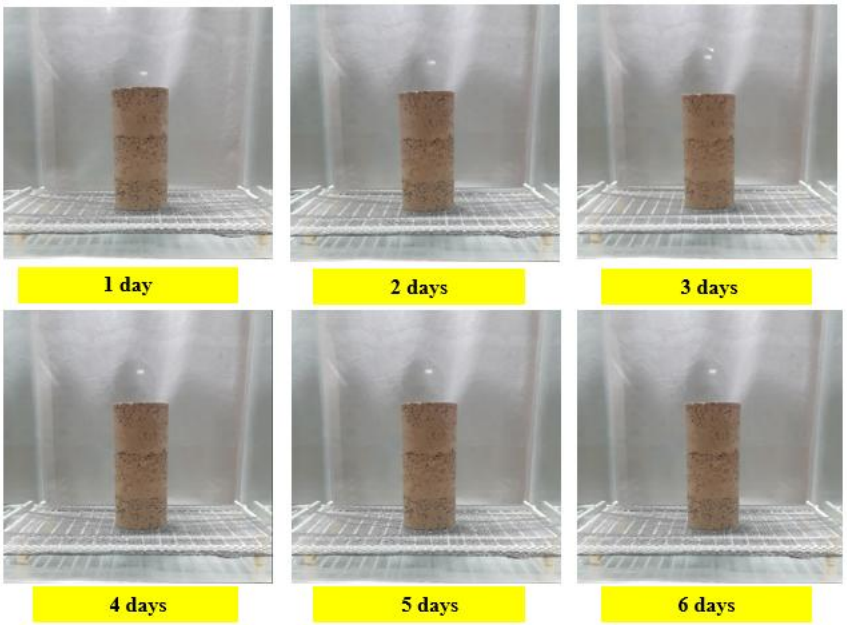

Figure 17: Shape of immerged sample (lime 2%- 1 day)

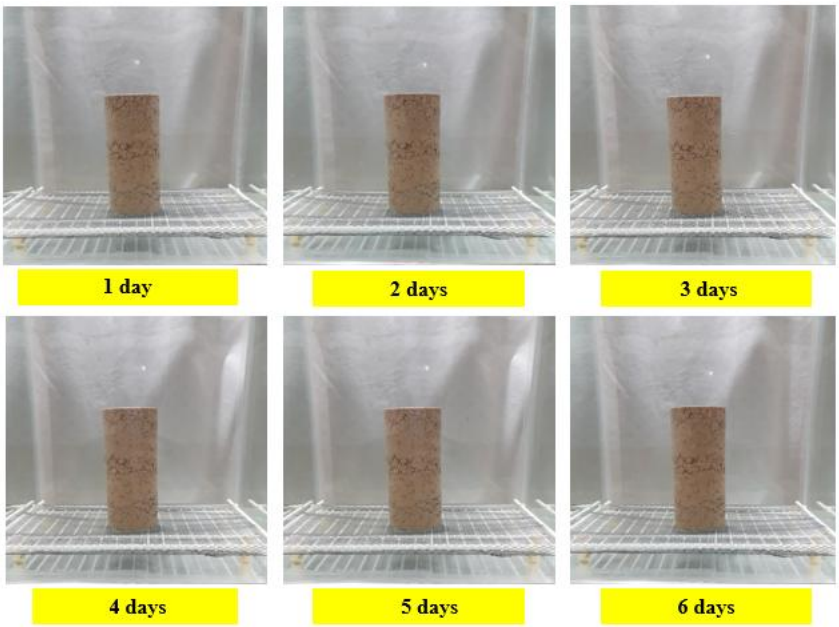

Figure 18: Shape of immerged sample (lime 2%- 7 days)

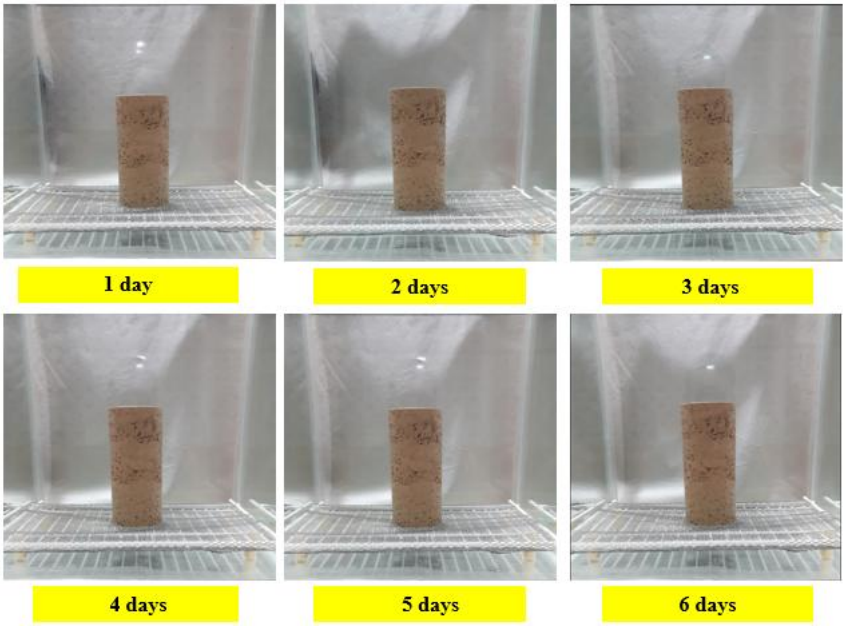

Figure 19: Shape of immerged sample (lime 2%- 28 days)

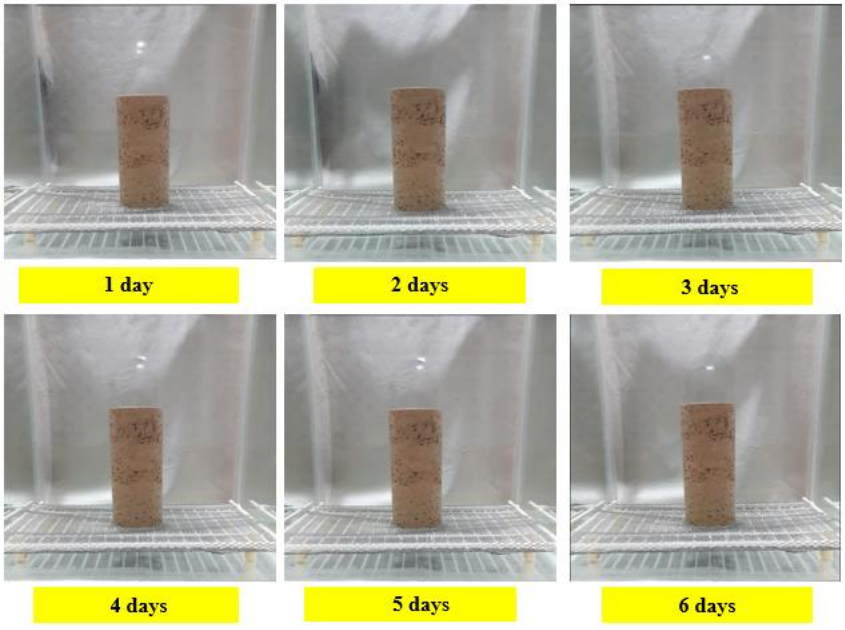

Figure 20: Shape of immerged sample (lime 2%- 90 days)

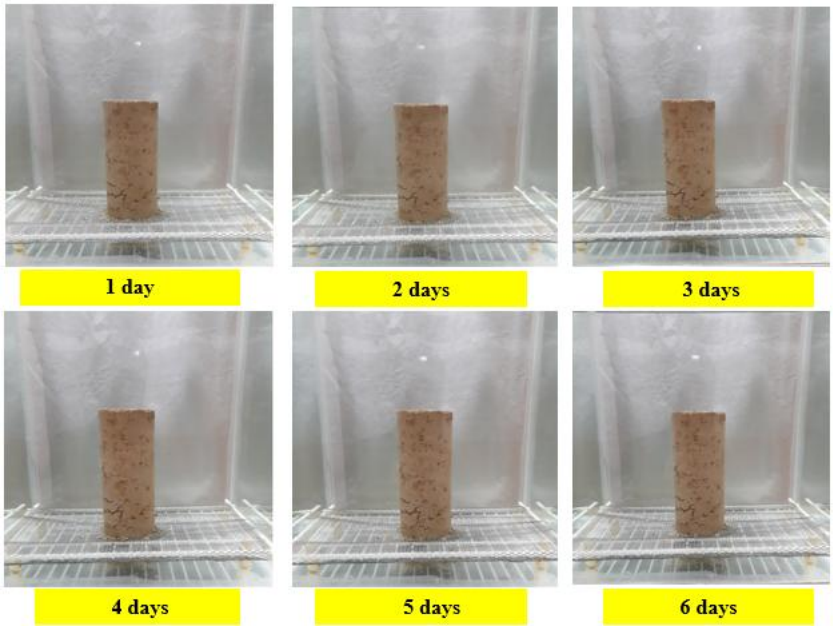

Figure 21: Shape of immerged sample (cement 2%- 1 day)

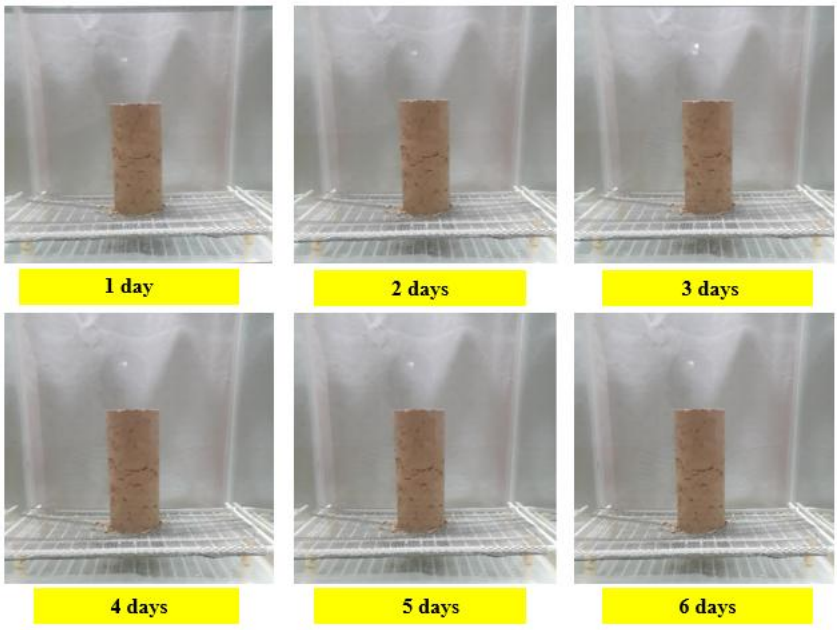

Figure 22: Shape of immerged sample (cement 2%- 7 days)

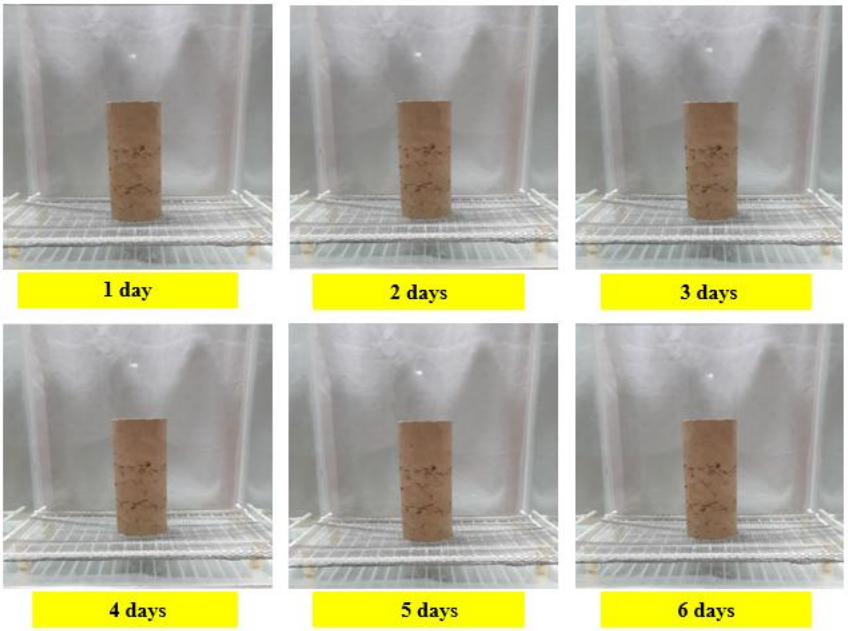

Figure 23: Shape of immerged sample (cement 2%- 28 days)

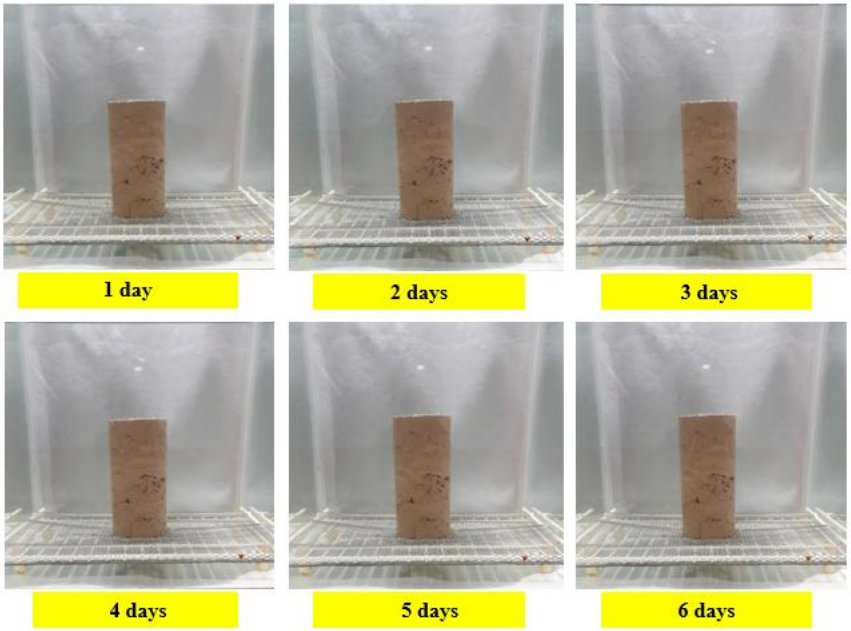

Figure 24: Shape of immerged sample (cement 2%- 90 days)

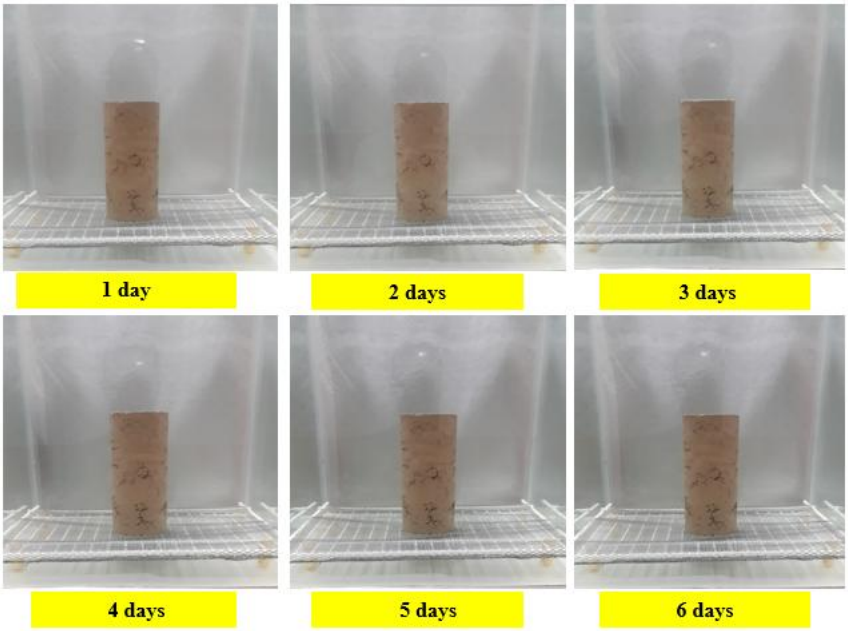

Figure 25: Shape of immerged sample (cement 3%- 1 day)

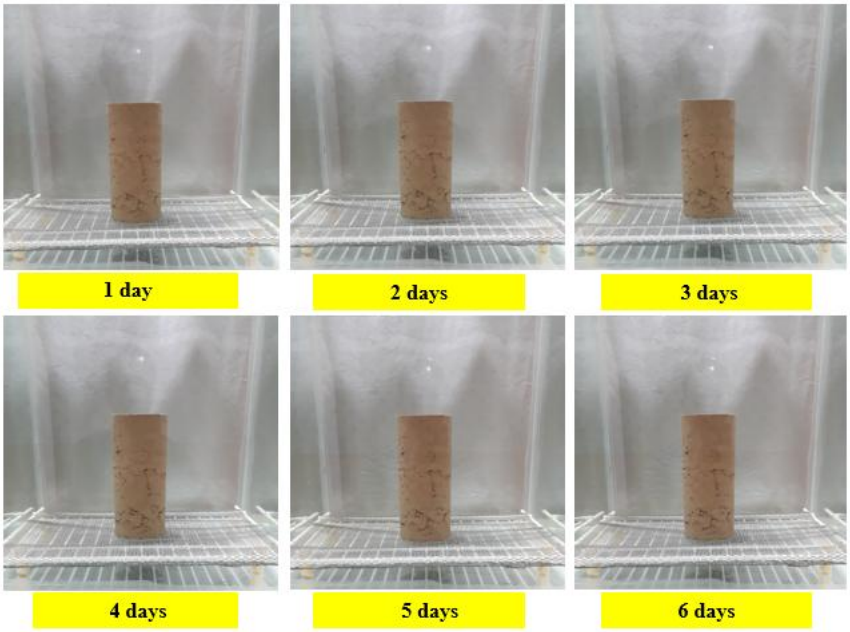

Figure 26: Shape of immerged sample (cement 3%- 7 days)

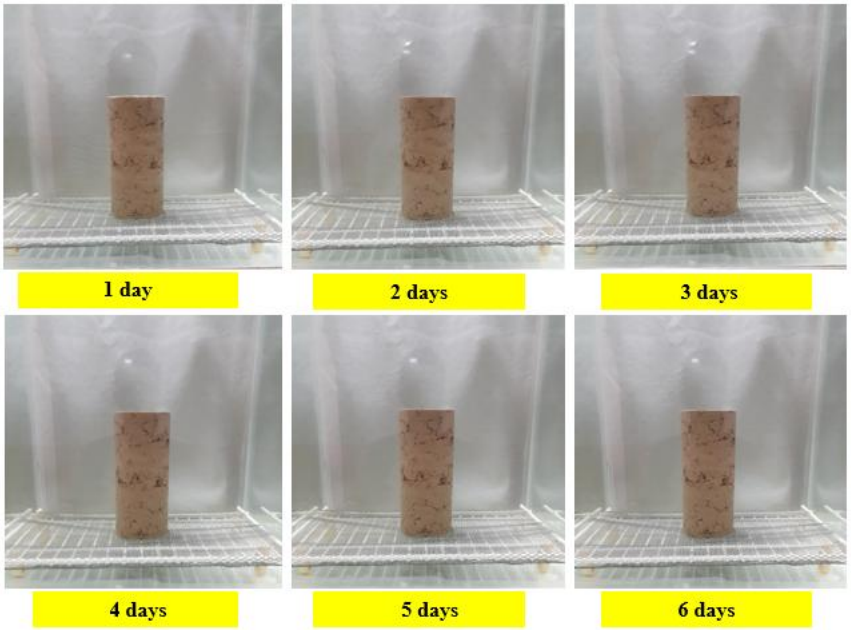

Figure 27: Shape of immerged sample (cement 3%- 28 days)

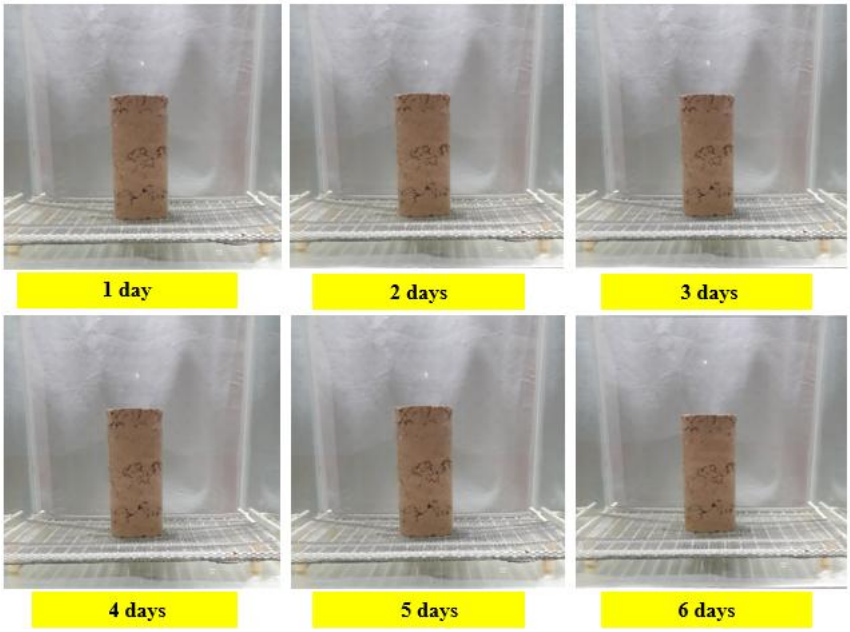

Figure 28: Shape of immerged sample (cement 3%- 28 days)

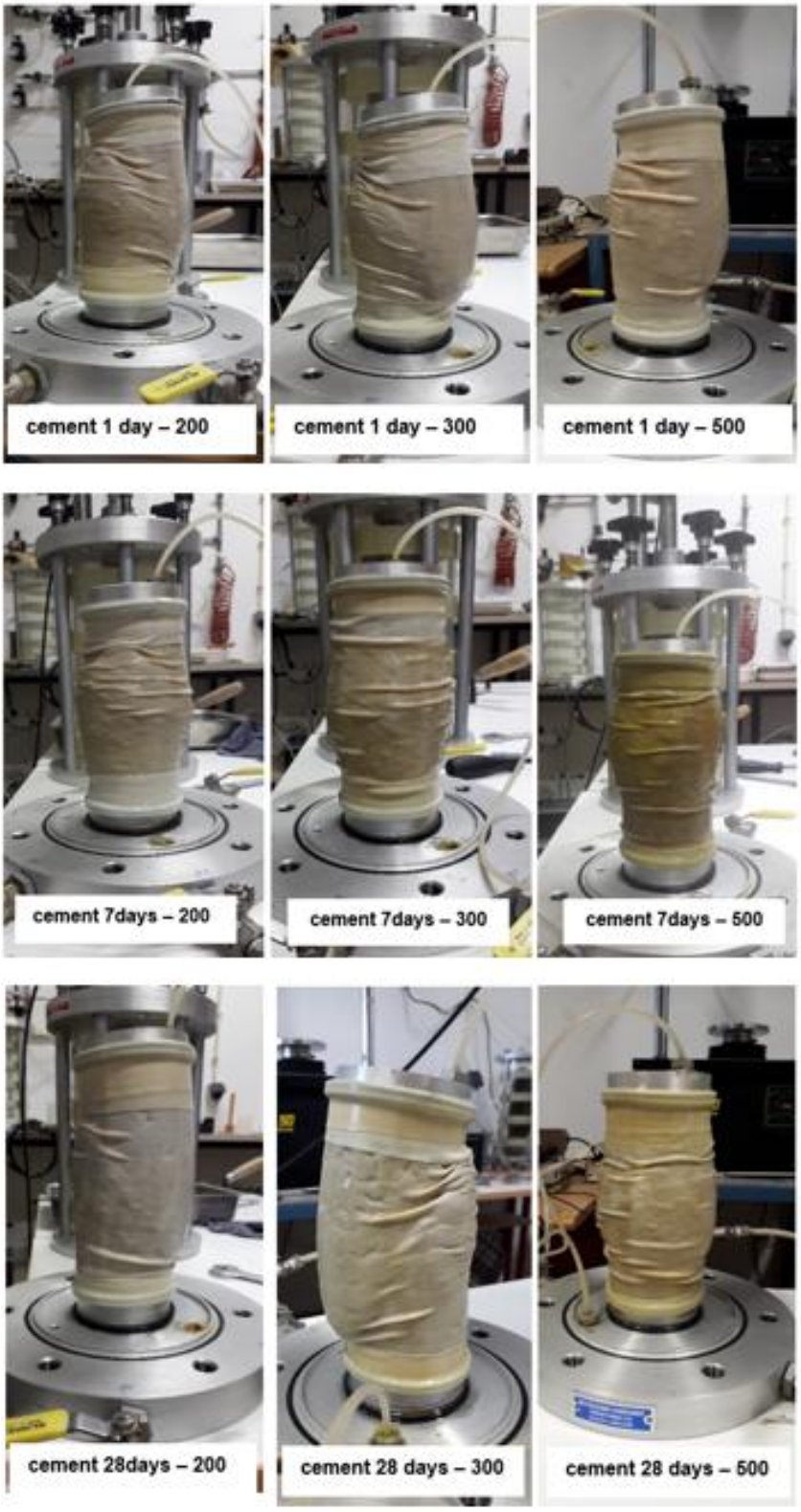

Figure 29: Cement treated specimen after test (7-28 and 90 days)

Figure 30: Lime treated specimen after test (7-28 and 90 days)